OPTIMAL CONTROL OF A ROTATING CYLINDER PARTIALLY FILLED WITH IDEAL FLUID

by

Robert D. Klauber

Dissertation submitted to the Faculty of the
Virginia Polytechnic Institute and State University
in partial fulfillment of the requirements for the degree of

DOCTOR OF PHILOSOPHY

in

Engineering Mechanics

APPROVED:

S. L. Hendricks, Chairman

M. S. Cramer

J. L. Junkins

L. L. Grigsby

L. Meirovitch

March 1982
Blacksburg, Virginia

ACKNOWLEDGEMENTS

One acquires many debts in life of a nonmaterial nature. In the course of earning this degree I have picked up more than my share.

The short acknowledgements that follow are an attempt, painfully inadequate, to express my gratitude to those who have given me more than I am able to return. They are restricted by space, and by the limited scope of human language and my ability to use it. It is my hope that they point, in some way, to feelings which transcend expression.

I would like to extend my heartfelt thanks

To my parents, Mr. and Mrs. Barney B. Klauber, whose innumerable unquestioning sacrifices first enabled me to get started on the long climb up the mountain to the Ph.D.,

and to my devoted wife, Susan, who so graciously and unselfishly helped on the last leg to the top;

To my friend, advisor, and confidant, Dr. Scott L. Hendricks, an individual who, through his continual, untiring, and knowledgeable guidance as well as through his personal integrity and devotion to truth at all levels, has won my deepest respect;

To Dr. Daniel Frederick and Dr. John L. Junkins, who never said "no," but always "we can find a way to do it." With people like that behind you, anything is possible;

To Dr. Leonard Meirovitch, who gave me one year of the best dynamics available anywhere;

To the members of my graduate advisory committee who, in addition to Professors Hendricks, Frederick, Junkins, and Meirovitch, have included Dr. Mark S. Cramer, Dr. Leo L. Grigsby, and Dr. Dean T. Mook. To a man they have left me with an indelible impression of exceptional professional ability coupled with sincere desire to help all others with whom they come in contact. These attributes I wish every member of the human race could share;

To Ms. Vanessa McCoy, who cheerfully did an exceptional job of typing the Department of Energy report which makes up the major portion of this dissertation, and to Mr. John Adams, for the very professional (and at times very entertaining) set of figures found within;

And finally, to Mahareshi Mahesh Yogi, whose great gifts of the Transcendental Meditation (TM) and TM-Sidhis Programs have raised my reasoning ability and overall mental clarity to a level well beyond that which they would otherwise now be. His techniques have enabled me to accomplish smoothly, in a relatively short period, a goal which could easily have engulfed considerably more time and struggle. I owe him a great deal.

TABLE OF CONTENTS

LIST OF SELECTED SYMBOLS

Roman

$\hat{P}(r^*,\theta,t)$ - total real dimensional pressure

$P(r,\theta,t)$ - nondimensional equivalent of $\hat{P}(r^*,\theta,t)$

$\hat{P}_n(r^*,t)$ - nth term in pressure expansion, complex and dimensional

$\hat{P}(r^*,t)$ - shorthand notation for $\hat{P}_1(r^*,t)$, the first term in the complex, dimensional pressure expansion

$P_n(r,t)$ - nondimensional equivalent of $\hat{P}_n(r^*,t)$

$P(r,t)$ - nondimensional equivalent of $\hat{P}(r^*,t)$

$P_{re}(r,t)$ - real part of $P(r,t)$

$P_{im}(r,t)$ - imaginary part of $P(r,t)$

$u_n(r,t)$ - nth term in expansion of radial velocity component, complex and nondimensional

$u(r,t)$ - shorthand notation for $u_1(r,t)$

$u_{re}(r,t)$ - real part of $u(r,t)$

$u_{im}(r,t)$ - imaginary part of $u(r,t)$

$u(t)$ - $u(r,t)/[1 - 1/r^2]$

u - shorthand for $u(t)$

$v_n(r,t)$ - nth term in expansion of tangential velocity component, complex and nondimensional

$v(r,t)$ - shorthand notation for $v_1(r,t)$

$v_{re}(r,t)$ - real part of $v(r,t)$

$v_{im}(r,t)$ - imaginary part of $v(r,t)$

Other

*	- superscript indicating dimensional quantity
^	- superscript indicates a dimensional quantity when used over scalars (also used over vectors to imply unit length).
†	- complex conjugate

CHAPTER I

INTRODUCTION

1.1 BACKGROUND

1.1.1 SYSTEM DYNAMICS

The dynamics of rotating shafts has long been a subject of fundamental importance in the design, operation, and analysis of most of the machinery of man. One of the primary concerns with such systems is that of transverse vibration, i.e., oscillatory rotor displacement in a direction perpendicular to the axis of rotation.

Motion of this type occurs when, for one reason or another, the shaft "bows outward" from its undeflected position and spins around the line of bearing centers. This general phenomenon, illustrated in Figure 1.1, is known by the generic name "whirl", though, kinematically, it can fall into either of two distinct categories. For both categories, the angular velocity with which the plane containing the axis of the bent shaft turns about the line of bearing centers is called, suitably, the "whirl speed". Also for both categories, the rotor center of mass traces out a circle (for steady state motion) about the same line. The two kinds of whirl are distinguished, however, by the relative magnitudes of the whirl and shaft spin speeds.

In the first case the two speeds are equal. The plane containing the bent axis rotates at exactly the same rate as does the shaft itself. This implies (see Figure 1.2a) that a point on the rotor

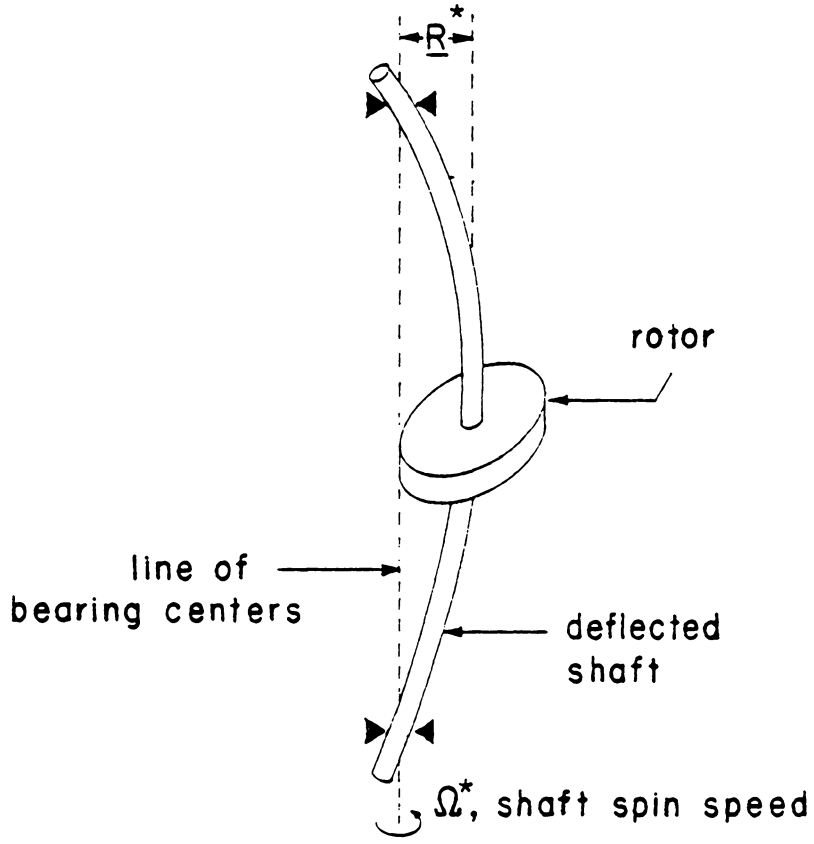

Side View

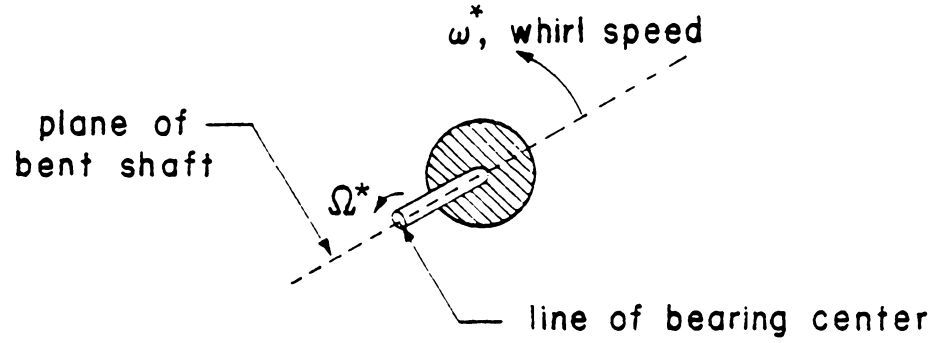

Top View

FIGURE 1.1. A WHIRLING ROTOR

Note: x-y axes shown are attached to rotor shaft; $T = 2\pi/\Omega^*$

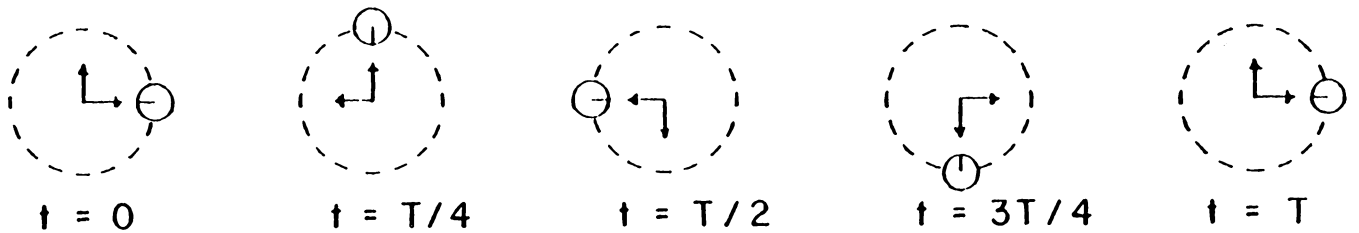

FIGURE 1.2a. SYNCHRONOUS WHIRL VIEWED FROM GROUND, $\Omega^* = \omega^*$

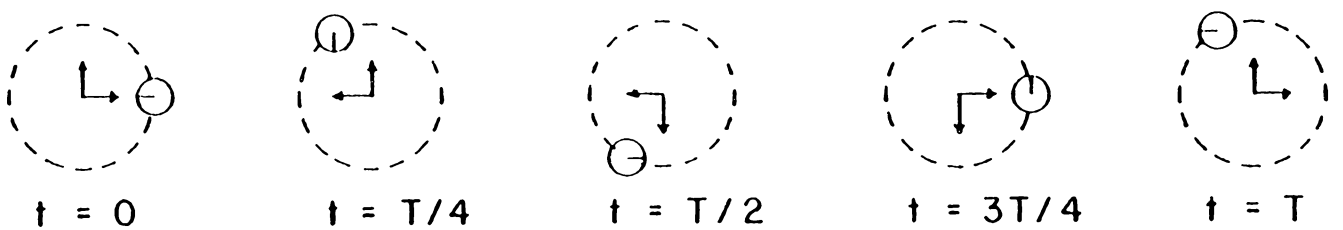

FIGURE 1.2b. ASYNCHRONOUS WHIRL VIEWED FROM GROUND, $\omega^* > \Omega^*$

surface which faces the line of bearing centers remains, analogous to the motion of the moon about the earth, facing that centerline throughout the history of the motion. This type of whirl is called "synchronous". The most significant point is that, from the point of view of the shaft, the deflection is static and the rotor experiences no alternating stresses (see Figure 1.3a).

The second kind of whirl is called, appropriately, "asynchronous" and occurs when the shaft experiences cyclic loading. It results from a difference in whirl and shaft angular velocities (see Figure 1.2b). In this case an observer moving with the rotor would see the shaft deflection varying sinusoidally in time (see Figure 1.3b). Since alternating stress loading leads to early failure from fatigue, asynchronous whirl is obviously the more serious of the two types.

It should be noted that asynchronous whirl does not give rise to simple oscillatory flexural loading in a single plane. Rather, it behaves, in general, in a manner similar to that depicted in Figure 1.3b, i.e., the bending is circulatory and its frequency is equal to the angular velocity of the center of mass as seen from the rotor fixed reference frame (the x-y axes in the illustration). By the addition of angular velocities rule, this frequency (denoted γ^*) can be shown to equal the difference between the whirl and shaft spin speeds.[1] If these

---

[1]Shaft spin and whirl speeds as measured from ground, that is. Since γ^* is measured in the rotating frame, $\omega^* = \gamma^* + \Omega^*$.

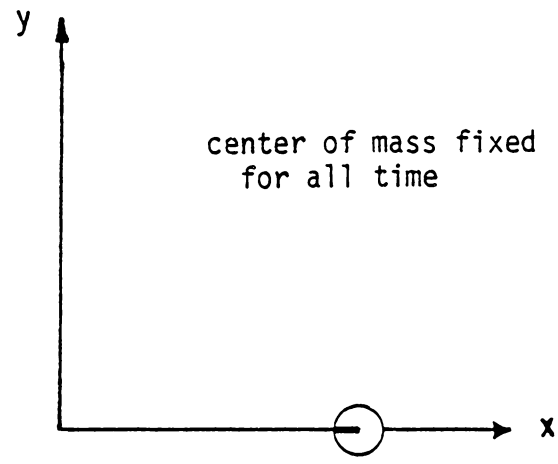

a. Synchronous Whirl

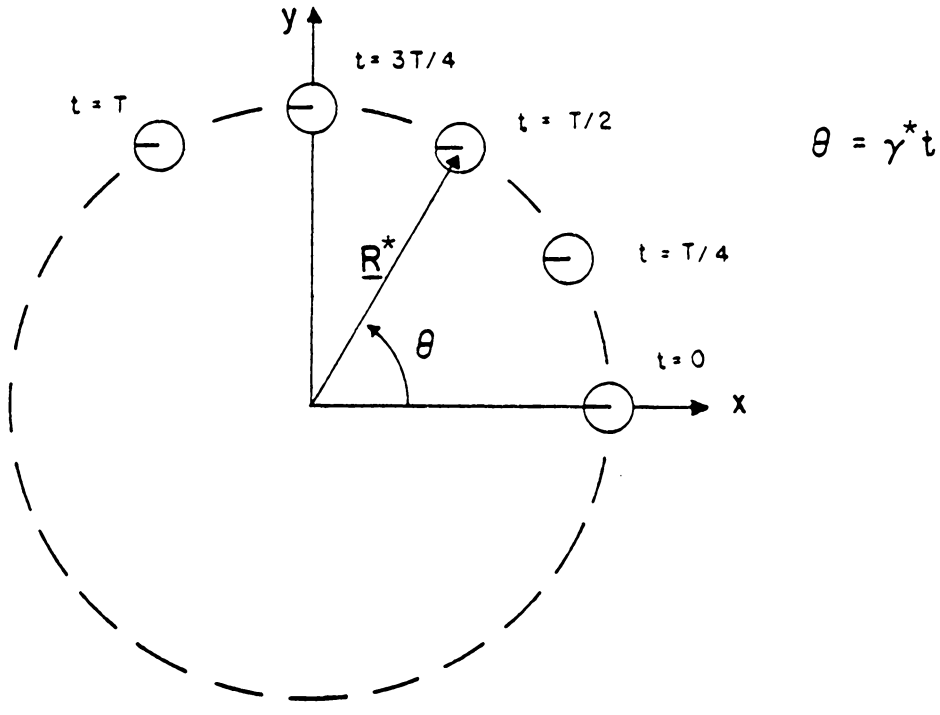

b. Asynchronous Whirl

FIGURE 1.3. WHIRL VIEWED FROM SHAFT FIXED REFERENCE FRAME

are equal, γ^* becomes zero, shaft deflection is static, and whirl reduces to the synchronous type.

Whirl can be further characterized by the direction of γ^* . Motion where it is in the same direction as Ω^* is referred to as forward whirl; that where it is in the opposite directon, as backward whirl.

In addition, the reader should note that, so far, only stable whirl has been discussed. For the unstable situation, rotor displacements are not constant in magnitude but increase exponentially with time. For this case the tip of the $\underline{R}^*$ vector traces out a spiral rather than a circle, behaving in a manner similar to that displayed in Figure 1.4.

The factors determining which kinematic configuration (stable or unstable, synchronous or asynchronous, etc.) arises are dynamical and vary with the nature of the spinning body and its supports.

Many situations can cause a rotor to whirl. The most common is that of mass unbalance, i.e., the rotor center of mass is not coincident with the rotational centerline. During spin the inertial force causes the center of mass to move even further outward, resulting in a flexurally stressed shaft[1]. Motion of this type has three characteristics which are conceptually relevant. They are: (1) the whirl is synchronous and hence not as damaging as it could be, (2) "critical" speeds exist for which deflection is greatly magnified (these

---

[1]For the mass unbalance configuration the zero deflection point is not an equilibrium point. Equilibrium for this case is depicted in Figure 1.3a.

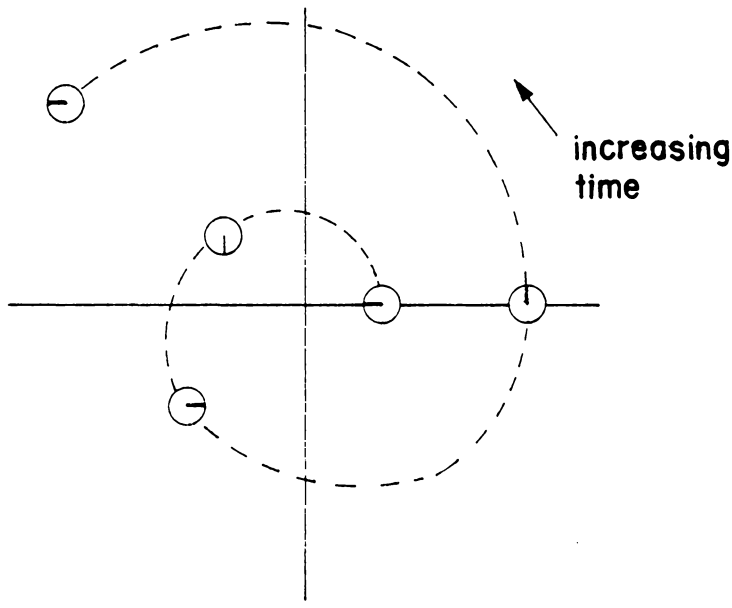

Viewed from Ground

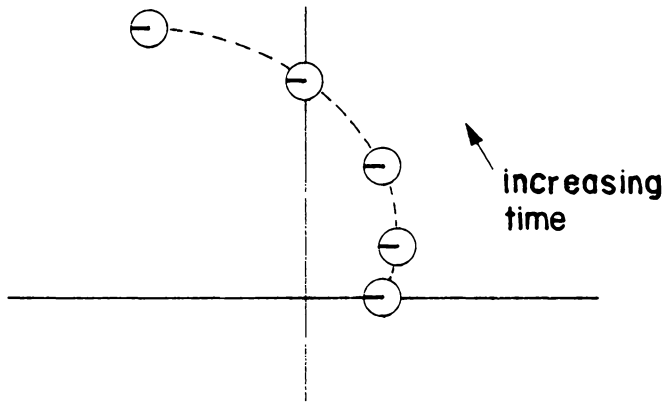

Viewed from Shaft Fixed Reference Frame

FIGURE 1.4. UNSTABLE ASYNCHRONOUS WHIRL

speeds are equal to the rotor resonant frequencies), (3) the motion is stable.

Other examples of whirl, more serious since they are asynchronous, and in some cases unstable, include shafts having internal damping forces [1,2] and rotors mounted in non-symmetrical supports [3].

The present research is concerned with yet another case, one caused by the presence of fluid inside the rotor, (see Figure 1.5 where for the present discussion the control force U is zero) and one which, in addition to being asynchronous, has been shown, under certain conditions, to be unstable as well.

The first evidence that such a phenomenon existed came from Kollman [4] in the early 1960's. Experimenting with a rotor partially filled with liquid, he discovered a wide range of spin speeds over which the system was unstable, i.e., slight transverse deflections grew rapidly, limited only by system non-linearities far from equilibrium[1]. Kollman's work was primarily empirical and he did not present an analytical explanation of the phenomenon.

Subsequent theoretical analyses by Kuipers [5], Phillips [6], Miles and Troesch [7], Wolfe [8], and more extensively, Hendricks and Morton [9,10] have evolved a comprehensive theory of centrifuge motion applicable to many different rotor geometries. They have shown, among other things, that the system instability results from an interaction

---

[1]There is no initial mass unbalance and the zero deflection point is the equilibrium point. However, it is an unstable equilibrium.

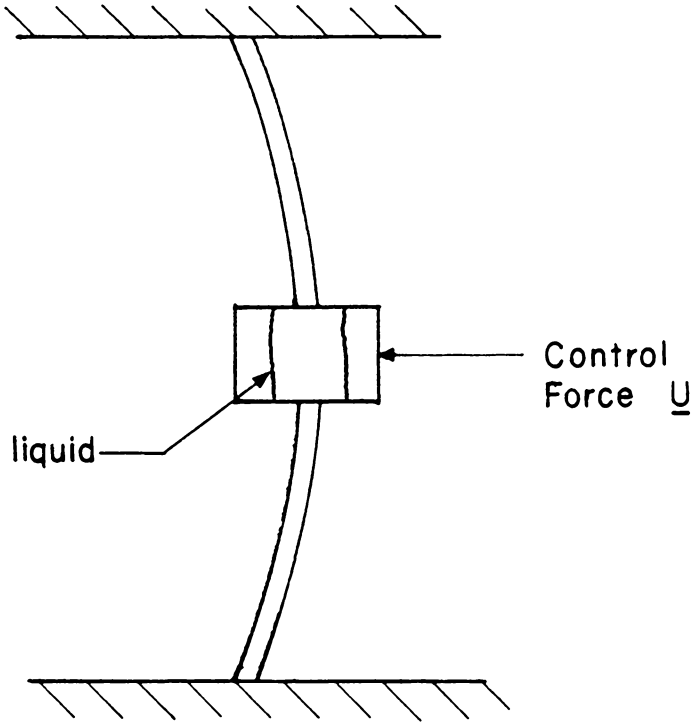

Single Mass Rotor

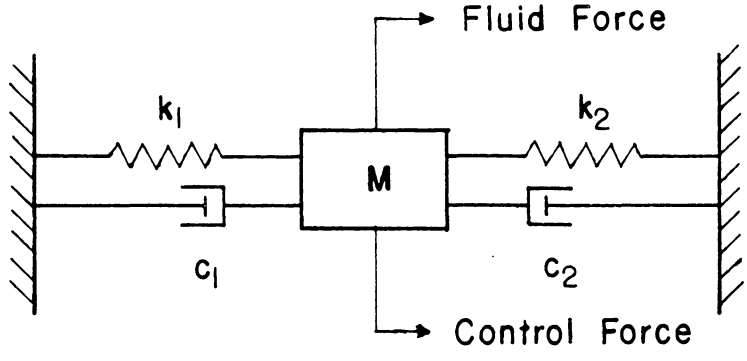

Equivalent Single Mass Rotor Model

FIGURE 1.5. SINGLE MASS ROTOR

between surface waves in the fluid and the solid rotor.

At the free surface of the fluid (radius = b) waves with wave lengths equal to $2\pi b/n$ ($n = 1,2,...$) can form, though as it turns out (see Section 2.1.2 and Appendix A2), only the longest of these (i.e., $n = 1$) can affect rotor motion. These surface waves can be initiated by slight transverse vibrations of the rotor and, in many instances, the wave can then feed energy back into the shaft, causing its oscillations to amplify rapidly.

The degree of instability is, as might be expected, related to how closely the first wave propagation frequency approaches one of the natural frequencies of the flexible rotor system. Since fluid surface wave frequencies are proportional to the half power of the body force, they vary monotonically with spin speed. As rotor velocity increases, therefore, wave propagation frequency does as well, resulting in severe instability in regions around system resonances.[1]

Significantly, instability is not always reduced by the introduction of external dampers on the rotor. Hendricks' [9]

---

[1]The reader should distinguish carefully between the various types of frequencies discussed. They are:

(1) shaft spin speed Ω^*,
(2) empty rotor resonance frequencies,
(3) fluid surface wave propagation frequency (considered independent of rotor deflection).
(4) natural frequencies of the coupled mass-fluid system (if all but one of the modes were damped out, the frequency of the undamped mode would become the whirl frequency γ^*.),

For the unbalanced solid rotor mentioned earlier, problems are encountered whenever (1) approaches any of (2). In the present case, however, the concern is with the proximity of (3) to (2).

theoretical results (see Figure 1.6) showed that:

(1) the ideal fluid undamped rotor case had regions of both stability and instability,

(2) addition of external (shaft) dampers caused the non-viscous fluid system to be unstable over all operating speeds, and

(3) viscous fluids with damped rotors had both stable and unstable regimes.

Presence of an external damper introduces a force on the fluid which is out of phase with the acceleration and displacement of the rotor. An ideal fluid has no mechanism for counteracting this force, the result being the behavior described in (2) above. The general feeling at present is that a non-viscous fluid analysis represents the "worst case" situation.

1.1.2 SYSTEM CONTROL

Extensive and definitive though the aforementioned research has been, it has, nevertheless, only covered half of the problem. Once the question of free system dynamics has been answered, the task of stabilization and control still remains.

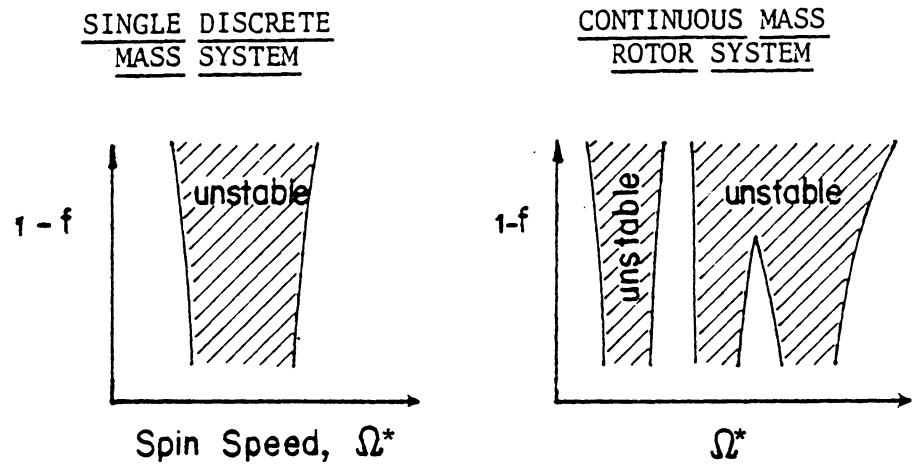

Ideal Fluid, No External Dampers

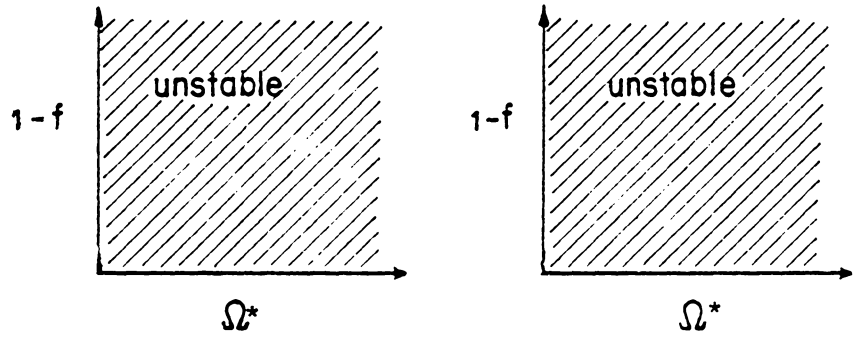

Ideal Fluid, External Dampers

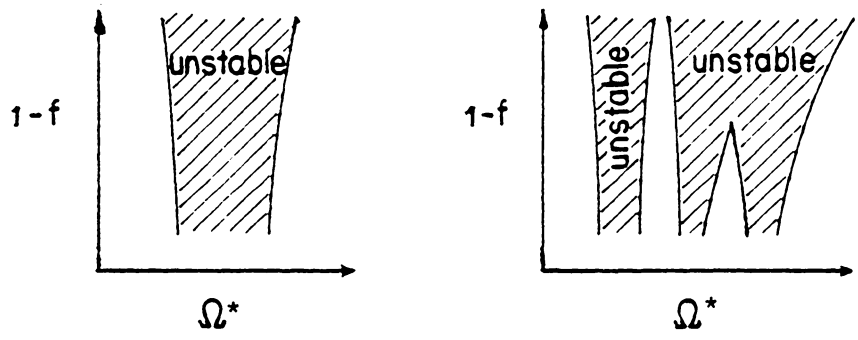

Viscous Fluid, External Dampers

Note: Fill ratio f = (radius to the fluid surface)/(inner radius of cup)

FIGURE 1.6. QUALITATIVE PRESENTATION OF THE GENERAL RESULTS OF HENDRICKS [9]

Taylor [11], evidently the only researcher in this area to date,[1] studied the control force necessary to stabilize the motion of a single discrete mass - two spring and damper rotor containing a small ball. This system exhibits many of the characteristics of a rotor containing fluid and was shown to be controllable, given that the closed loop feedback force is applied directly to the rotor mass itself (see Figure 1.5).

The present effort extends Taylor's work to a more realistic case in which (1) higher degree of freedom systems are treated, (2) the rotor contains fluid, and (3) the control force is applied at a more practical location. In addition, a control force solution technique, more modern and accurate than that used in his studies, is employed (see Section 2.2).

The question of controllability when the feedback force does not act directly on the cup is by no means a trivial one. The situation is somewhat analogous to that of a master trying to control his rather recalcitrant dog (see Figure 1.7). By pulling on the animal's collar, he can, given sufficient strength, force his pet in any direction he chooses. Whether he can have the same effect by tugging on the dog's tail (at the optimal frequency, phase, direction, etc.) is a totally different matter. The first case is much like Taylor's problem, while

---

[1]Reference [12] looks briefly at a cylinder completely filled with liquid which, since it does not have surface wave phenomena, is not relevant here. Reference [13], despite its title, does not attack the specific problem at hand.

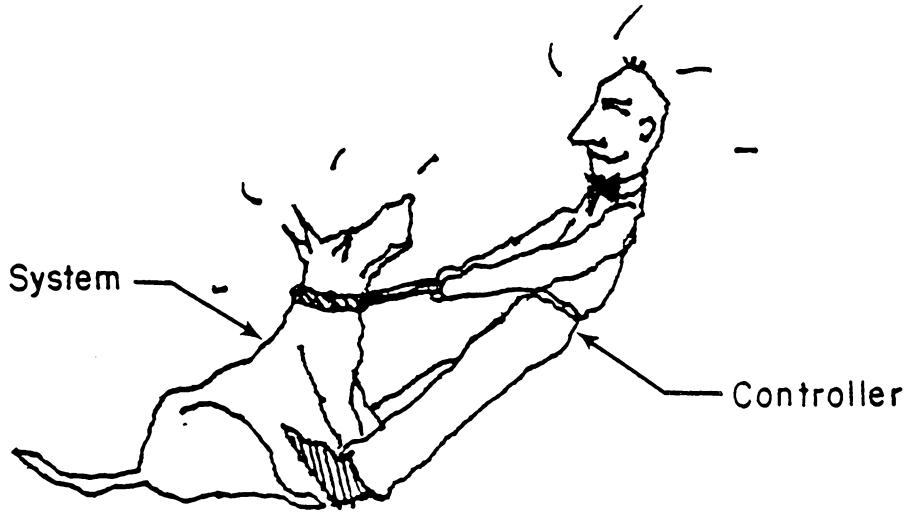

Taylor's Approach

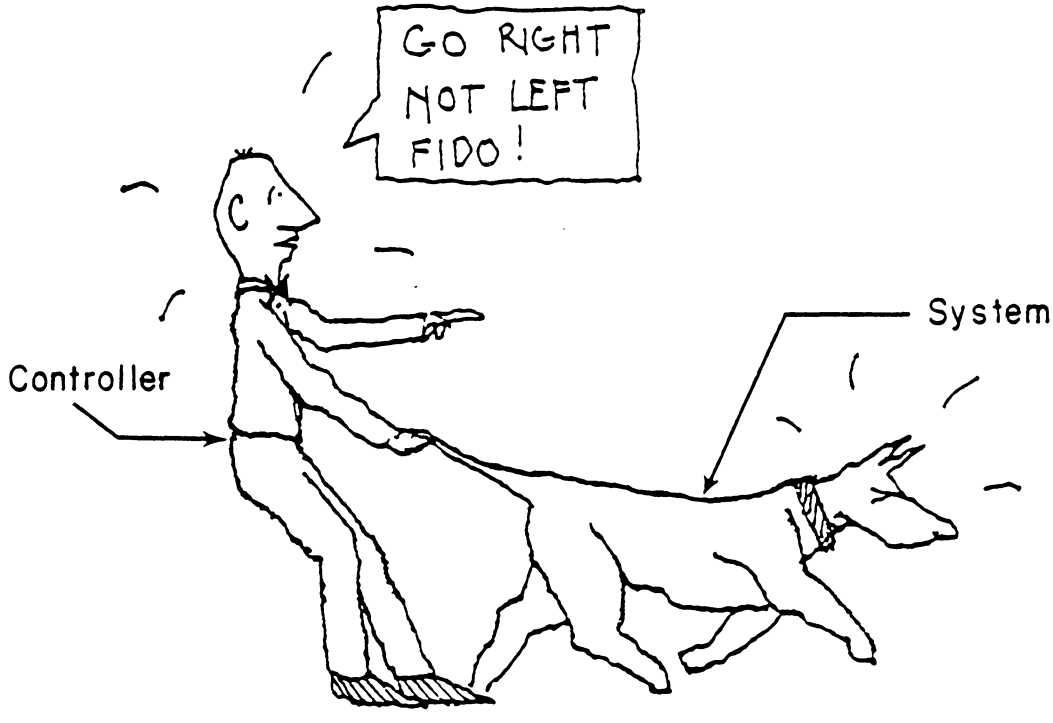

Present Approach

FIGURE 1.7. TWO DIFFERENT APPROACHES TO CONTROL

the second is more like the one considered here. The destabilizing influence is in the cup, but it remains to be seen whether or not it can be controlled by a force applied elsewhere.

Liquid filled centrifuges, liquid cooled gas turbines, and spinning rockets containing fuel are examples for which this analysis is applicable.

1.2 PROBLEM DEFINITION

The present study applies optimal control theory analysis to two different inviscid liquid centrifuge configurations, one modeled simply as a two mass-three spring and damper system, and the other, as a continuous mass rotor. Controllability for a feedback force input at a location other than the principal system mass is investigated, and the governing control relations determined.

The development is carried out in non-dimensional form, allowing ready application to a wide range of physical systems, similar in form but differing parametrically. In addition, for reasons of efficiency and elegance, it is expressed using complex variable notation.

The general formulation of Hendricks [9] is used to write the equations of motion for a multicritical rotor containing an incompressible inviscid fluid. The resulting system of linear equations is then cast in state space form and used to derive the appropriate feedback controls.

1.2.1 DISCRETE TWO MASS ROTOR

The first part of this research extend's Taylor's [11] work to a two degree of freedom system having an ideal fluid contained in the first mass and a control force applied to the second (see Figures 1.8 and 1.9). The equations of motion are developed in Chapter II, first for the two mass rotor model using Lagrange's formulation and then for the liquid via the Euler and continuity equations.

Being non-viscous, the liquid cannot transmit a tangential force to the cup, so fluid input to the rotor is found simply by integrating the wall pressure over the container inner surface. Thus pressure enters both the rotor and the fluid equations of motion, and is, in effect, the coupling agent between the two.

Simple substitution eliminates the pressure and tangential fluid velocity, culminating in a set of three coupled complex equations in three unknowns (two mass displacements and the normal free surface velocity) plus the yet to be determined control force. These are subsequently cast into state space form to yield six equations in six unknowns. The state space equations are then used as constraints on the minimization of a suitable cost function. Solution of the associated Riccati matrix equation and related feedback control follows, with results presented in Sections 2.3 and 2.4.

1.2.2 CONTINUOUS MASS ROTOR

After solving and fully digesting the two mass cases, the next logical step in producing a realistic mathematical representation is the

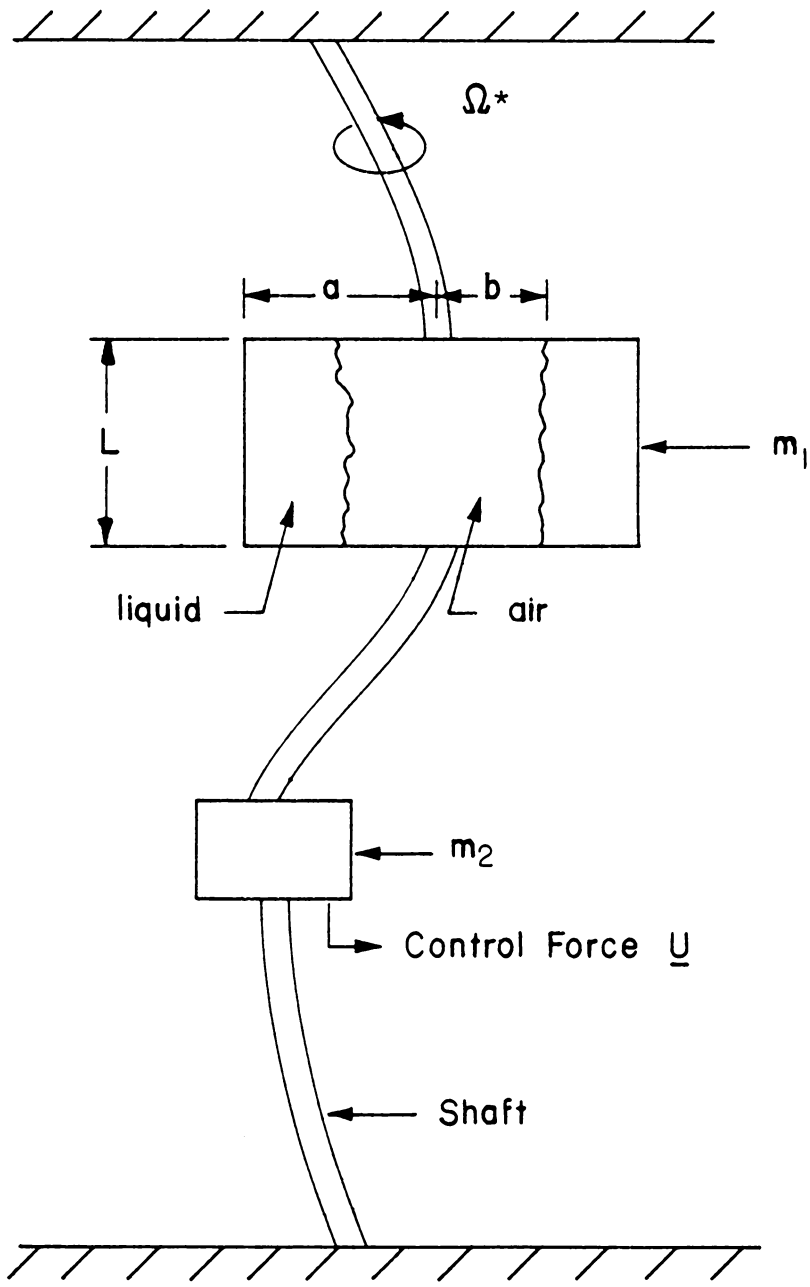

FIGURE 1.8. TWO-MASS ROTOR

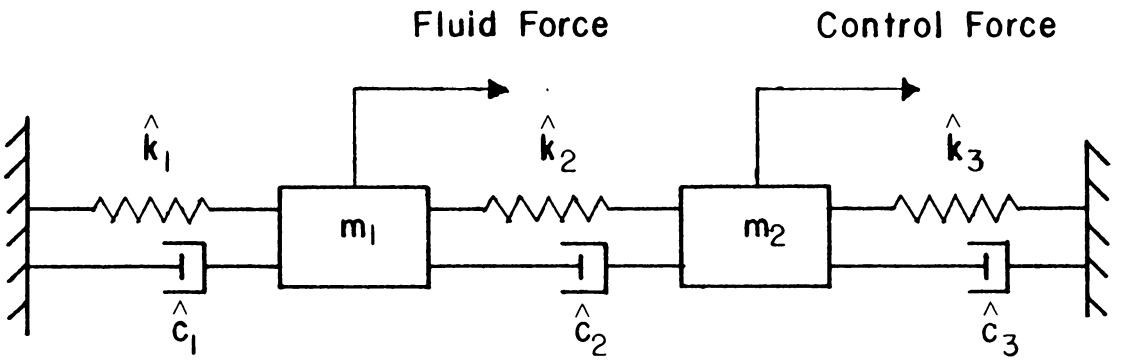

FIGURE 1.9. EQUIVALENT TWO-MASS ROTOR MODEL

development of a continuous mass rotor theory (see Figure 1.10). The methodology used in Chapter II and the resultant knowledge gleaned from it provide the foundation upon which this, the essence and ultimate objective of the present research is structured.

The solution development, presented in Chapter III, is similar to that of the earlier problem, modified by the inclusion of local and global rotations as well as a conversion to continuous rotor displacement coordinates.

In order to discretize the system and make it amenable to the solution techniques of Chapter II, the method of assumed modes (see reference [14], p. 293) is employed. Rotor deflection and rotation coordinates are expanded in a set of N admissible functions chosen from a complete set and substituted into the expressions for kinetic energy, Rayleigh dissipation function, potential energy, and generalized displacements of the Lagrangian formulation. Similar substitution for the base point acceleration in the Euler equation, followed by appropriate integration and variable elimination, yields a completely discretized set of 2N + 5 complex time dependent ordinary differential equations in 2N + 5 complex variables (plus, as before, the unknown control force.)

Subsequent transformation to state space results in a 4N + 10 order[1] system which is used, in conjunction with the performance index,

---

[1]Throughout this report "N" will denote the number of admissible functions. "n" will denote the total system order in state space (i.e., n = 4N + 10).

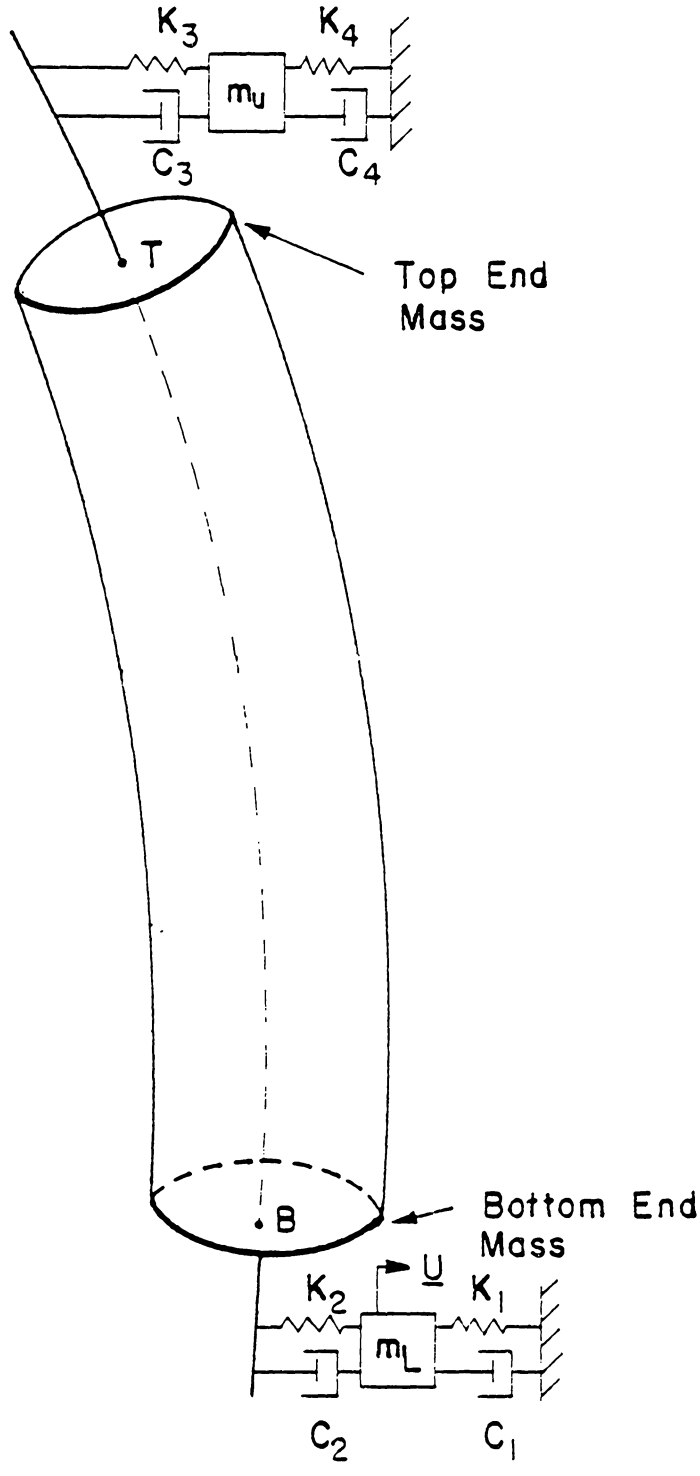

FIGURE 1.10. FLEXIBLE ROTOR MODEL

to pose the optimal feedback control problem. Solution methodology parallels that for the two mass system and results are presented in Sections 3.3 and 3.4.

1.3 SCOPE OF THE RESEARCH

A complete list of the assumptions employed, some mentioned previously, is given below.

(1) The fluid is ideal, i.e., incompressible and inviscid.

(2) Spring and damper forces are linearly related to displacements and velocities respectively.

(3) The fluid and rotor equations of motion are linearized. All second and higher order terms are ignored.

(4) The influence of gravity is considered negligible.

(5) Unbalance due to misalignment of the rotor center of mass from the axis of rotation can be readily corrected by standard dynamic balancing techniques and is therefore taken to be zero.

(6) Rotational modes for all discrete masses are ignored.

(7) Axial acceleration is assumed to be insignificant in the fluid equations.

CHAPTER II

TWO MASS ROTOR

2.1 GOVERNING EQUATIONS

This section generates the differential equations needed to analyze a two-mass rotor partially filled with an inviscid incompressible fluid. The equations are put in state space form by eliminating the spatial dependence of the fluid variable.

The basic system consists of a long, flexible shaft, two masses and a controller (Figure 1.8). The first mass is a hollow circular cup partially filled with an inviscid incompressible fluid. The second mass is mounted further down the shaft and the control force is applied to this mass.

To keep the system general the shaft is modeled as a series of springs and dampers placed between the two masses and between each mass and ground (Figure 1.9).

2.1.1 ROTOR EQUATIONS OF MOTION

The equations of motion for the rotor are written in rotating coordinates utilizing Lagrange's equations. The effect of the entrapped fluid and the controller enter as generalized forces.

Consider two coordinate systems (Figure 2.1): $\{\hat{\underline{N}}\}$ fixed in space (inertial); $\{\hat{\underline{n}}\}$ fixed in the cup (rotating with angular velocity Ω^*). Then

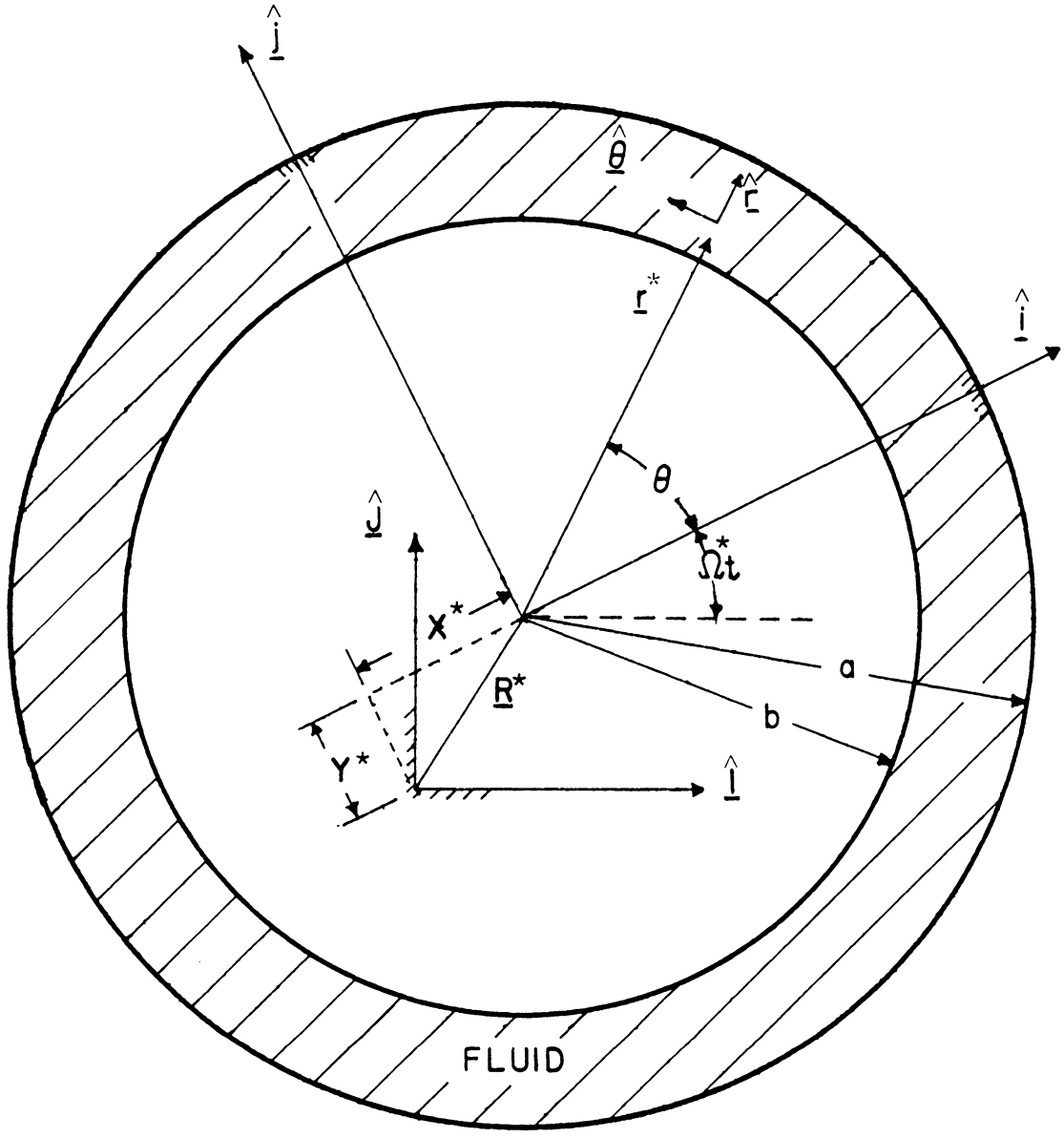

FIGURE 2.1. DEFINITION OF COORDINATE SYSTEMS (TOP VIEW)

$$\{\hat{\underline{n}}\} = \begin{Bmatrix} \hat{\underline{i}} \\ \hat{\underline{j}} \\ \hat{\underline{k}} \end{Bmatrix} = \begin{bmatrix} \cos\Omega^*t & \sin\Omega^*t & 0 \\ -\sin\Omega^*t & \cos\Omega^*t & 0 \\ 0 & 0 & 1 \end{bmatrix} \begin{Bmatrix} \hat{\underline{I}} \\ \hat{\underline{J}} \\ \hat{\underline{K}} \end{Bmatrix} \quad : \{\hat{\underline{N}}\} = \begin{Bmatrix} \hat{\underline{I}} \\ \hat{\underline{J}} \\ \hat{\underline{K}} \end{Bmatrix}. \quad (2.1)$$

The position, velocity, and acceleration of the center of mass 1 (the cup) relative to the inertial frame but expressed in the cup fixed coordinate system are:

$$\underline{R}_1^* = x_1\hat{\underline{i}} + y_1\hat{\underline{i}} \quad (2.2a)$$

$$\dot{\underline{R}}_1^* = (\dot{x}_1 - \Omega^* y_1)\hat{\underline{i}} + (\dot{y}_1 + \Omega^* x_1)\hat{\underline{j}} \quad (2.2b)$$

$$\ddot{\underline{R}}_1^* = (\ddot{x}_1 - 2\Omega^*\dot{y}_1 - \Omega^{*2}x_1)\hat{\underline{i}} + (\ddot{y}_1 + 2\Omega^*\dot{x}_1 - \Omega^{*2}y_1)\hat{\underline{j}} \quad (2.2c)$$

The inertial frame position and velocity of mass 2, measured in the same cup fixed axes are:

$$\underline{R}_2^* = x_2\hat{\underline{i}} + y_2\hat{\underline{i}} \quad (2.3a)$$

$$\dot{\underline{R}}_2^* = (\dot{x}_2 - \Omega^* y_2)\hat{\underline{i}} + (\dot{y}_2 + \Omega^* x_2)\hat{\underline{j}} \quad (2.3b)$$

$\underline{R}_1^*$ and $\underline{R}_2^*$ are the two mass system equivalents of the $\underline{R}^*$ vector depicted in Figures 1.1 and 1.3.

Recall that constancy of $\underline{R}_1^*$ and $\underline{R}_2^*$, as measured in the $\hat{\underline{i}}$-$\hat{\underline{j}}$-$\hat{\underline{k}}$ system, indicates static shaft flexure and hence synchronous whirl. If, however, $\underline{R}_1^*$ and $\underline{R}_2^*$ are not constant but rotate relative to the cup at a given frequency, then cyclic loading occurs at the same frequency and whirl is asynchronous. Growth without limit in the magnitude of these vectors indicates instability. The final time dependent form for x_1, y_1, x_2, and y_2 (part of the eventual solution) will reveal these

characteristics readily. The kinetic energy T, the dissipation function D, and the potential energy V are

$$T = \frac{1}{2} m_1[(\dot{x}_1-\Omega^* y_1)^2 + (\dot{y}_1+\Omega^* x_1)^2] + \frac{1}{2} m_2[(\dot{x}_2-\Omega^* y_2)^2 + (\dot{y}_2+\Omega^* x_2)^2] \tag{2.4a}$$

$$D = \frac{1}{2} \hat{c}_1[(\dot{x}_1-\Omega^* y_1)^2 + (\dot{y}_1+\Omega^* x_1)^2] + \frac{1}{2} \hat{c}_3[(\dot{x}_2-\Omega^* y_2)^2 + (\dot{y}_2+\Omega^* x_2)^2]$$

$$+ \frac{1}{2} \hat{c}_2[(\dot{x}_2-\dot{x}_1-\Omega^* y_2+\Omega^* y_1)^2 + (\dot{y}_2-\dot{y}_1+\Omega^* x_2-\Omega^* x_1)^2] \tag{2.4b}$$

$$V = \frac{1}{2} \hat{k}_1(x_1^2+y_1^2) + \frac{1}{2} \hat{k}_3(x_2^2+y_2^2) + \frac{1}{2} \hat{k}_2[(x_1-x_2)^2 + (y_1-y_2)^2]. \tag{2.4c}$$

The control force $\underline{U}^*$

$$\underline{U}^* = U_x^*\hat{\underline{i}} + U_y^*\hat{\underline{j}} \text{ is applied at } \underline{R}_2^*. \tag{2.5}$$

The entrapped fluid pressure $\hat{P}(r^*,\theta,t)$ creates a normal force distributed over the cylinder wall (Figure 2.2):

$$d\underline{F}_{f1} = \hat{P}(r^*=a,\theta,t)ad\theta dz[\cos\theta\hat{\underline{i}} + \sin\theta\hat{\underline{j}}] \tag{2.6a}$$

applied at

$$\underline{R}_{f1}^* = \underline{R}_1^* + a[\cos\theta\hat{\underline{i}} + \sin\theta\hat{\underline{j}}] + z\hat{\underline{k}}. \tag{2.6b}$$

To enter the equations of motion the fluid force will be integrated over the wall of the cylinder.

To develop the equations of motion, Lagrange's equation for each of the generalized coordinates is employed,

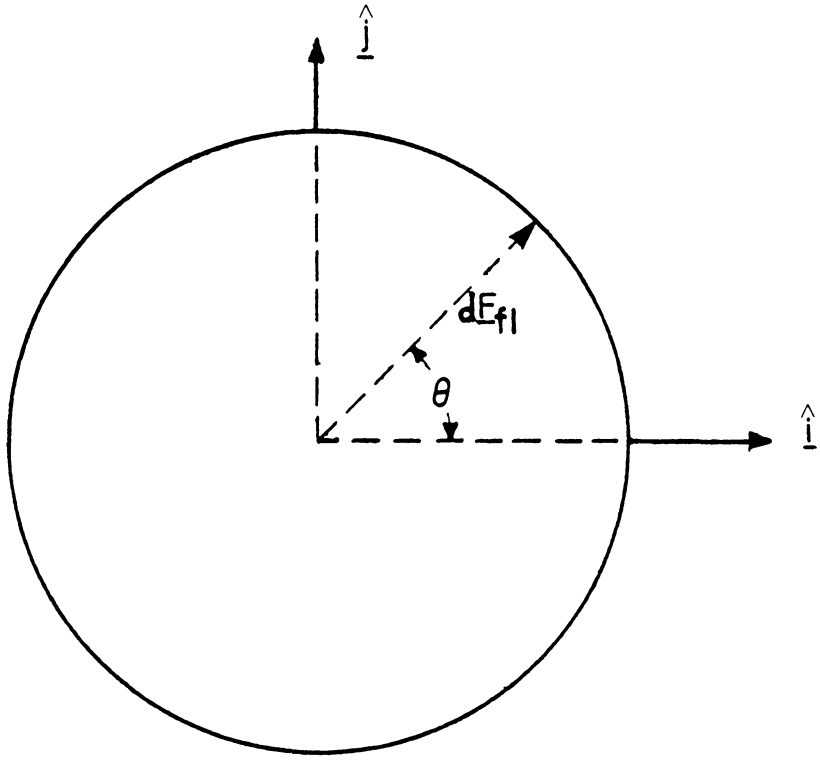

FIGURE 2.2. APPLICATION OF FLUID FORCE

$$\frac{d}{dt}\left(\frac{\partial T}{\partial \dot{q}}\right) - \frac{\partial T}{\partial q} + \frac{\partial D}{\partial \dot{q}} + \frac{\partial V}{\partial q} = \frac{\partial \underline{R}_2^*}{\partial q} \cdot \underline{U}^* + \int_0^L \int_0^{2\pi} \frac{\partial \underline{R}_1^*}{\partial q} \cdot d\underline{F}_{f1} \qquad (2.7)$$

where it is noted that $\frac{\partial \underline{R}_{f1}^*}{\partial q} = \frac{\partial \underline{R}_1^*}{\partial q}$ since q is respectively x_1, x_2, y_1, y_2.

In order to generalize the solution to systems of arbitrary size, it will prove useful to nondimensionalize the problem with

m_1 = mass of the empty cup

a = radius of the cup inner surface

$\omega_o = (\hat{k}_1/m_1)^{1/2}$

as the characteristic mass, length, and frequency (reciprocal of characteristic time). This gives rise to the following nondimensional terms:[1]

$$m = m_2/m_1 \qquad \underline{R}_1 = \underline{R}_1^*/a$$
$$c_1 = \hat{c}_1/2m_1\omega_o \qquad \underline{R}_2 = \underline{R}_2^*/a$$
$$c_2 = \hat{c}_2/2m_1\omega_o \qquad f = b/a$$
$$c_3 = \hat{c}_3/2m_1\omega_o \qquad \Omega = \Omega^*/\omega_o$$
$$k_1 = \hat{k}_1/m_1\omega_o^2 = 1 \qquad \mu = \pi\rho a^2 L/m_1 \qquad (2.8)$$
$$k_2 = \hat{k}_2/m_1\omega_o^2 \qquad \eta_1 = (x_1 - iy_1)/a$$
$$k_3 = \hat{k}_3/m_1\omega_o^2 \qquad \eta_2 = (x_2 - iy_2)/a$$
$$r = r^*/a \qquad \phi = (U_x^* - iU_y^*)/m_1 a\omega_o^2$$

---

[1]Note that the symbols"*" or "^" are used above a quantity to denote that it is dimensional. For example R_1^*, $\hat{P}$ are dimensional, R_1, P are nondimensional.

$z_o = L/a$ $\qquad\qquad$ $P(r,\theta,t) = \hat{P}(r,\theta,t)a/m_1\omega_o^2$

where ρ is fluid density, nondimensional cup mass is unity, and μ is the nondimensional fluid density.

As the rotor equations are written more succinctly in complex form, three complex quantities have been introduced:

η_1 gives the displacement of mass 1

η_2 gives the displacement of mass 2

ϕ is the complex control force.

These quantities may be interpreted as follows:

$\underline{R}_1 = \text{real } (\eta_1)\hat{\underline{i}} - \text{imag } (\eta_1)\hat{\underline{j}}$

$\underline{R}_2 = \text{real } (\eta_1)\hat{\underline{i}} - \text{imag } (\eta_2)\hat{\underline{j}}$

$\underline{U} = \text{real } (\phi)\hat{\underline{i}} - \text{imag } (\phi)\hat{\underline{j}}$

where $\underline{R}_1$, $\underline{R}_2$, and $\underline{U}$ are the nondimensional equivalents of equations (2.2a), (2.3a) and (2.5).

The pressure $\hat{P}$ (which appears in the fluid force) is in general a function of (θ,z,r^*,t). In this application, however, the cup will not be allowed to tilt, so the fluid will be uniform in the z direction (thus two dimensional). To conform with the other terms in the equations of motion, pressure must be recast in nondimensional complex form. This follows, but as several different "kinds" (real or complex, physical or nondimensional, total or partial, etc.) of pressure are

considered, the reader may care to make frequent reference to the list of symbols at the beginning.[1]

The θ dependence of the real physical pressure $\hat{P}(r^*,\theta,t)$ can be expanded in a complex Fourier series as

$$\hat{P}(r^*,\theta,t) = \mathrm{Re}\{\sum_{n=0}^{\infty} \hat{P}_n(r^*,t)e^{in\theta}\} \tag{2.10a}$$

where

$$\hat{P}_n(r^*,t) = \hat{P}_{n_{re}}(r^*,t) + i\hat{P}_{n_{im}}(r^*,t) \tag{2.10b}$$

so that

$$\hat{P}(r^*,\theta,t) = \sum_{n=0}^{\infty} (\hat{P}_{n_{re}}(r^*,t)\cos(n\theta) - \hat{P}_{n_{im}}(r^*,t)\sin(n\theta)) \tag{2.10c}$$

When $\hat{P}(r^*,\theta,t)$, so expressed, is inserted in (2.6a) and the resulting wall force $d\underline{F}_{fl}$ used in the Lagrange equation (2.7), all terms with $n\neq 1$ integrate to zero, proving that only $\hat{P}_1(r^*,t)e^{i\theta}$ can affect the motion of the rotor. (This and much of what remains in this section is carried out in greater detail in Appendix A.) Thus, for this analysis, pressure can be regarded as simply equal to the real part of $\hat{P}(r^*,t)e^{i\theta}$, where for simplicity $\hat{P}(r^*,t)$ is now used in place of

---

[1]Note carefully that, in the notation employed, the same symbol used with different arguments can represent different quantities. For instance $\hat{P}(r^*,\theta,t)$ is not the same as $\hat{P}(r^*,t)$. Arguments will be retained in all cases where any ambiquity might otherwise result.

$\hat{P}_1(r^*,t)$. Note that, as shown in Appendix A, this is compatible with a physical interpretation of the components in the series expansion.

The dimensionless pressure becomes

$$P(r,\theta,t) = Re\{\hat{P}(r,t)e^{i\theta}\ a/m_1\omega_o^2\} = Re\{P(r,t)e^{i\theta}\} \qquad (2.10d)$$

where $P(r,t) = \hat{P}(r,t)e^{i\theta}a/m_1\omega_o^2$ evaluated at $r = 1$ will be of relevance here. For future reference, it will be well to remember that $P_{re}(r,t)$ is the value of dimensionless pressure at $\theta = 0^0$, while $P_{im}(r,t)$ is that at $\theta = -90^0$ (see again, Appendix A).

Using all real, physical quantities in Lagrange's equations (2.7), working through the algebra, and reformulating the result in nondimensional complex form, one finds the equations of motion for this rotor are:

$$\begin{bmatrix} 1 & 0 \\ 0 & m \end{bmatrix} \begin{Bmatrix} \ddot{\eta}_1 \\ \ddot{\eta}_2 \end{Bmatrix} + \begin{bmatrix} 2(c_1+c_2-i\Omega) & -2c_2 \\ -2c_2 & 2(c_2+c_3 - im\Omega) \end{bmatrix} \begin{Bmatrix} \dot{\eta}_1 \\ \dot{\eta}_2 \end{Bmatrix}$$

$$+ \begin{bmatrix} 1 + k_2-\Omega^2-2i\Omega(c_1+c_2) & -k_2+2i\Omega c_2 \\ -k_2+2i\Omega c_2 & k_2+k_3-m\Omega^2-2i\Omega(c_2+c_3) \end{bmatrix} \begin{Bmatrix} \eta_1 \\ \eta_2 \end{Bmatrix}$$

$$= \begin{Bmatrix} \pi z_o\ P(r=1,t) \\ \psi \end{Bmatrix} \qquad (2.11)$$

2.1.2 FLUID EQUATIONS OF MOTION

The cup fixed coordinate system most readily facilitates application of the fluid boundary conditions. For this reason it is chosen both as the reference frame relative to which the vector equations of motion are written and as the coordinate system in which the scalar components of the vectors are expressed.

Since the fluid is incompressible and inviscid, the pertinent equations are Euler's equation (conservation of momentum) and the continuity equation (conservation of mass). In terms of real physical quantities they are

$$\dot{\underline{q}} + (\underline{\nabla}\cdot\underline{q})\underline{q} + (\Omega^*)^2\hat{\underline{k}} \times (\hat{\underline{k}} \times \underline{r}^*) + 2\Omega^*\hat{\underline{k}} \times \underline{q} + \ddot{\underline{R}}_1^* + \frac{1}{\rho}\nabla\hat{P}(r^*,\theta,t)=0 \tag{2.12a}$$

$$\underline{\nabla} \cdot \underline{q} = 0 \tag{2.12b}$$

where $\underline{q} = \underline{q}(r^*,\theta,t)$ is the real physical fluid velocity relative to the cup and $\hat{P}(r^*,\theta,t)$ is the total real physical pressure.

The first five terms in equation (2.12a) equal the total inertial acceleration experienced by a fluid particle. The initial two represent the local (cup fixed) Eulerian acceleration where the second of these, the convective part, is second order and is ignored in the linear treatment that follows. The third and fourth terms are the normal and Coriolus accelerations that appear because the equation is formulated in a rotating (cup fixed) reference frame. The fifth term (see equation 2.2c), arising because the cup moves laterally, is the inertial acceleration of the origin of the cup fixed axes. It serves to couple

the rotor motion into the fluid motion. The final term is the usual pressure term.

To nondimensionalize equations (2.12a,b), partially separate variables, and incorporate complex notation, the following representations are introduced:

$$\hat{P}(r^*,\theta,t)=\frac{1}{2}\rho(\Omega^*)^2(r^{*2}-b^2)+\mathrm{Re}\{\sum_{n=0}^{\infty}P_n(r,t)e^{in\theta}\frac{m_1\omega_o^2}{a}\} \quad (2.13a)$$

$$\underline{q}=\mathrm{Re}\{\sum_{n=0}^{\infty}[(u_n(r,t)\hat{\underline{r}}+v_n(r,t)\hat{\underline{\theta}})e^{in\theta}\,a\omega_o]\} \quad (2.13b)$$

where $r = r^*/a$ $(0 < r < 1)$ is the nondimensional equivalent of r^*,

$$P_n(r,t) = P_{n_{re}}(r,t) + iP_{n_{im}}(r,t) \quad (2.13c)$$

$$u_n(r,t) = u_{n_{re}}(r,t) + iu_{n_{im}}(r,t) \quad (2.13d)$$

$$v_n(r,t) = v_{n_{re}}(r,t) + iV_{n_{im}}(r,t) \quad (2.13e)$$

are nondimensional complex scalar variables, and

$$\hat{\underline{r}} = \cos\theta\hat{\underline{i}} + \sin\theta\hat{\underline{j}} \quad (2.13f)$$

$$\hat{\underline{\theta}} = -\sin\theta\hat{\underline{i}} + \cos\theta\hat{\underline{j}} \quad (2.13g)$$

are unit vectors which point in the radial and azimuthal directions respectively (see Figure 2.1).[1]

The first term in (2.13a) is zeroth order and represents the pressure due to rigid body rotation of the cylinder. It arises solely as a result of the centrifugal acceleration and will be seen (in the derivation of equations (2.14), Appendix B1) to balance the third term (also zeroth order) in the momentum equation (2.12a).

The remaining terms in (2.13a) represent pressure contributions from surface perturbations (waves) which are assumed small (first order) relative to the first term. As shown in Appendices A and B, all but the n = 1 term have no effect on rotor motion and can be ignored.

Similarly, wave symmetries dictate that only the n = 1 term in the velocity expansion plays any role in influencing cup motion (see Appendices A2 and B1) and like pressure, the other velocity terms can be dropped.

Use of (2.13a,b) in (2.12a,b) yields the following linearized nondimensional complex fluid equations (the derivation can be found in Appendix B1):

$$\dot{u}(r,t) - 2\Omega v(r,t) + \frac{\pi z_o}{\mu}\frac{\partial P(r,t)}{\partial r} + (\ddot{\eta}_1 - 2i\Omega\dot{\eta}_1 - \Omega^2\eta_1) = 0 \quad (2.14a)$$

$$\dot{v}(r,t) + 2\Omega u(r,t) + \frac{i\pi z_o}{\mu r} P(r,t) + i(\ddot{\eta}_1 - 2i\Omega\dot{\eta}_1 - \Omega^2\eta_1) = 0 \quad (2.14b)$$

---

[1]Note carefully that, as before, function arguments are used to distinguish between different entities, e.g., $u_n(r,t)$ is not the same as $u_n(t)$. The list of symbols should help to avoid confusion.

$$\frac{u(r,t) + iv(r,t)}{r} + \frac{\partial u(r,t)}{\partial r} = 0 \qquad (2.14c)$$

where for simplicity the n = 1 subscripts have been dropped, i.e.,

$$P(r,t) = P_1(r,t) = P_{re}(r,t) + iP_{im}(r,t)$$
$$u(r,t) = u_1(r,t) = u_{re}(r,t) + iu_{im}(r,t)$$
$$v(r,t) = v_1(r,t) = v_{re}(r,t) + iv_{im}(r,t).$$

Note that the θ dependence has been eliminated by integrating from 0 to 2π.

Note also that $u_{re}(r,t)$ and $v_{re}(r,t)$ are respectively the real nondimensional values for the n = 1 normal and tangential fluid velocities at $\theta = 0°$; similarly, $u_{im}(r,t)$ and $v_{im}(r,t)$ are those at $\theta = -90°$. This is similar in form to the interpretations given to $P_{re}(r,t)$ and $P_{im}(r,t)$ in Appendix A3.

Three things remain to be done in this section: i) reduce the three differential equations (2.14) in P(r,t), u(r,t), and v(r,t) to one differential equation in u(r,t) and find the general solution, ii) apply the wall boundary condition to deduce the precise r dependence of u(r,t), and iii) use u(r,t) in the boundary condition at the free surface to eliminate the r dependence and accomodate the state space formulation of the equation of motion in terms of the single independent variable t (time). (This last step is a prerequisite for the application of optimal control theory.)

i) Finding the general solution u(r,t)

The third of equations (2.14) can be solved for v(r,t) and substituted into the second to yield

$$P(r,t) = \frac{\mu}{\pi z_o}\left[\left(2i\Omega r - r^2\frac{\partial^2}{\partial r\partial t} - r\frac{\partial}{\partial t}\right)u(r,t)\right.$$

$$\left. - r\left(\frac{\partial^2}{\partial t^2} - 2i\Omega\frac{\partial}{\partial t} - \Omega^2\right)\eta_1\right]. \qquad (2.15a)$$

Use of this in (2.14a) results in the following simple equation:

$$\frac{d}{dt}\left[3\frac{\partial}{\partial r} + \frac{\partial^2}{\partial r^2}\right]u(r,t) = 0. \qquad (2.15b)$$

This is solved by employing the standard separation of variables technique on u(r,t) (although the reader can verify the solution by simple substitution), so that

$$u(r,t) = u_1(t) + \frac{u_2(t)}{r^2} \qquad (2.16)$$

where $u_1(t)$ and $u_2(t)$ are, at this point, unknown functions not to be confused with the n = 1,2 terms of $u_n(r,t)$ used previously.

ii) Applying the wall boundary condition

At the cup wall, the no penetration boundary condition is

$$u(r=1,t) = 0. \qquad (2.17)$$

Making use of this in (2.16), one finds $u_1(t) = -u_2(t) = u(t)$ and

$$u(r,t) = u(t)\left[1 - \frac{1}{r^2}\right]. \qquad (2.18a)$$

Since u(t) turns out to be a fundamental dependent variable

employed in subsequent sections, it should be noted that at r = f the free surface normal wave velocity equals the normal fluid velocity u(f,t) and

$$u(t) = u(f,t)/[1 - \frac{1}{f^2}]. \qquad (2.18b)$$

As u(f,t) represents a sinusoidally varying wave, the amplitude of the function u(t) is, by (2.18b), equal to the amplitude of the wave velocity itself divided by $[1 - 1/f^2]$. Maximum u(t) is not, therefore, as one may later be tempted to think, simply equal to wave velocity amplitude.

iii) Eliminating r dependence in the free surface boundary condition

When a wave forms, the radial position of the fluid surface can be expressed as

$$r^* = b + \lambda^*(\theta,t) \qquad (2.19a)$$

or nondimensionally (by dividing (2.19a) by "a") as

$$r = f + \lambda(\theta,t) \qquad (2.19b)$$

where b and f represent the unperturbed (wave free) surface position and λ^* and λ represent a perturbation (wave).

At the free surface the pressure must be zero and the radial velocity of the wave must match the radial velocity of the fluid. Applying these conditions to (2.13a), one finds the linearized nondimensional boundary condition at the free surface is (see Appendix B2)

$$u(r=f,t) = -\frac{\pi z_o}{\mu \Omega^2 f} \hat{P}(r=f,t) \qquad (2.20)$$

The goal is to eliminate the r dependence and transform (2.20) into a second order equation in u(t). To this end the time derivative of (2.15a) at r = f is first evaluated using relation (2.18a). The result is then substituted along with (2.18a) into (2.20), producing:

$$[1 + \frac{1}{f^2}]\ddot{u}(t) - 2i\Omega[1 - \frac{1}{f^2}]\dot{u}(t) - \Omega^2[1 - \frac{1}{f^2}]u(t)$$

$$+ (\dddot{\eta}_1 - 2i\Omega\ddot{\eta}_1 - \Omega^2\dot{\eta}_1) = 0 \qquad (2.21)$$

Equation (2.21) is free of any dependence on r but it is third order in time. Reduction to second order is accomplished by using equation (2.15a) at r = 1 in the first of equations (2.11), taking the time derivative of the result, solving for $\ddot{\eta}_1'$, and using it in (2.21) (see Appendix B3). All terms then become second or lower order in time and the original fluid system has been reduced to one ordinary differential equation in three complex variables (the cup displacement η_1, the second mass displacement η_2, and a function u(t) which is proportional to free surface wave velocity).

The equation is

$$- 2(c_1 + c_2)\ddot{\eta}_1 + 2c_2\ddot{\eta}_2 + (1 - \mu + \frac{1}{f^2}[1 + \mu])\ddot{u}$$

$$+ (-1 - k_2 + 2i\Omega[c_1 + c_2])\dot{\eta}_1 + (k_2 - 2i\Omega c_2)\dot{\eta}_2 - 2i\Omega(1 - \frac{1}{f^2})(1 + \mu)\dot{u}$$

$$- \Omega^2(1 - \frac{1}{f^2})(1 + \mu)u = 0 \qquad (2.22)$$

where from here on the symbol "u" stands for what has previously been "u(t)".

2.1.3 COMBINED ROTOR FLUID EQUATIONS

Equations (2.11) and (2.22) can be combined into the single complex matrix equation

$$[M"]\{\ddot{Z}\} + [C"]\{\dot{Z}\} + [K"]\{Z\} = \phi \begin{Bmatrix} 0 \\ 1 \\ 0 \end{Bmatrix} \qquad (2.23)$$

where

$$\{Z\} = \begin{Bmatrix} \eta_1 \\ \eta_2 \\ u \end{Bmatrix}; \quad [M"] = \begin{bmatrix} 1+\mu & 0 & 0 \\ 0 & m & 0 \\ -2(c_1+c_2) & 2c_2 & (1 - \mu + \frac{1}{f^2}[1+\mu]) \end{bmatrix}$$

$$[C"] = \begin{bmatrix} -2(c_1+c_2-i\Omega[1+\mu]) & -2c_2 & 2\mu \\ -2c_2 & 2(c_2+c_3-i\Omega m) & 0 \\ -1-k_2+2i\Omega(c_1+c_2) & k_2-2i\Omega c_2 & -2i\Omega(1 - \frac{1}{f^2})(1+\mu) \end{bmatrix}$$

$$[K"] = \begin{bmatrix} 1+k_2-\Omega^2(1+\mu)-2i\Omega(c_1+c_2) & -k_2+2i\Omega c_2 & 0 \\ -k_2+2i\Omega c_2 & k_2+k_3-m\Omega^2-2i\Omega(c_2+c_3) & 0 \\ 0 & 0 & -\Omega^2(1 - \frac{1}{f^2})(1+\mu) \end{bmatrix}$$

2.1.4 STATE SPACE FORMULATION

By premultiplying (2.23) by $[M"]^{-1}$ (hereafter called [D]), the three second-order equations (2.23) can be replaced by six first-order equations in the following form:

$$\{\dot{Y}\} = [A]\{Y\} + \phi\{E\} \tag{2.24}$$

where

$$\{Y\} = \begin{Bmatrix} \eta_1 \\ \eta_2 \\ u \\ \dot{\eta}_1 \\ \dot{\eta}_2 \\ \dot{u} \end{Bmatrix} \quad ; \quad \{E\} = \begin{Bmatrix} 0 \\ 0 \\ 0 \\ 0 \\ 1/m \\ -2c_2 f^2/([1+\mu-f^2(1-\mu)]m) \end{Bmatrix}$$

$$[A] = \begin{bmatrix} [0] & [I] \\ -[D][K"] & -[D][C"] \end{bmatrix}$$

$$[D] = \frac{f^2}{2[(1+\mu)^2+(1-\mu^2)f^2]} \begin{bmatrix} 2(1-\mu+\frac{1}{f^2}[1+\mu]) & 0 & 0 \\ 0 & \frac{2}{m}(1-\mu^2+\frac{1}{f^2}[1+\mu]^2) & 0 \\ 4(c_1+c_2) & -4c_2(1+\mu)/m & 2(1+\mu) \end{bmatrix}$$

Equation (2.24) is the desired state space form of the equations which can be applied directly to an optimal control law.

The following list summarizes the important nondimensional parameters that control this system:

$m = m_2/m_1$ = mass ratio

$\mu = \pi\rho a^2 L/m_1$ = fluid density

$\Omega = \Omega^*/\omega_o$ = spin speed

$f = b/a$ = fill ratio

c_1, c_2, c_3 = damping coefficients

k_2, k_3 = stiffness coefficients

2.2 OPTIMAL CONTROL PROBLEM

Two different approaches to the control problem were considered. The first, the classical optimal theory method, is described in detail in subsequent sections. The second, developed by Meirovitch, $\ddot{Oz}$, and Baruh, is presented in detail in references [15] and [16]. It makes extensive use of the concept of vibration mode independence, reaping considerable computational benefit from the uncoupling of the equations of motion in modal space. In decoupled form the equations can be solved separately resulting in controls which are first determined in the modal space. These controls are then transformed to configuration space to obtain the physical feedback inputs required.

The independent modal space control (IMSC) approach can be very advantageous for large order systems (100 or more degrees of freedom) where size and coupling lead to severe computational difficulties. However, as pointed out in the aforementioned references, it does require a separate physical force input for every mode controlled. For instance, if the ten lowest modes are to be controlled, then ten feedback forces would have to be applied at ten separate locations.

While IMSC has unquestioned potential for application in areas such as large scale spacecraft control, it turns out to be less suitable for the problem at hand. The present chapter deals with only a six degree of freedom system and Chapter III with no more than twenty six. In actual practice this number may go higher, but it should never exceed 50 or 60. The classical control approach in conjunction with the solution technique described in Section 2.2.2 has little numerical difficulty in solving problems of this order. In addition, it requires only one feedback force. If the system analyzed herein can in fact be controlled with a single input, hardware savings alone would dictate choice of the classical method. For these reasons, it is the one selected for use here.

2.2.1 FEEDBACK CONTROL EQUATIONS

In the previous section the differential equations which describe the motion of a two mass flexible rotor partially filled with an inviscid incompressible fluid were expressed via the state space formulation. These equations have the form

$$\{\dot{Y}\} = [A]\{Y\} + \psi\{E\} \tag{2.25}$$

where ψ is the complex scalar control force, in general a function of time, which is to be determined so that the system will be stable.

The following performance index, only one of many possible indices, is chosen:

$$J = \frac{1}{2}\int_0^{t_f} [\{Y^\dagger\}^T[Q]\{Y\} + \psi^\dagger R\psi]dt \tag{2.26}$$

where

t_f is final time,

[Q] is a positive definite hermitian weighting matrix,

R is a positive weighting scalar, and

$\dagger$ denotes the complex conjugate of a quantity.

[Q] and R can be varied to emphasize different aspects of the performance index[1]. ψ is to be determined so that J will be a minimum. Thus ψ will be an "optimal" control for this performance index.[2]

To find ψ, the Hamiltonian is constructed:

---

[1]The positive definite hermitian character for both weighting parameters is needed to insure that both terms inside the integrand of (2.26) are penalized in the same directions, i.e., that both control force and state vector are denied large values. If, for instance, R were negative here, {Y} would be minimized and ψ would be maximized, hardly a desirable situation. (To be precise, [Q] need only be positive semi-definite. R, since it appears later in the denominator of the expression for the control force, must, however, be non-zero.)

[2]The control problem as posed here is often referred to as the "linear regulator problem".

$$H = \frac{1}{2}\{Y^{\dagger}\}^{T}[Q]\{Y\} + \frac{\psi^{\dagger}R\psi}{2} + \{\lambda^{\dagger}\}^{T}([A]\{Y\} + \psi\{E\}) \qquad (2.27)$$

where $\{\lambda^{\dagger}\}^{T}$ are Lagrange multipliers, in general functions of time, and $\{\lambda\}$ are their complex conjugate transposes (the system costate variables). The necessary conditions for optimal control are then

$$\{\dot{\lambda}^{\dagger}\}^{T} = -\frac{\partial H}{\partial\{Y\}} = -\{Y^{\dagger}\}^{T}[Q] - \{\lambda^{\dagger}\}^{T}[A] \qquad (2.28a)$$

$$0 = \frac{\partial H}{\partial\psi} = \psi^{\dagger}R + \{\lambda^{\dagger}\}^{T}\{E\}. \qquad (2.28b)$$

A derivation of these relationships can be found in Appendix C. Solving equation (2.28b) for ψ yields

$$\psi = -\frac{\{\lambda\}^{T}\{E^{\dagger}\}}{R^{\dagger}} = -\frac{\{E^{\dagger}\}^{T}\{\lambda\}}{R}. \qquad (2.29)$$

With equation (2.29), equation (2.25) becomes

$$\dot{\{Y\}} = [A]\{Y\} - \frac{1}{R}\{E\}\{E^{\dagger}\}^{T}\{\lambda\}. \qquad (2.30)$$

Equation (2.30) and the complex conjugate transpose of equation (2.28a) can then be written as

$$\begin{Bmatrix} \dot{\{Y\}} \\ \dot{\{\lambda\}} \end{Bmatrix} = \begin{bmatrix} [A] & -\frac{1}{R}\{E\}\{E^{\dagger}\}^{T} \\ -[Q] & -[A^{\dagger}]^{T} \end{bmatrix} \begin{Bmatrix} \{Y\} \\ \{\lambda\} \end{Bmatrix}. \qquad (2.31)$$

The solution of equation (2.31) is

$$\begin{Bmatrix} \{Y(t_f)\} \\ \{\lambda(t_f)\} \end{Bmatrix} = [\phi(t_f,t)] \begin{Bmatrix} \{Y(t)\} \\ \{\lambda(t)\} \end{Bmatrix} \qquad (2.32)$$

where

$$[\phi(t_f,t)] = \begin{bmatrix} [\phi_{11}(t_f,t)] & [\phi_{12}(t_f,t)] \\ [\phi_{21}(t_f,t)] & [\phi_{22}(t_f,t)] \end{bmatrix} \tag{2.33}$$

is the state transition matrix.

The final boundary condition on the costate variable vector emerges from the same variational treatment used to generate equations (2.28) (see (c.9) in Appendix C). For the performance index chosen this is

$$\{\lambda(t_f)\} = \{0\}. \tag{2.34}$$

With this the second half of equation (2.32) can be solved for the feedback form of the costate variables

$$\{\lambda(t)\} = -[\phi_{22}]^{-1}[\phi_{21}]\{Y(t)\} = [K(t)]\{Y(t)\} \tag{2.35}$$

where from now on $[K(t)]$ denotes $[K(t_f,t)]$. Note that if the $[K(t)]$ matrix can be determined, then by equations (2.29) and (2.35), the control is

$$\psi = -\frac{1}{R}\{E^\dagger\}^T[K(t)]\{Y(t)\} \tag{2.36}$$

and all that remains is to find $[K(t)]$.

To this end equation (2.35) is differentiated and used in the complex conjugate of equation (2.28a), resulting in

$$[\dot{K}(t)]\{Y(t)\} + [K(t)]\{\dot{Y}(t)\} = -[Q]\{Y(t)\} + [A^\dagger]^T\{\lambda\}. \tag{2.37}$$

Insertion of (2.30) for $\{\dot{Y}(t)\}$ and (2.35) for $\{\lambda\}$, along with cancellation of $\{Y(t)\}$ produces, after minor rearrangement, the matrix

Riccati equation

$$[\dot{K}(t)] = - [K(t)][A] - [A^{\dagger}]^{T}[K(t)] - [Q] + [K(t)]\{E\}\{E^{\dagger}\}^{T}[K(t)]/R \ . \tag{2.38}$$

From (2.32) at $t = t_f$, $[\phi(t_f,t_f)] = [I]_{2nx2n}$, the identity matrix. Therefore $[\phi_{22}(t_f,t_f)] = [I]_{nxn}$ and $[\phi_{21}(t_f,t_f)] = [0]_{nxn}$. From the definition of $[K(t)]$ implicit in (2.35),

$$[K(t_f)] = - [\phi_{22}(t_f,t_f)]^{-1}[\phi_{21}(t_f,t_f)]$$

and the final boundary condition associated with (2.38) is

$$[K(t_f)] = [0] \tag{2.39}$$

Solving (2.38) for $[K(t)]$, subject to (2.39), then determines the feedback control force ψ.

2.2.2 RICCATI EQUATION SOLUTION TECHNIQUE

Attempts at direct integration of the matrix Riccati equation (2.38) for systems of order comparable to that of the present chapter lead to numerical difficulties. A number of different integration schemes for the problem at hand were tried, all without success.

The steady state approach ($[\dot{K}(t)] = [0]$ in (2.38)) proves more tractable and leads to a solution which does in fact control the system. Justification for accepting this as a suitable solution is presented in Appendix D1. There it is shown that the assumption of steady state control gain is equivalent to taking final time, t_f, as approaching infinity. This is a common practice in control

applications, and it is adopted here. The performance index is thus modified slightly to

$$J = \lim_{t_f \to \infty} \frac{1}{2} \int_0^{t_f} [\{Y^\dagger\}^T [Q] \{Y\} + \phi^\dagger R \phi] dt.$$

The control force will then be optimal for the case of very large t_f. As discussed in Appendix D1 this will even be an extremely good approximation for t_f of all but the smallest magnitudes.

The same appendix justifies two other significant conditions on the Riccati equation solution (steady state or time dependent) which are necessary if [K(t)] is to solve the given problem. They are:

(1) [K(t)] is hermitian

(2) [K(t)] is positive definite.

Note that solutions to the Riccati equation exist which do not satisfy (2). However, only the one which does will result in a correct solution to the optimal control problem as posed.

At least two different approaches to solving the algebraic (steady state) matrix Riccati equation are available. The first, a Newton-Raphson iterative technique, entails about as many numerical roadblocks as does integration. The second, a method apparently first proposed by Potter [20], proves to be superior, being non-iterative and possessing the highly desirable attributes of ease and accuracy. For these reasons Potter's method is used here.

A proof of Potter's method, highlighting the salient points, is

presented in Appendix D2. The pertinent steps for applying the technique are given below.

Consider the steady state algebraic Riccati equation where, all coefficient matrices are constant in time (i.e., an autonomous system).[1]

$$[0] = -[K][A] - [A^{\dagger}]^{T}[K] - [Q] + [K]\{E\}\{E^{\dagger}\}^{T}[K]/R. \quad (2.40)$$

For the method presented, $[Q]$ and $\{E\}\{E^{\dagger}\}^{T}/R$ are assumed to be positive definite hermitian.[2]

The solution steps are:

1. From the nxn matrices used in (2.40) construct the following 2nx2n matrix

$$[M] = \begin{bmatrix} [A^{\dagger}]^{T} & [Q] \\ \{E\}\{E^{\dagger}\}^{T}/R & -[A] \end{bmatrix} \quad (2.41)$$

2. Find the eigenvalues and eigenvectors of $[M]$. Note: i) for this matrix, if $\Lambda_j = \Lambda_{re} + i\Lambda_{im}$ is an eigenvalue, then so is $-\Lambda_j^{\dagger} = -\Lambda_{re} + i\Lambda_{im}$, ii) it is not necessary to normalize the eigenvectors, iii) the following notation is introduced:

If $\{a\} = \left\{ \begin{matrix} \{b\} \\ --- \\ \{c\} \end{matrix} \right\}$ is a 2n dimensional

eigenvector of $[M]$, the n dimensional vectors $\{b\}$ and $\{c\}$ represent,

---

[1]Since, under these conditions, $[K(t)]$ is not a function of time, the notation $[K]$ will be used to indicate constant $[K(t)]$.

[2]In practical application $[Q]$ is almost invariably a diagonal matrix with positive real components.

respectively, the top and bottom halves of that vector. There will be 2n eigenvectors of the form

$$\{a\} = \begin{Bmatrix} \{b\} \\ \hline \{c\} \end{Bmatrix} .$$

3. Discard the n eigenvectors whose associated eigenvalues have negative real parts.

4. From the n eigenvectors that are left, construct the 2n x n matrix

$$[P] = \begin{bmatrix} \{b_1\} \ \{b_2\} \ldots \{b_n\} \\ \hline \{c_1\} \ \{c_2\} \ldots \{c_n\} \end{bmatrix}$$

Note: columns of [P] can be in any order without affecting the solution.

5. Find the inverse of $[\{c_1\}, \{c_2\}, \ldots, \{c_n\}]$

6. The solution is then:

$$[K] = [\{b_1\}, \{b_2\}, \ldots, \{b_n\}][\{c_1\}, \{c_2\}, \ldots \{c_1\}]^{-1} \qquad (2.42)$$

It can be shown that equation (2.42) justifies note ii) of step 2 since $[\{c_1\}, \{c_2\}, \ldots, \{c_n\}]^{-1}$ contains the inverses of the normalization constants used in $[\{b_1\}, \{b_2\}, \ldots, \{b_n\}]$.

2.2.3 METHODOLOGY FOR CONTROL AND STABILITY DETERMINATION

At this point is may be beneficial to summarize the overall solution approach and review the final goal briefly.

Given a rotor containing fluid, such as the one described herein,

the equations governing its motion, free of any feedback control, can be expressed as

$$\{\dot{Y}\} = [A]\{Y\}. \tag{2.43}$$

This is simply equation (2.24) with $\psi = 0$.

To answer the question of stability for such a system, the evolution of the state vector $\{Y\}$ in time must be determined. Since the first two components of $\{Y\}$ represent the nondimensional equivalents of $\underline{R}_1^*$ and $\underline{R}_2^*$ respectively, exponentially explosive behavior of the state vector will indicate instability. Conversely, exponential decay characterizes asymptotic stability.

Assuming a solution of the form

$$\{Y(t)\} = e^{\lambda t}\{Y(t_o)\} \tag{2.44}$$

where λ and time, t, are nondimensional, one can convert (2.43) into the standard eigenvalue problem, i.e.,

$$\lambda\{Y(t)\} = [A]\{Y(t)\}. \tag{2.45}$$

This will lead to nondimensional complex eigenvalues of the form

$$\lambda_s = \lambda_{s_{re}} + i\lambda_{s_{im}}, \quad (s = 1,\ldots,n) \tag{2.46a}$$

where $\lambda_{s_{re}}$ and $\lambda_{s_{im}}$ are real numbers and n is equal to the order of [A].

The solution to (2.45) then becomes

$$\{Y(t)\} = \sum_{s=1}^{n} e^{\lambda_{s_{re}} t} e^{i\lambda_{s_{im}} t}\{Y_s(t_o)\}. \tag{2.47}$$

The largest $\lambda_{s_{re}}$ determines overall system stability. Positive values

for it indicate instability; negative values, stability; and the magnitude, the relative degree of either.[1]

If n were equal to 1, the system would have one degree of freedom (one $\underline{R}$ vector to the only mass and no fluid present) and λ_{im} would be the frequency with which the $\underline{R}$ vector rotates relative to the $\hat{\underline{i}}$-$\hat{\underline{j}}$ (rotor fixed) reference frame. This was implicit in the sample discussed in the introduction.[2] For $n > 1$ the motion is analogous though more complicated, since the state vector is then a summation of terms each having different time dependence.

The general procedure described above is used to determine stability of each of the centrifuge configurations found in this report. For the controlled system, the equations of motion take the form of (2.24) (repeated below)

$$\{\dot{Y}\} = [A]\{Y\} + \{E\}\phi. \tag{2.48}$$

From (2.36) this is seen to be

$$\{\dot{Y}\} = \left([A] - \frac{1}{R}\{E\}\{E^{\dagger}\}^{T}[K]\right)\{Y\}, \tag{2.49a}$$

or, notationally simplified,

$$\{\dot{Y}\} = [A_c]\{Y\}. \tag{2.49b}$$

---

[1]All $\lambda_{s_{re}}$'s must be negative for stability. If any one is positive, the system is unstable.

[2]Note that λ_{im} here equals the negative of the whirl speed γ (nondimensionalized). This is a result of the definition of the displacement as (x-iy)/a rather than (x+iy)/a.

Like the control free case this can be treated as an eigenvalue problem with the same interpretation given to the real and imaginary parts of the λ_s.[1]

If a given system is unstable without a control force, but can be stabilized with it, then it is controllable. Comparison of the respective λ_{re}'s indicates the degree of stability supplied.

An alternative procedure for numerically demonstrating stability is simply to integrate equations (2.43) and (2.49) subject to certain initial conditions (i.e., initial disturbances) and observe whether the state vector norm grows or diminishes in time. At any given spin speed, the two methods are essentially equivalent, though for graphic and self-checking reasons both are employed in this chapter. For comparing system behavior at different rotor velocities, however, the eigenvalue approach has a distinct advantage, since it permits the display of stability versus spin speed on a single plot.

The feedback force ϕ will be different for different performance indices of course. It will also vary with time (even for a steady state, i.e., constant [K] matrix) since it depends on the state vector $\{Y(t)\}$ (see equation (2.36)).

---

[1]For a summary of the number of distinct eigenvalues to be found in the complex formulation of a system with symmetry such as that found here, see Appendix E.

The immediate goal is therefore twofold:

i) evaluate stability for the controlled and uncontrolled systems. (This can be done by finding the eigenvalues or equivalently, the state vector time dependence),

ii) determine the control force ψ (for a given performance index).

In addition, it may be of value to know the system gains. In this context "gain" refers to the contribution to the control force ψ made by a single state vector component with numerical value unity. More specifically, if (2.36) is rewritten as

$$\psi = \{G\}^T\{Y(t)\}, \tag{2.50}$$

the components of $\{G\}$ are the gains.

2.3 NONDIMENSIONAL NUMERICAL RESULTS

The results of the nondimensional optimal control analysis for a specific two mass system are presented in three parts: system stability, system gains, and feedback control force. In all of these the following parameter values are used:

$R = 100.$

$[Q] = [I]$

$k_2, k_3 = 5.0, 1.0$

$c_1, c_2, c_3 = .1, .2, .3$

$f = .8$

$m = .7$

$\mu = .5$

$\Omega = 1.5$ (when spin speed is not an axis variable)

Additional sections compare the effects of different weighting factors (R = 1.0 vs. R = 100.) and investigate stability and feedback force at different spin speeds

($\Omega = 0.5$ vs $\Omega = 1.5$).

The following outline summarizes the arrangement of the results:

For R = 100, $\Omega = 1.5$

2.3.1 System Stability

Figure 2.3: Maximum Real Part of All Eigenvalues vs Spin Speed (Controlled and Uncontrolled)

Figure 2.4-2.6: Uncontrolled State Vector Components vs Time

Figures 2.7-2.8: Polar Plots[1] of Uncontrolled Mass Displacements

Figures 2.9-2.11: Controlled State Vector Components vs Time

Figures 2.12-2.13: Polar Plots of Controlled Mass Displacements

2.3.2 System Gains

Figures 2.14-2.19: Gain for Each State Vector Component vs Spin Speed

2.3.3 Feedback Control Force

Figure 2.20: Control Force vs Time

---

[1]Polar plots are plots of x displacement vs y displacement with time as a parameter. Note that on all polar plots the final point in time is denoted by a small symbol, usually a triangle, and time progresses along the plot towards that point.

Figure 2.21: Polar Plot of Control Force

For R = 100, Ω = .5

2.3.4 Influence of Operating Speed

Figures 2.22-2.23: Uncontrolled State Vector Components vs Time (Compare with Figures 2.4-2.5)

Figures 2.24-2.25: Controlled State Vector Components vs Time (Compare with Figures 2.9-2.10)

Figures 2.26-2.27: Polar Plots of Controlled Mass Displacements (Compare with Figures 2.12-2.13).

Figure 2.28: Control Force vs Time (Compare with Figure 2.20)

Figure 2.29: Polar Plot of Control Force (Compare with Figure 2.21)

For R = 1.0, Ω = 1.5

2.3.5 Influence of Performance Index Weighting Factors

Figure 2.30: Maximum Real Part of all Eigenvalues vs Spin Speed (Compare with Figure 2.3)

Figures 2.31-2.32: Controlled State Vector Components vs Time (Compare with Figures 2.9-2.10)

Figures 2.33-2.34: Polar Plots of Controlled Mass Displacements (Compare with Figures 2.12-2.13)

Figure 2.35: Control Force vs Time (Compare with Figure 2.20)

Figure 2.36: Polar Plot of Control Force (Compare with Figure 2.21)

To facilitate comparison, all plots of controlled quantities have the same axis scaling even though other parameters may vary. The same internal consistency holds true for uncontrolled quantities. Note, however, that controlled and uncontrolled scalings are different.

All time dependent plots (that is all except Figures 2.3, 2.14-2.19, and 2.30) were generated by setting the initial (time = 0) x direction displacement of mass 1 equal to .01 and all other real and imaginary parts of the state vector equal to 0.

2.3.1 SYSTEM STABILITY

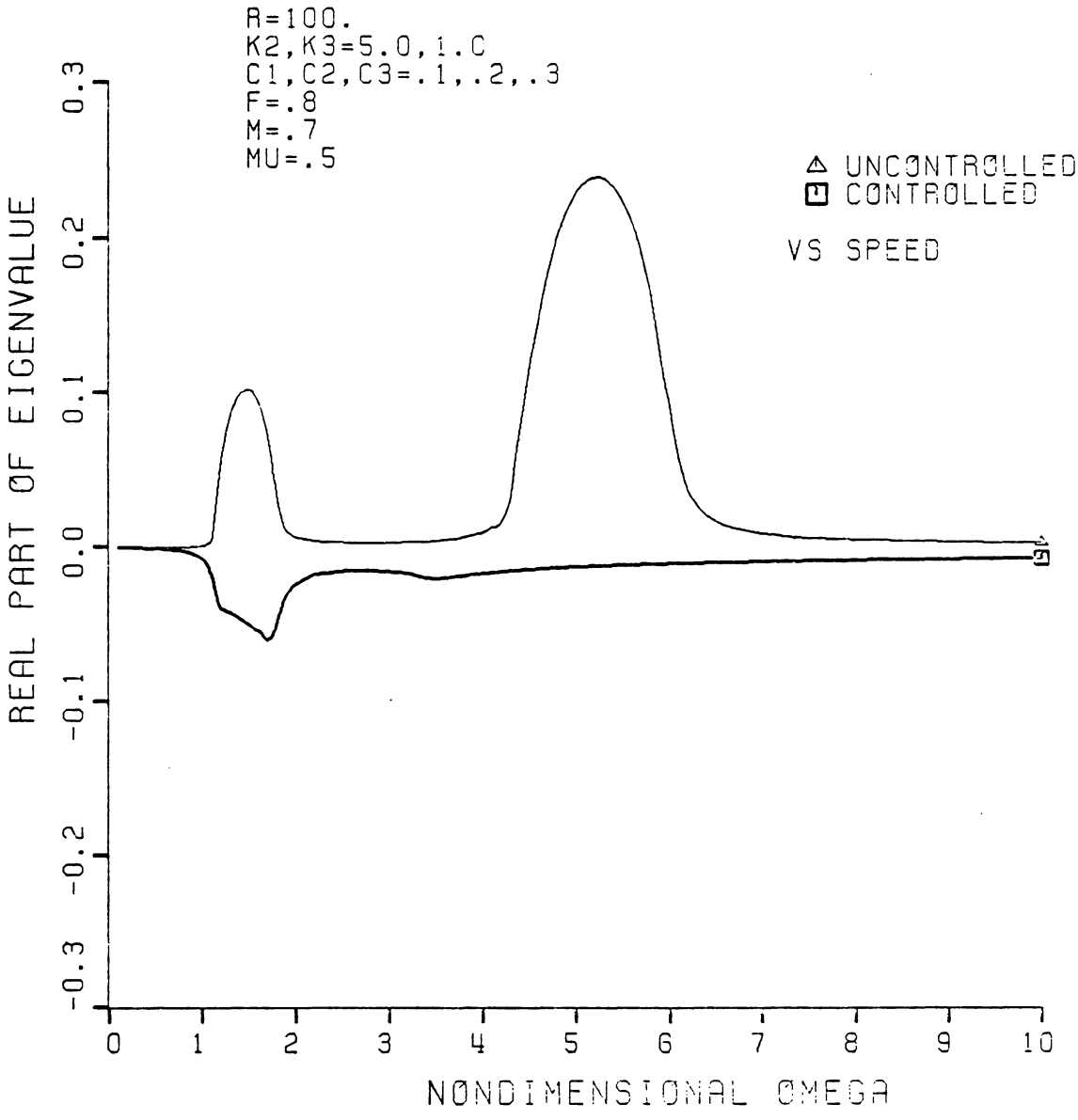

FIGURE 2.3 TWO MASS SYSTEM STABILITY: MAXIMUM REAL PART OF EIGENVALUES

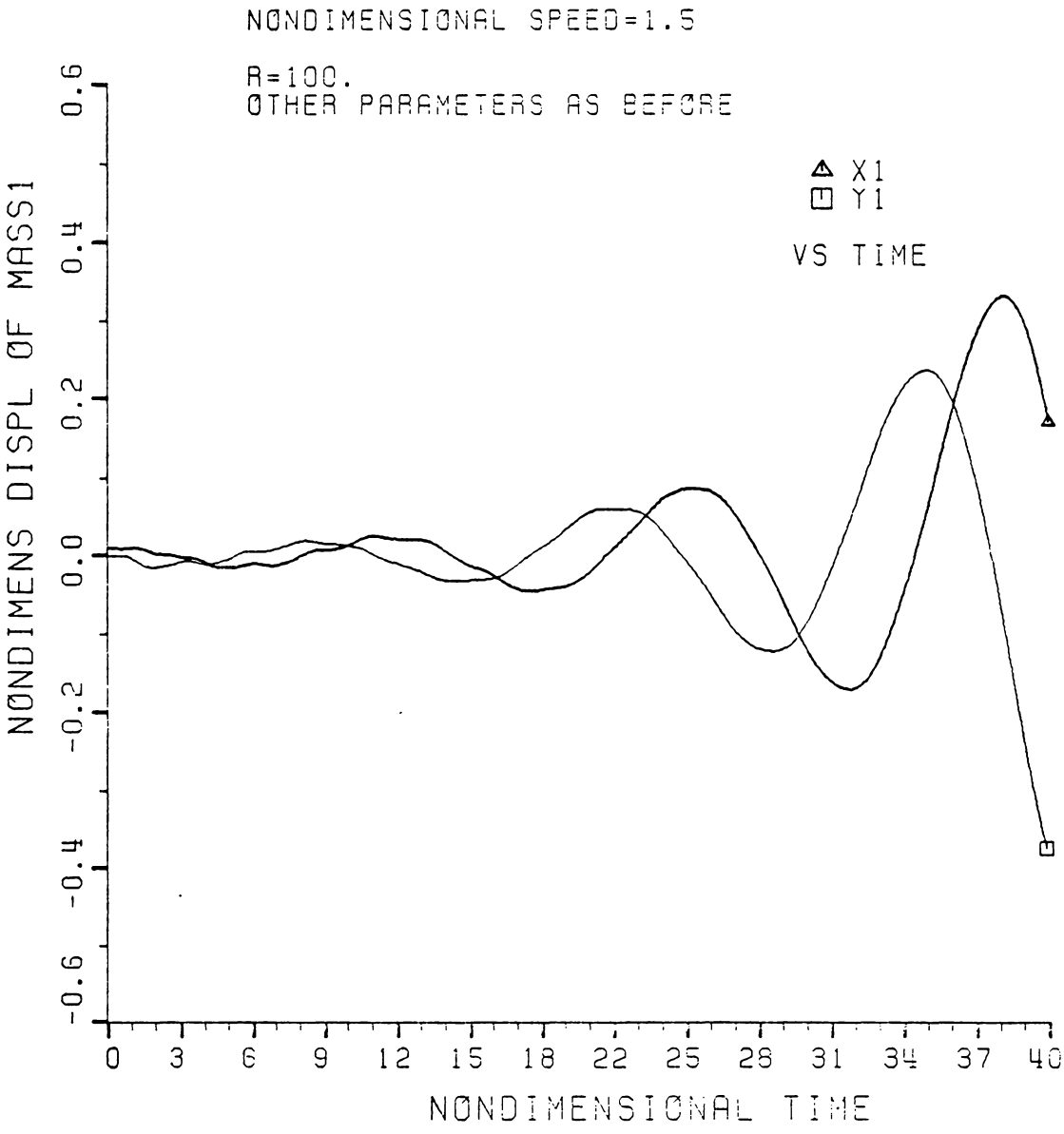

FIGURE 2.4 UNCONTROLLED TWO MASS SYSTEM: MASS 1 DISPLACEMENTS

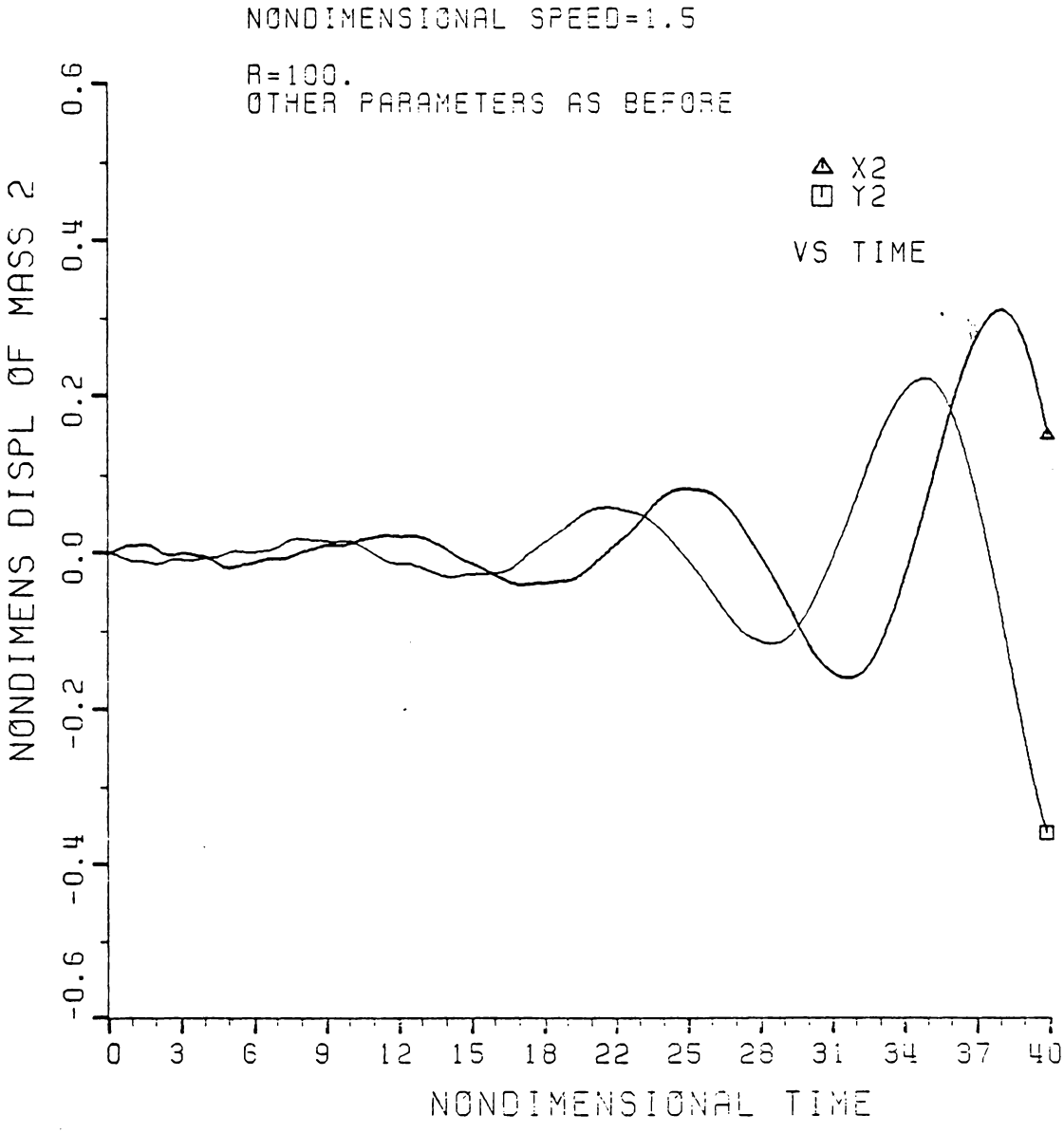

FIGURE 2.5 UNCONTROLLED TWO MASS SYSTEM: MASS 2 DISPLACEMENTS

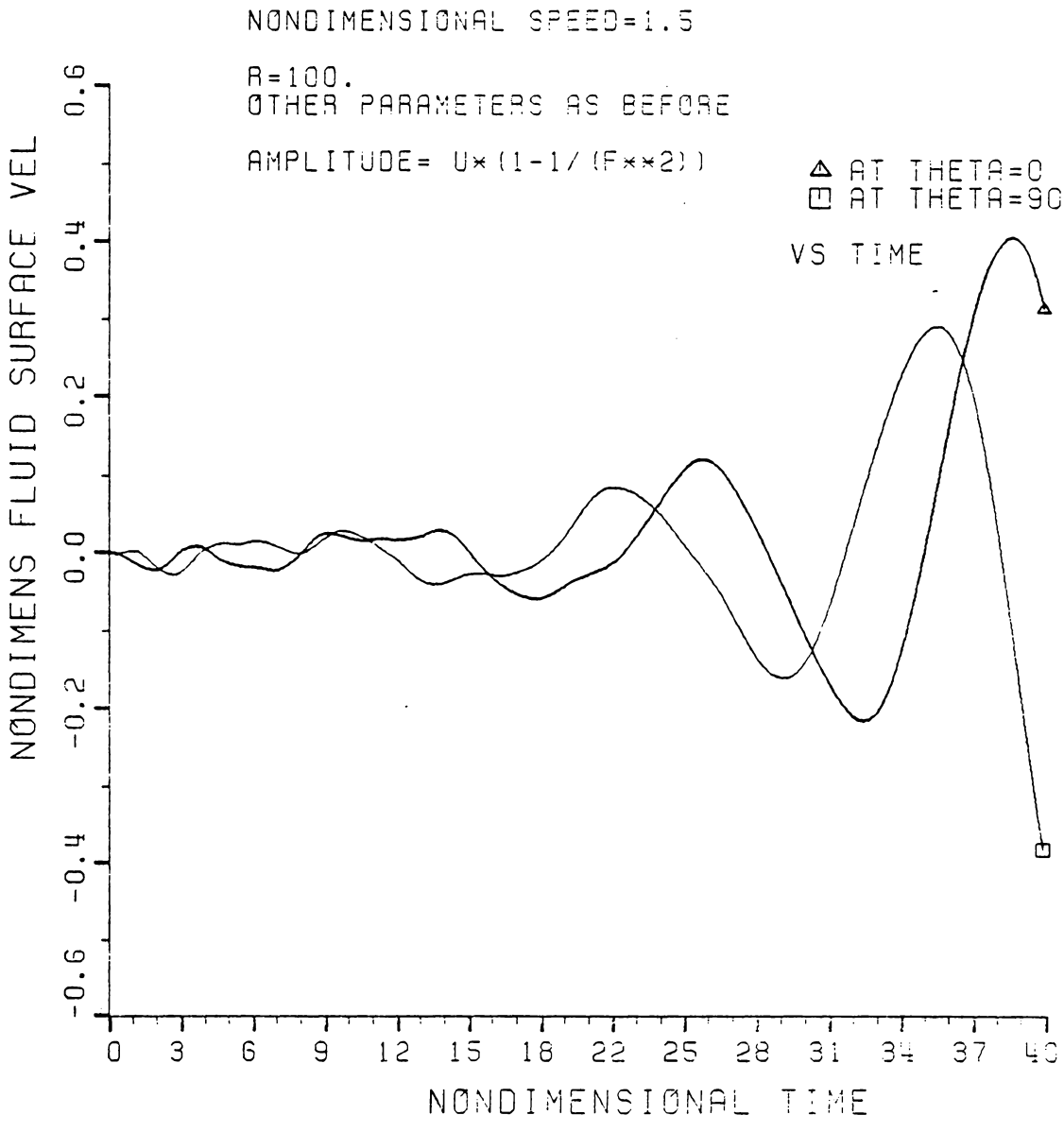

FIGURE 2.6 UNCONTROLLED TWO MASS SYSTEM: NORMAL FLUID VELOCITY U

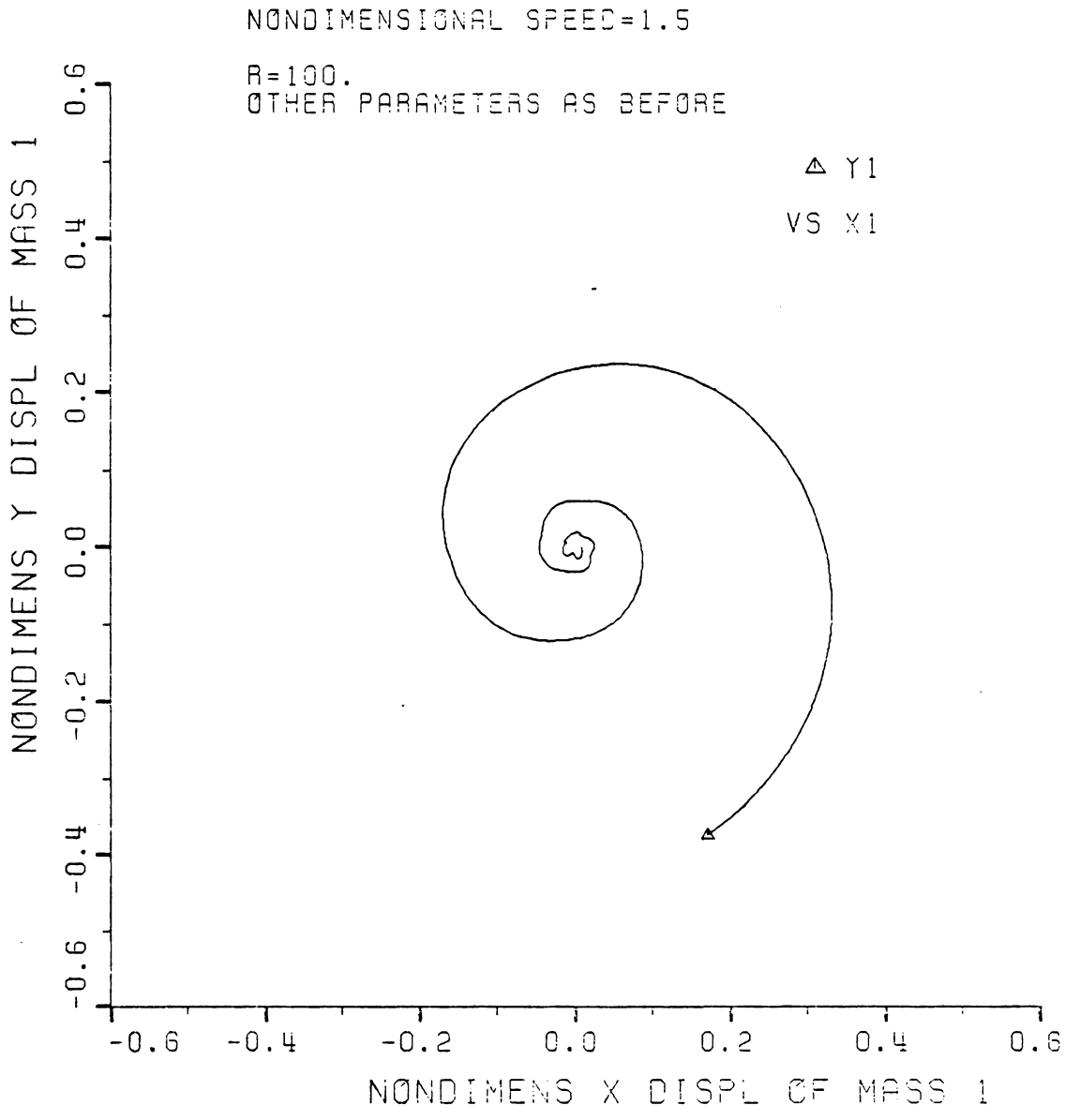

FIGURE 2.7 UNCONTROLLED TWO MASS SYSTEM: POLAR PLOT OF MASS1 DISPLACEMENTS

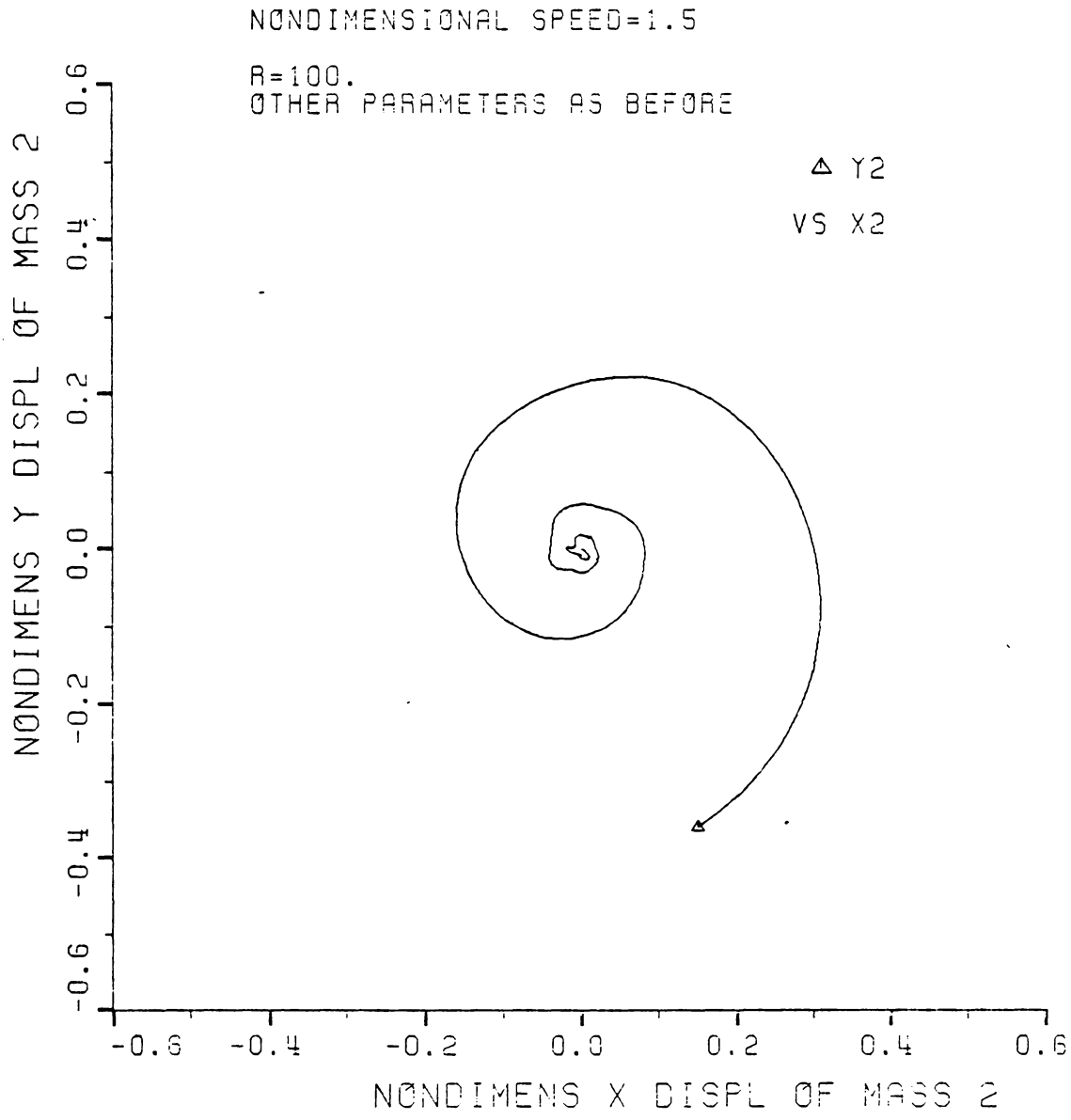

FIGURE 2.8 UNCONTROLLED TWO MASS SYSTEM: POLAR PLOT OF MASS2 DISPLACEMENTS

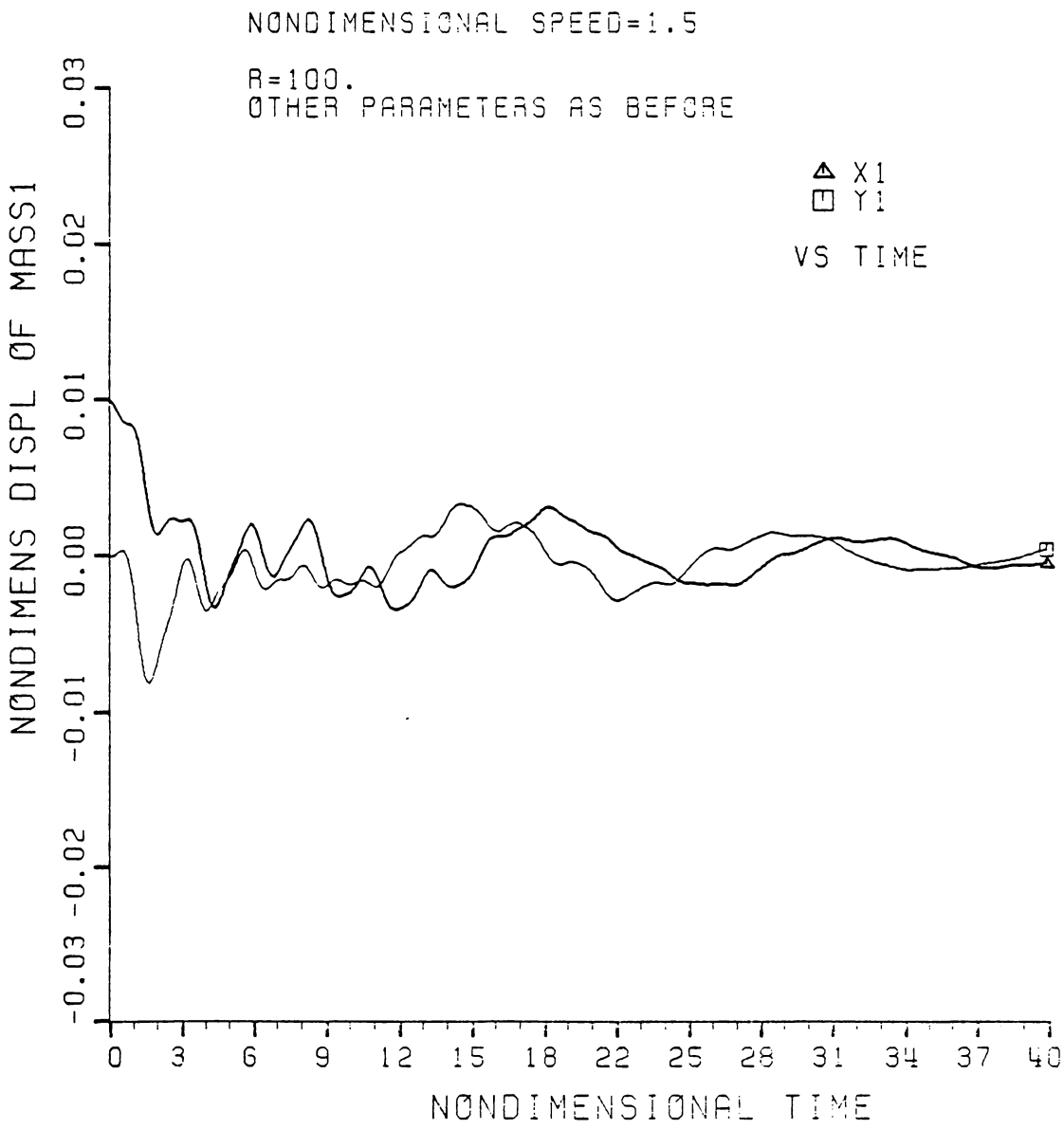

FIGURE 2.9 CONTROLLED TWO MASS SYSTEM: MASS 1 DISPLACEMENTS

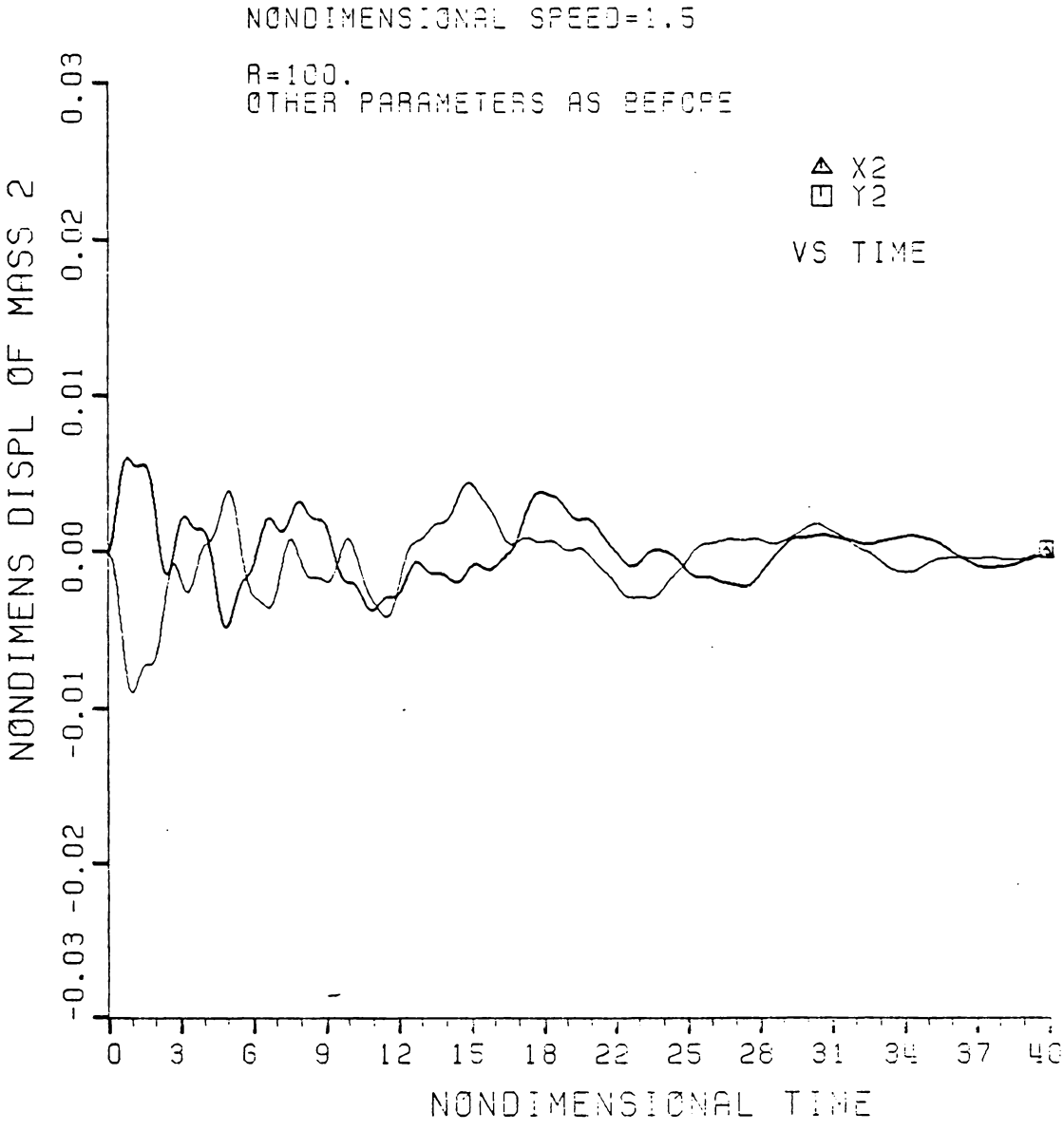

FIGURE 2.10 CONTROLLED TWO MASS SYSTEM: MASS 2 DISPLACEMENTS

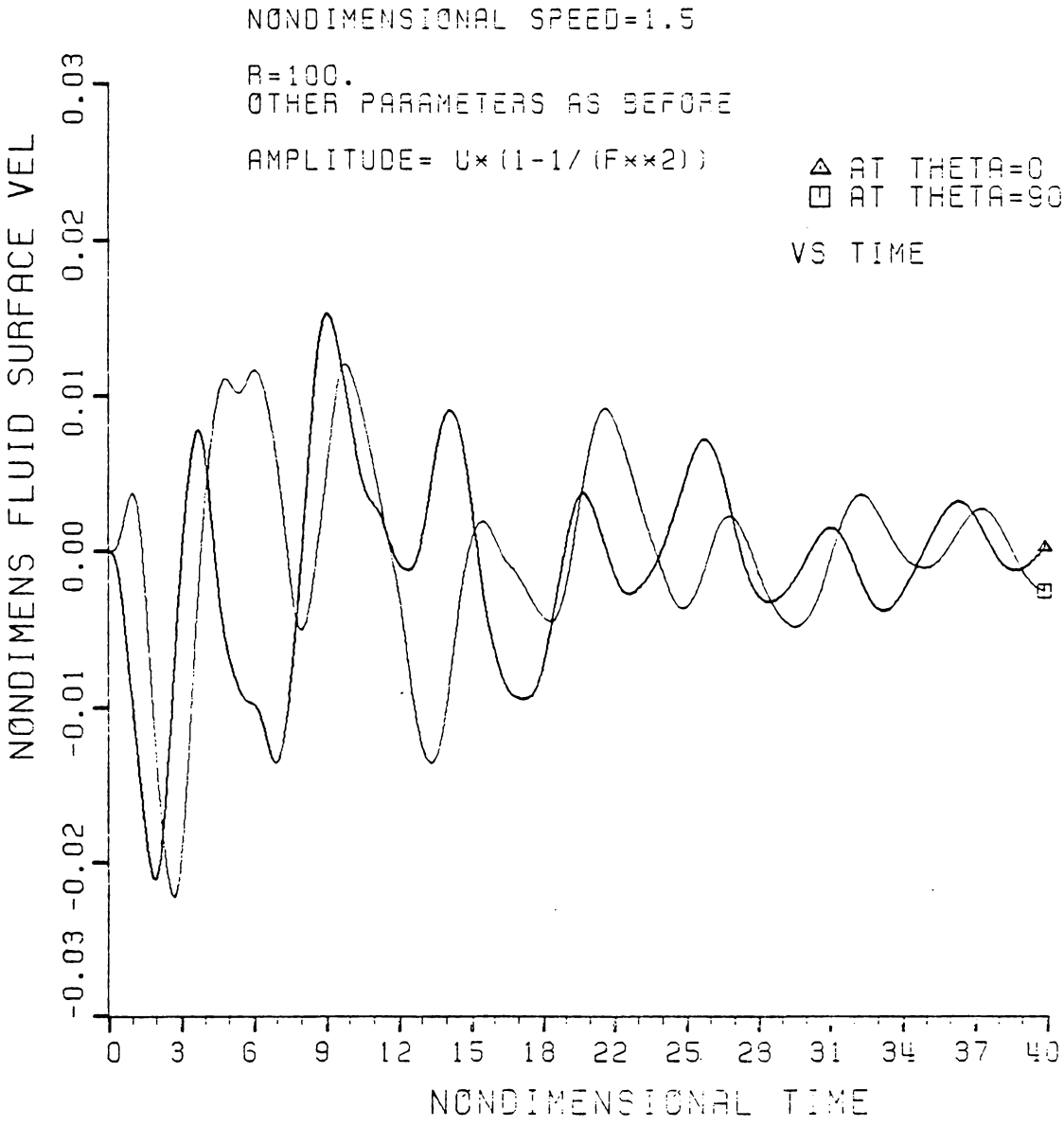

FIGURE 2.11 CONTROLLED TWO MASS SYSTEM:
NORMAL FLUID VELOCITY U

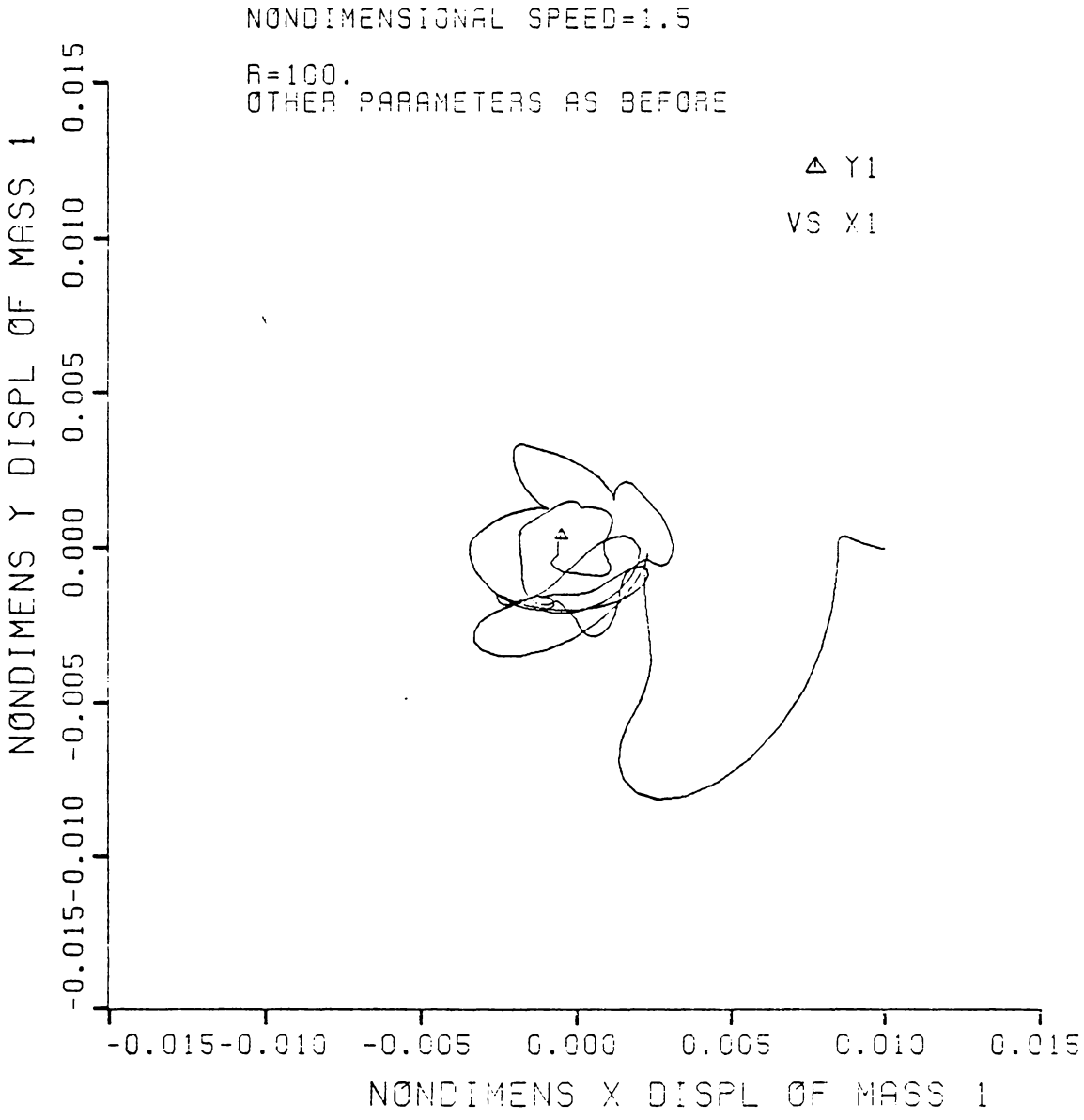

FIGURE 2.12 CONTROLLED TWO MASS SYSTEM:
POLAR PLOT OF MASS1 DISPLACEMENTS

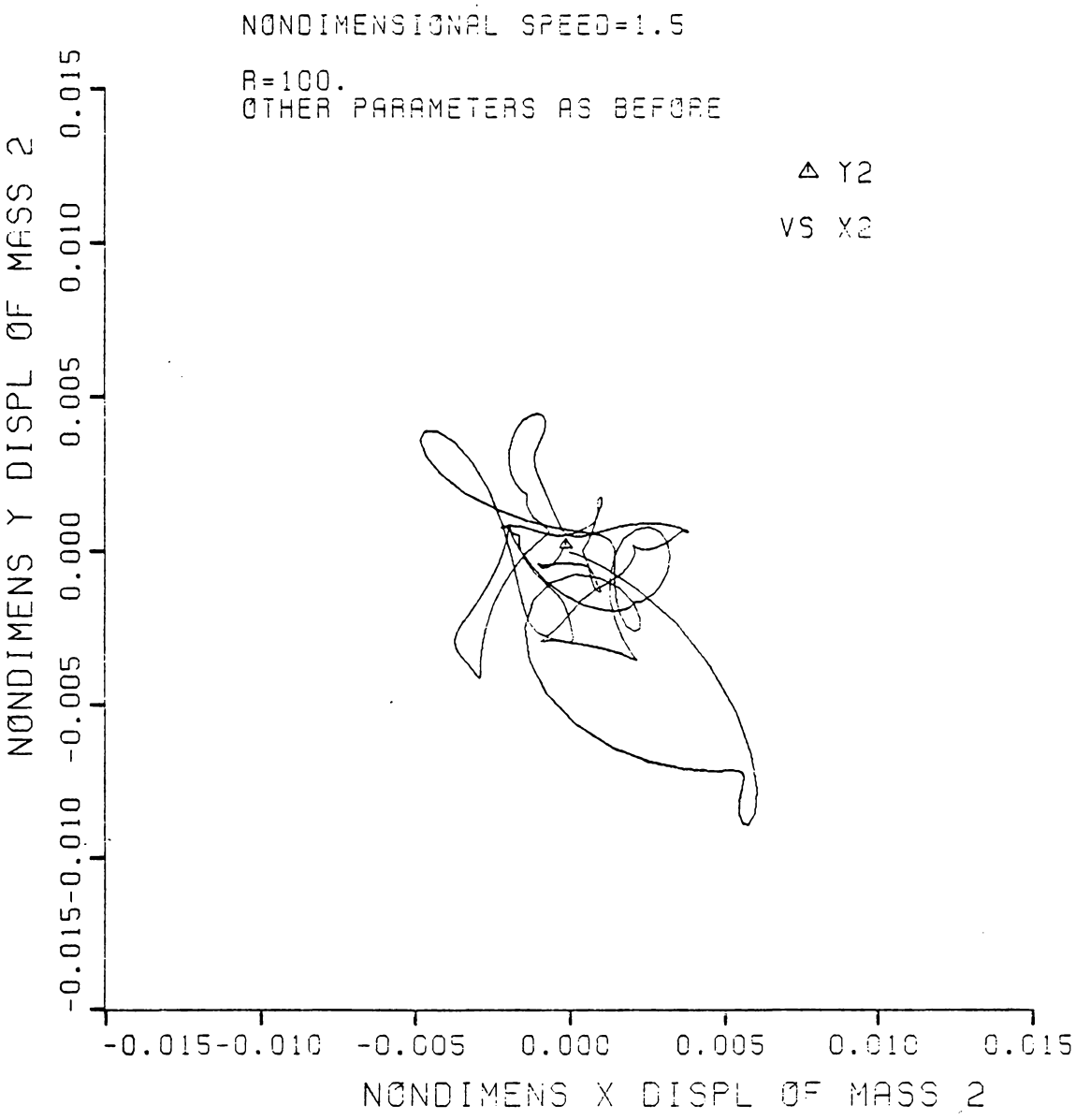

FIGURE 2.13 CONTROLLED TWO MASS SYSTEM;
POLAR PLOT OF MASS2 DISPLACEMENTS

2.3.2 SYSTEM GAINS

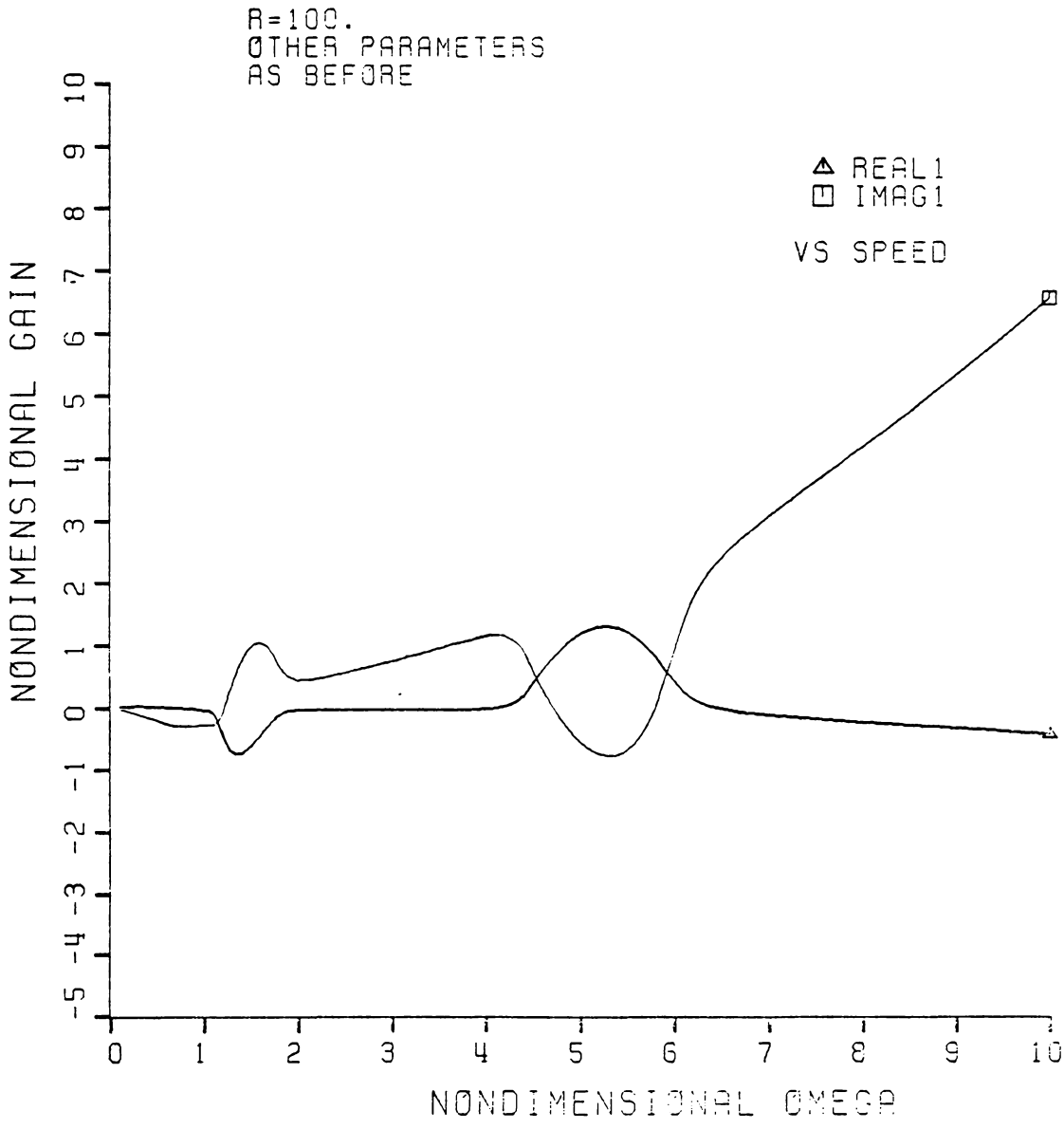

FIGURE 2.14 TWO MASS SYSTEM: GAIN(1)

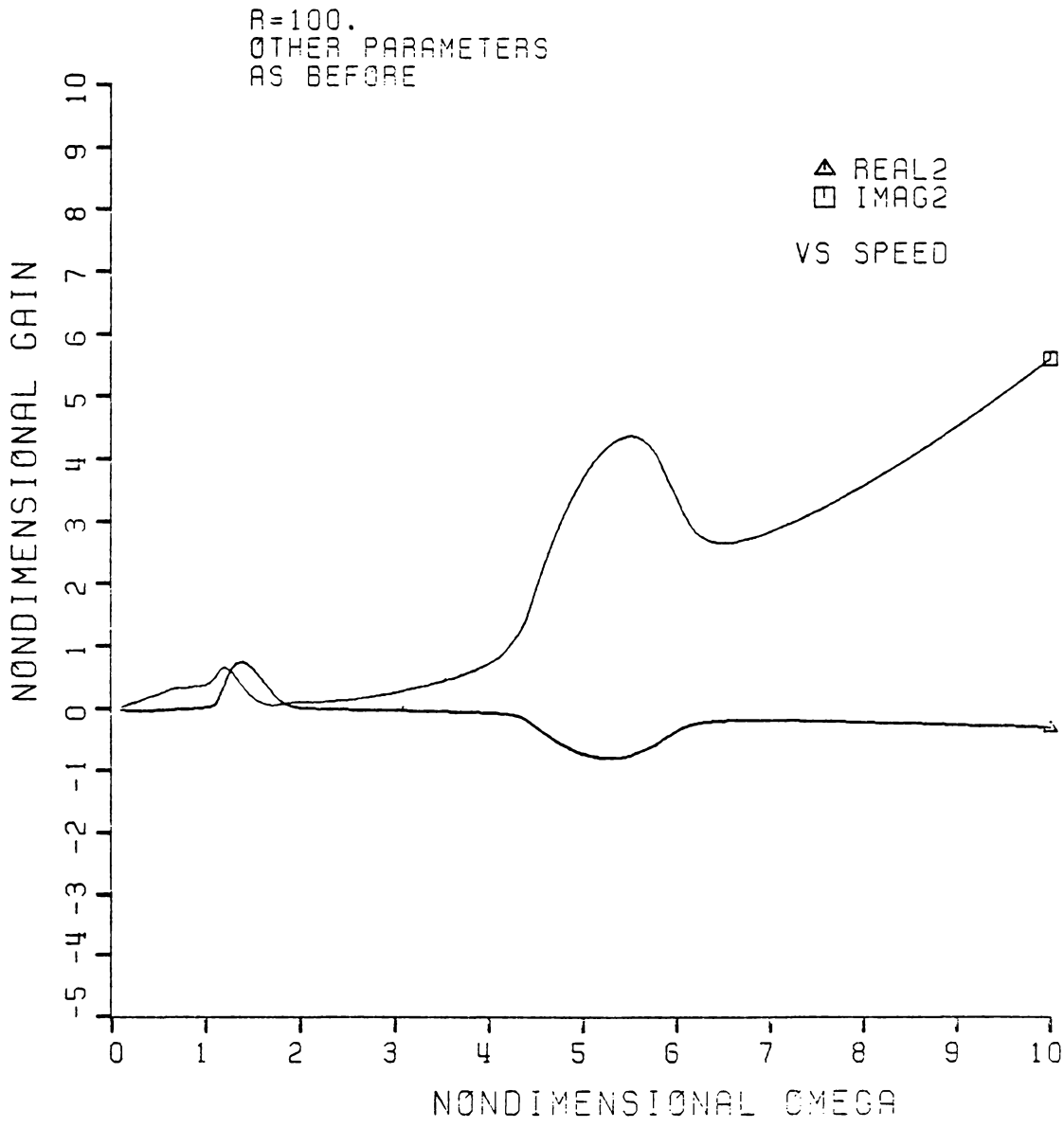

FIGURE 2.15 TWO MASS SYSTEM: GAIN(2)

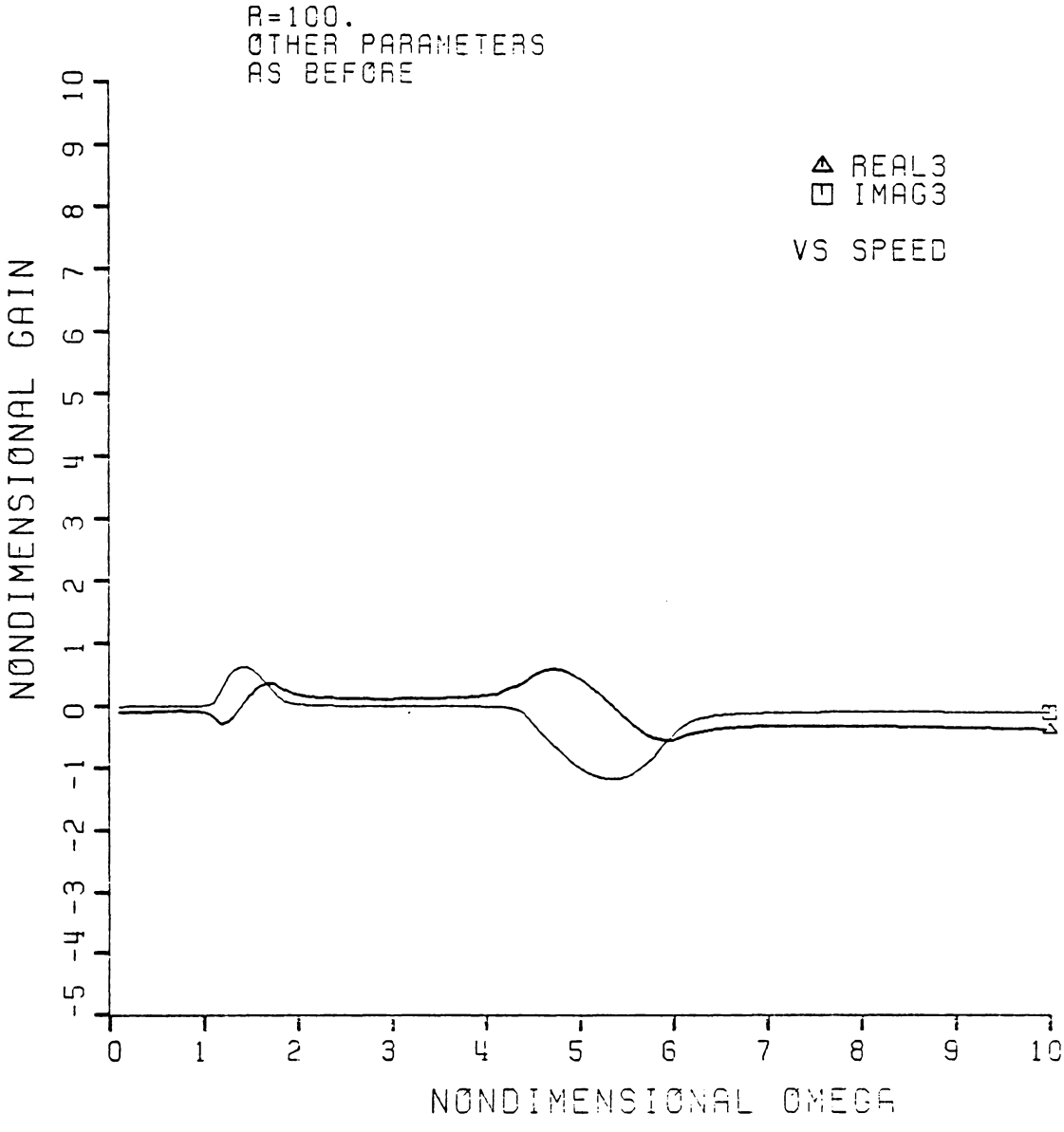

FIGURE 2.16 TWO MASS SYSTEM: GAIN(3)

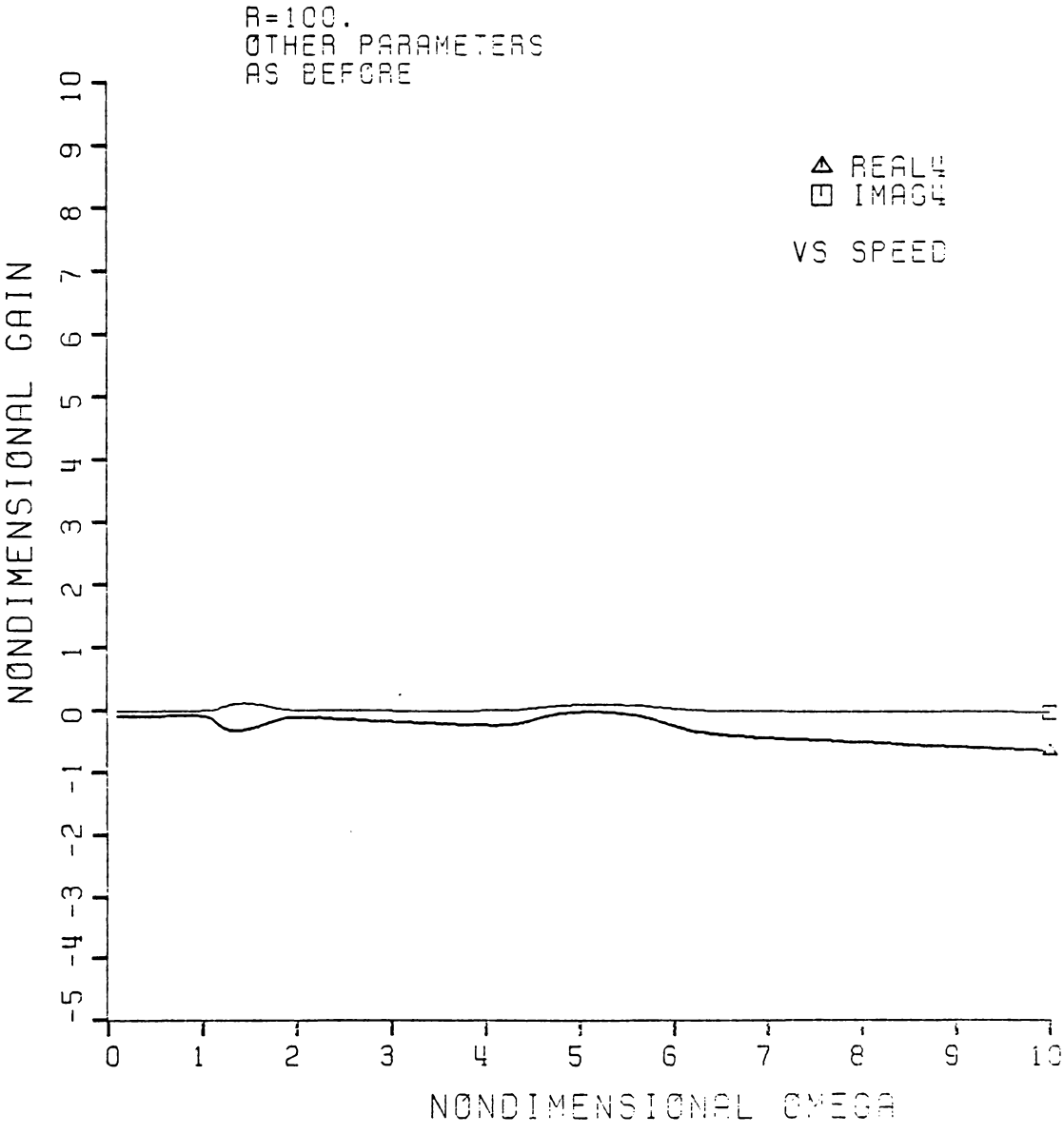

FIGURE 2.17 TWO MASS SYSTEM: GAIN(Ω)

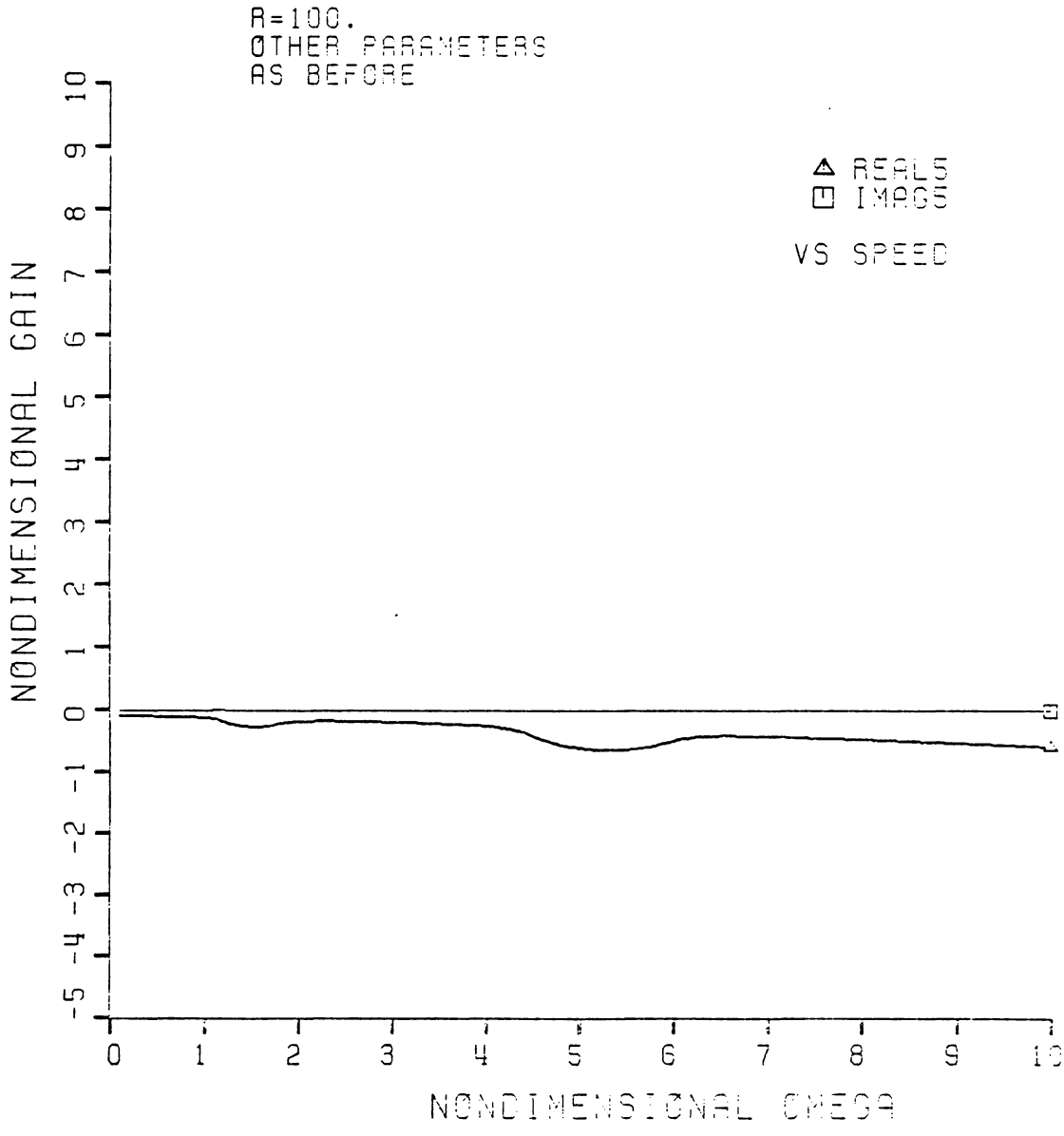

FIGURE 2.18 TWO MASS SYSTEM: GAIN(E)

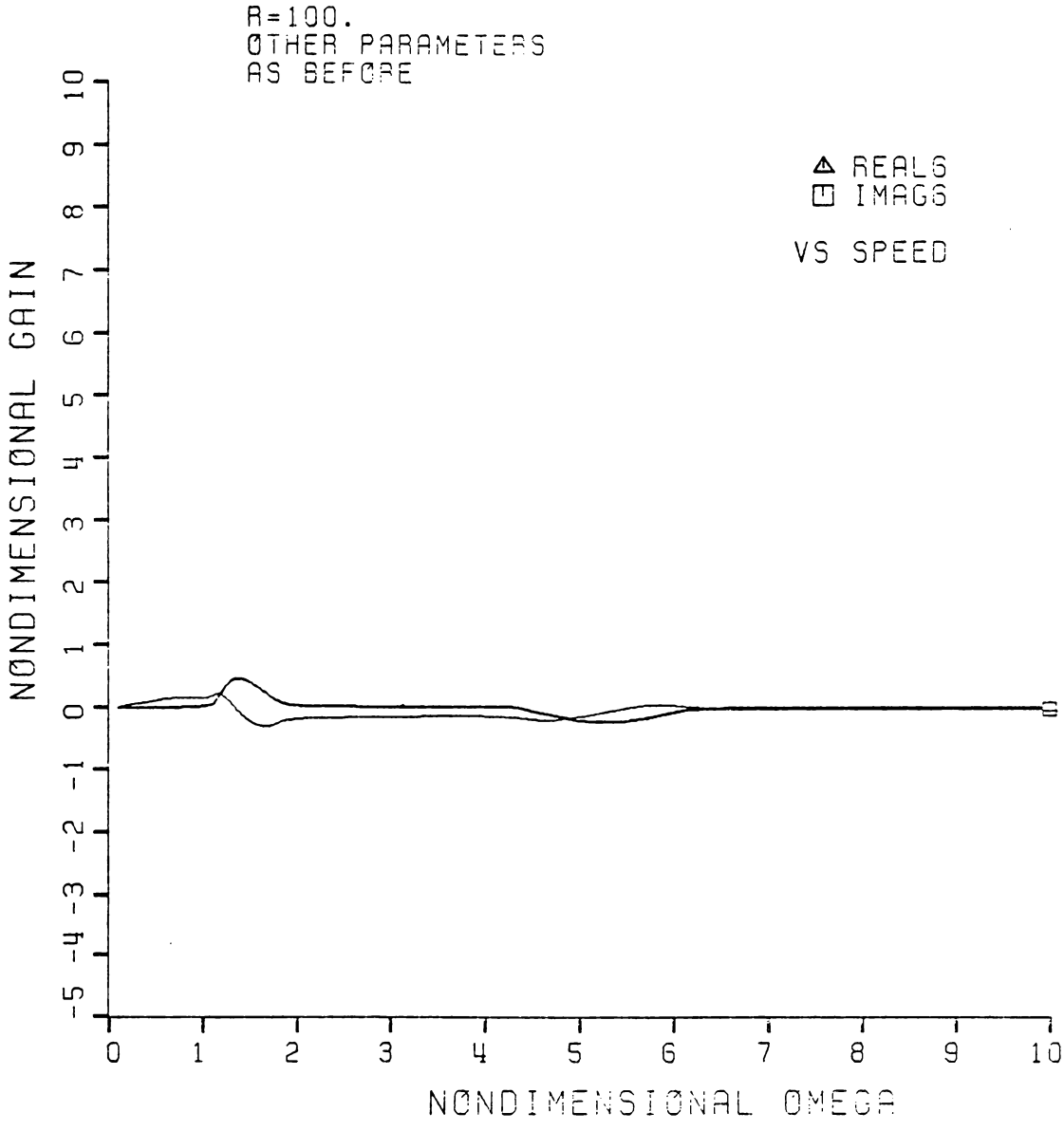

FIGURE 2.19 TWO MASS SYSTEM: GAIN(G)

2.3.3 FEEDBACK CONTROL FORCE

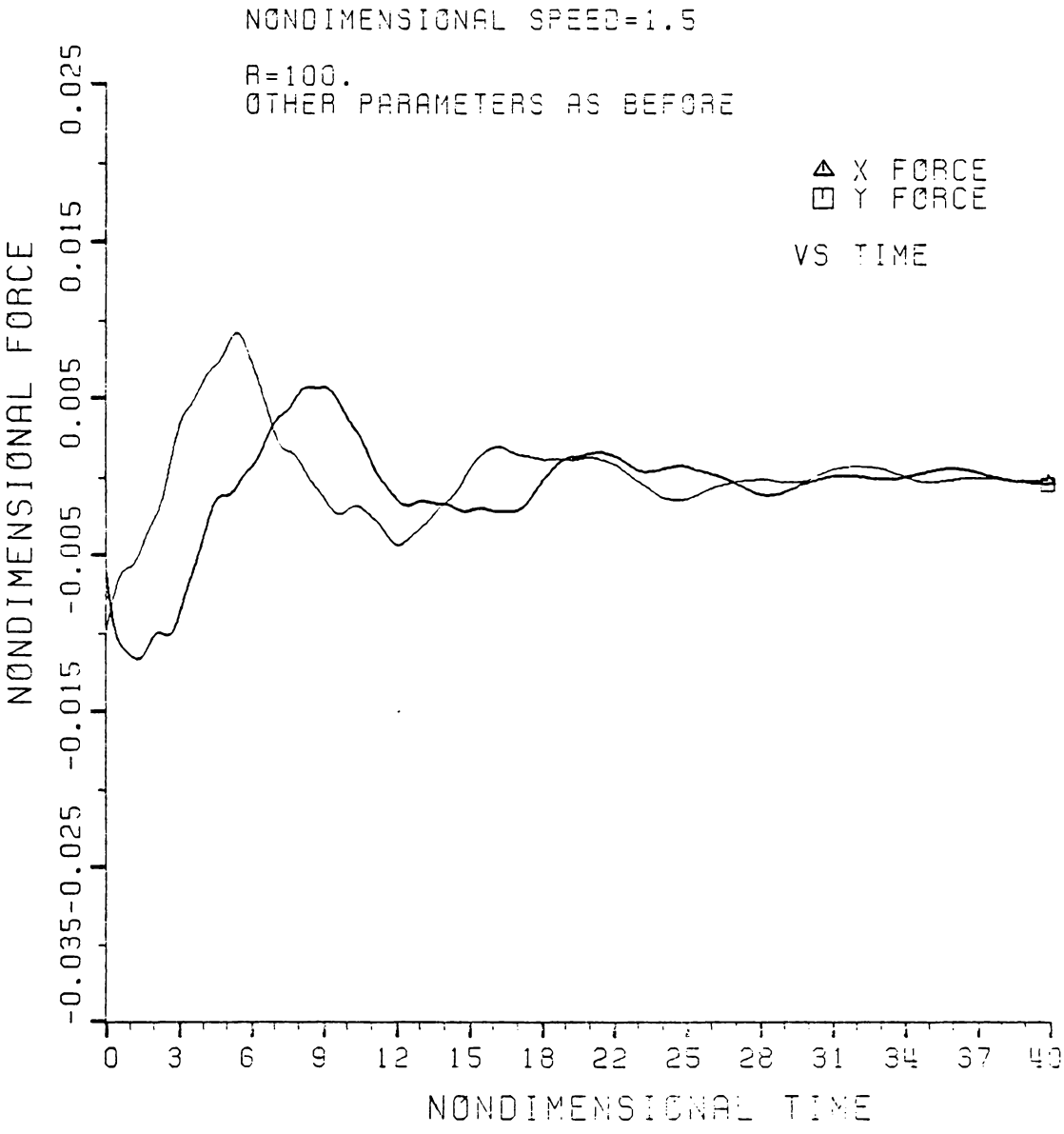

FIGURE 2.20 CONTROLLED TWO MASS SYSTEM: NONDIMENSIONAL FORCE

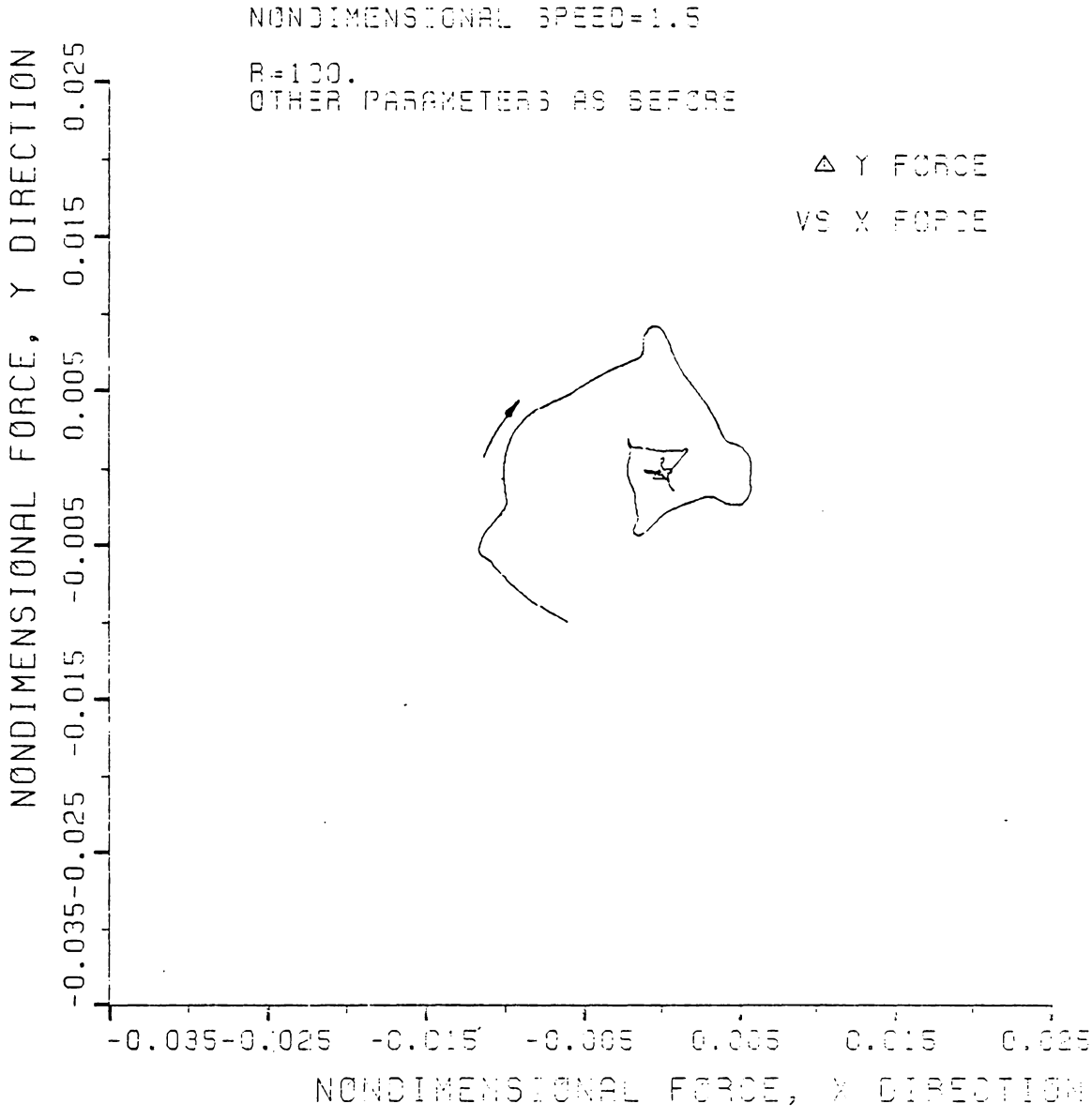

FIGURE 2.21 CONTROLLED TWO MASS SYSTEM:
POLAR PLOT OF FORCE

2.3.4 INFLUENCE OF OPERATING SPEED

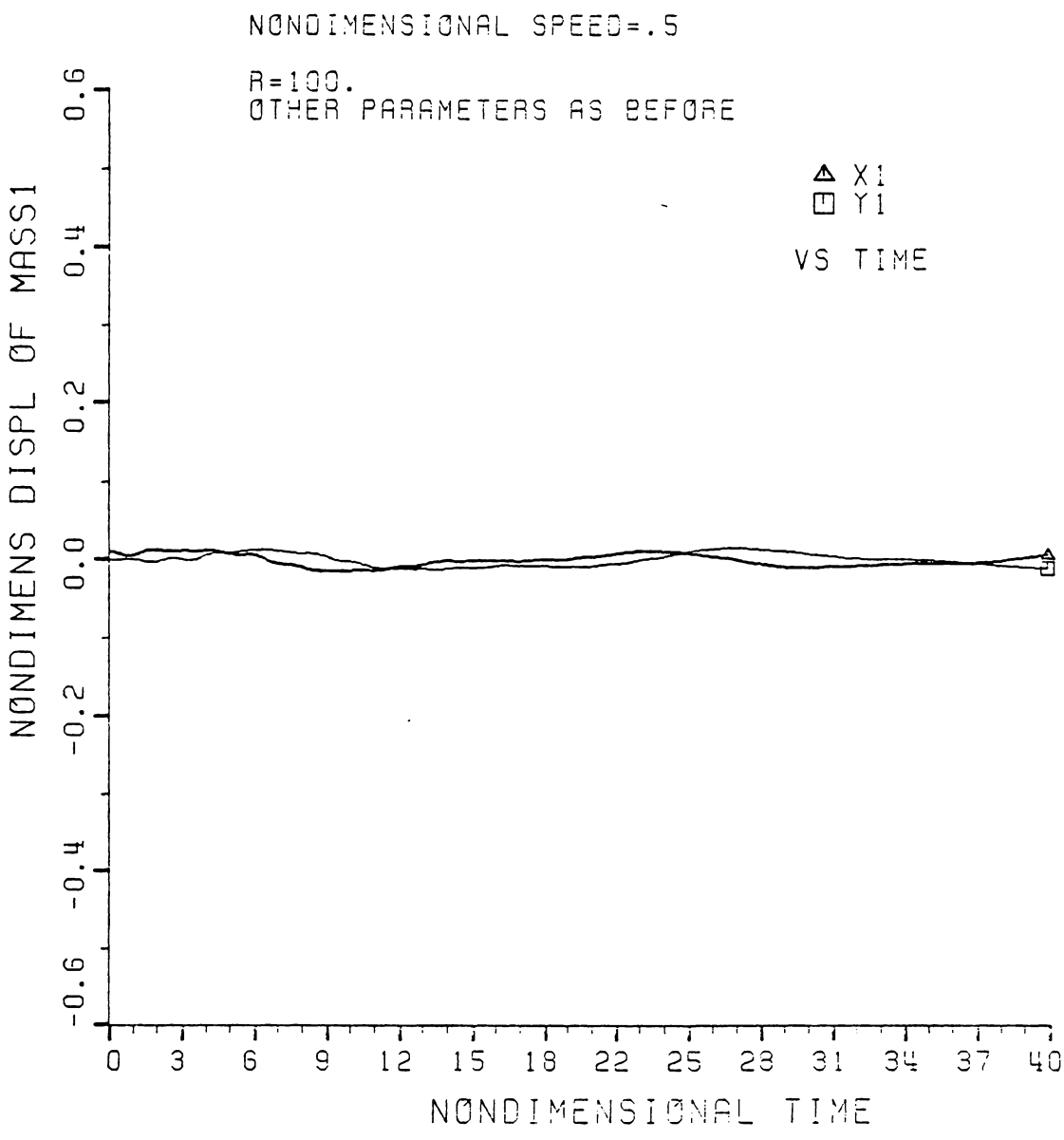

FIGURE 2.22 UNCONTROLLED TWO MASS SYSTEM: MASS 1 DISPLACEMENTS

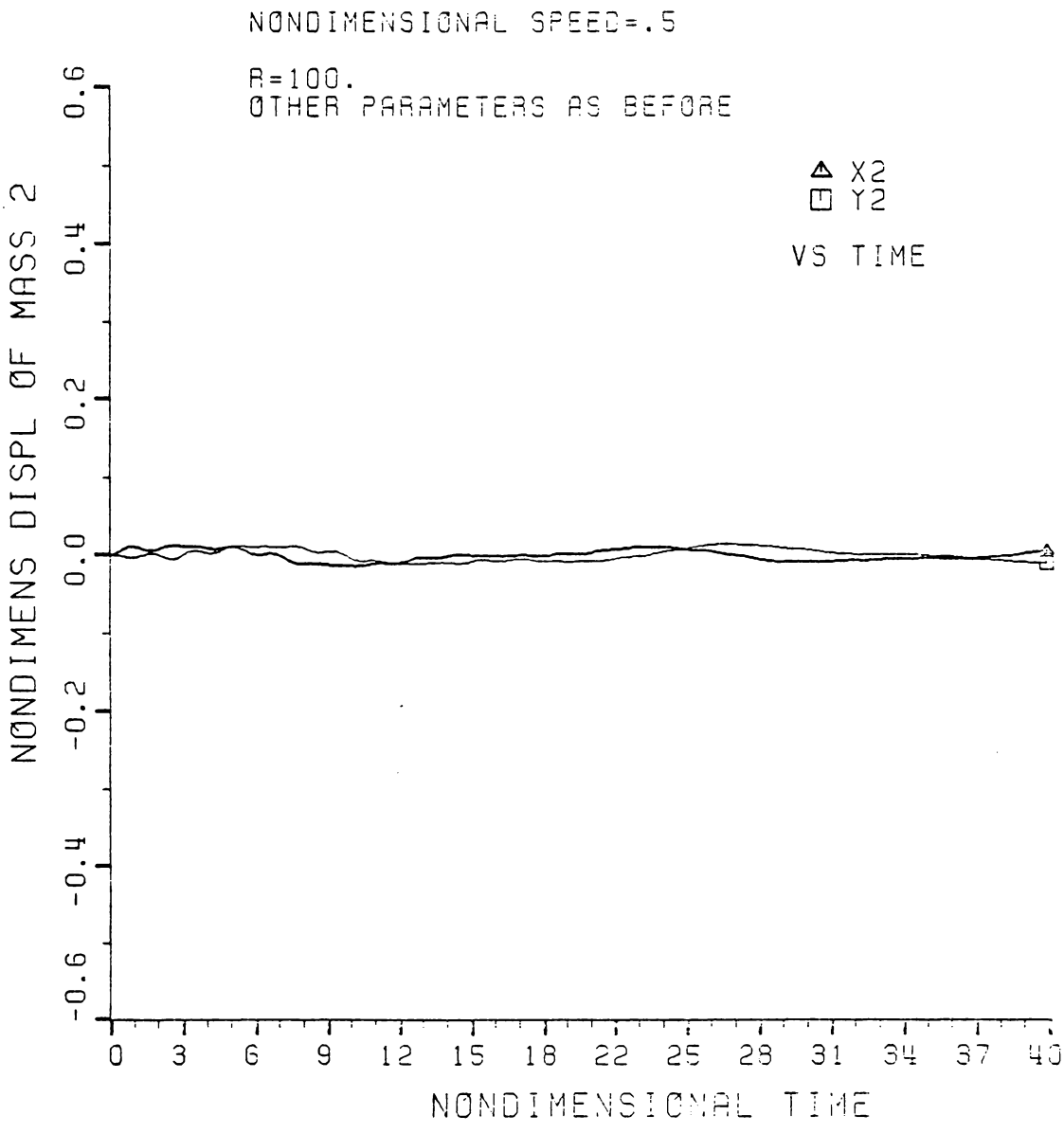

FIGURE 2.23 UNCONTROLLED TWO MASS SYSTEM: MASS 2 DISPLACEMENTS

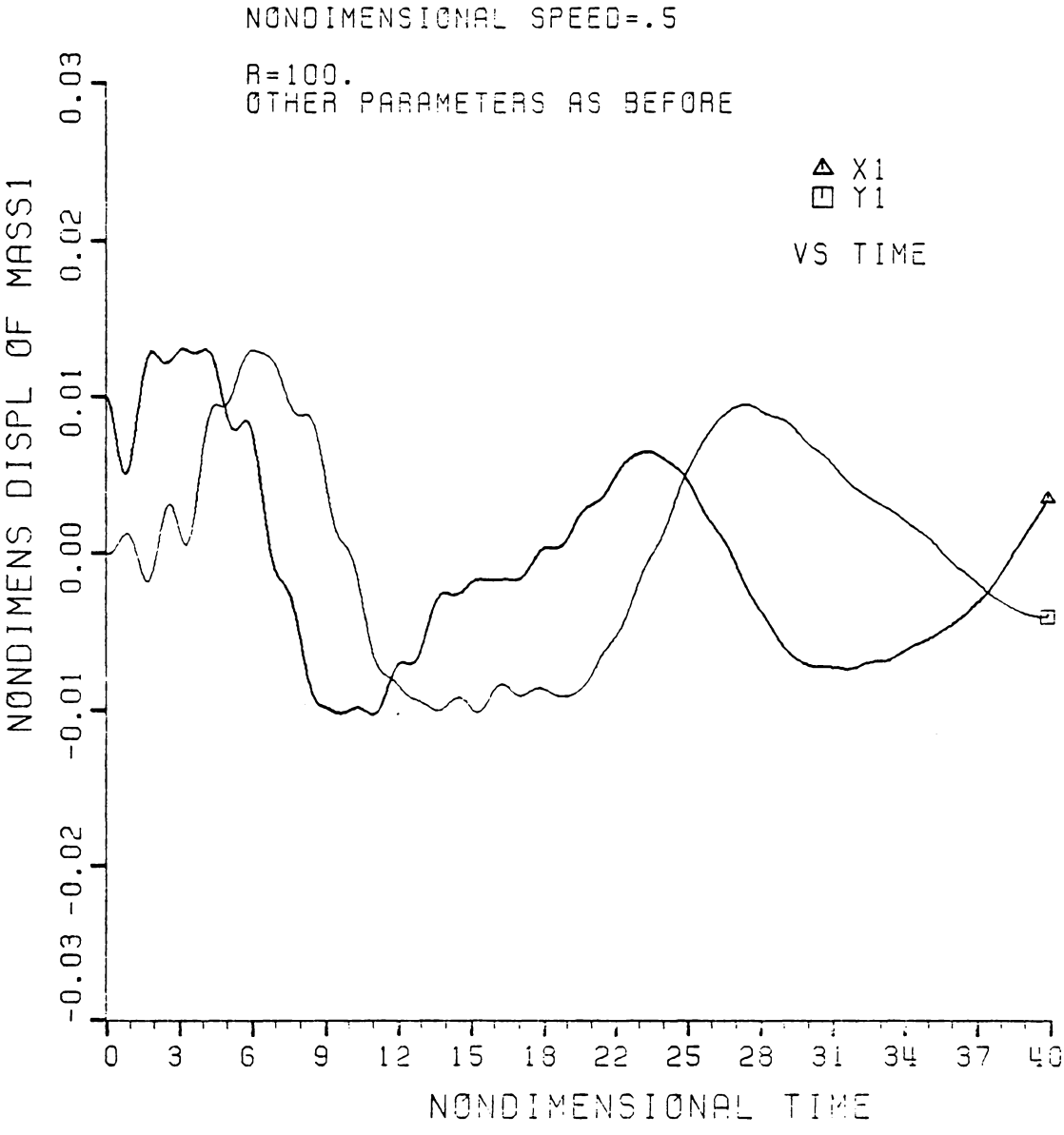

FIGURE 2.24 CONTROLLED TWO MASS SYSTEM:
MASS 1 DISPLACEMENTS

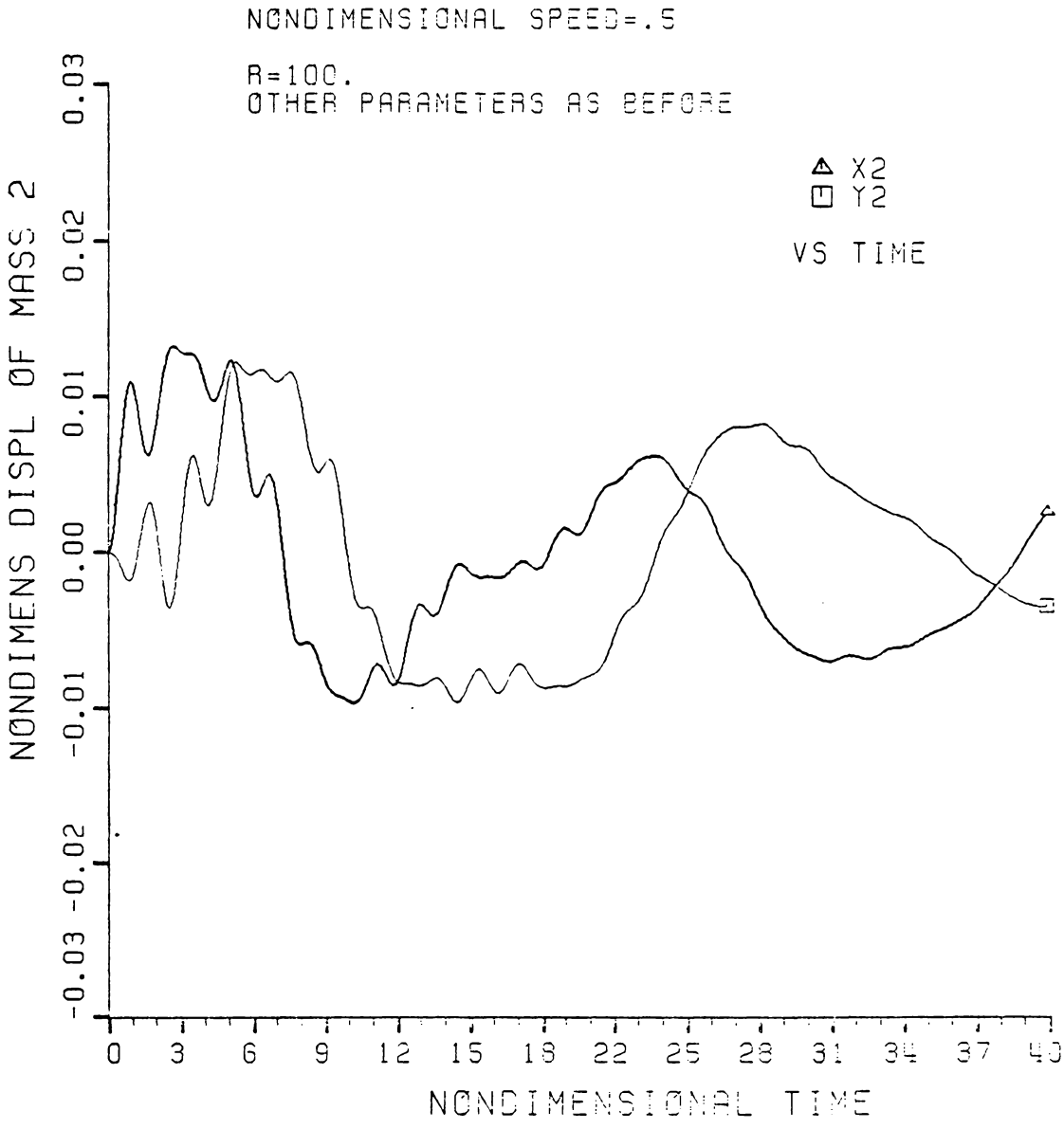

FIGURE 2.25 CONTROLLED TWO MASS SYSTEM: MASS 2 DISPLACEMENTS

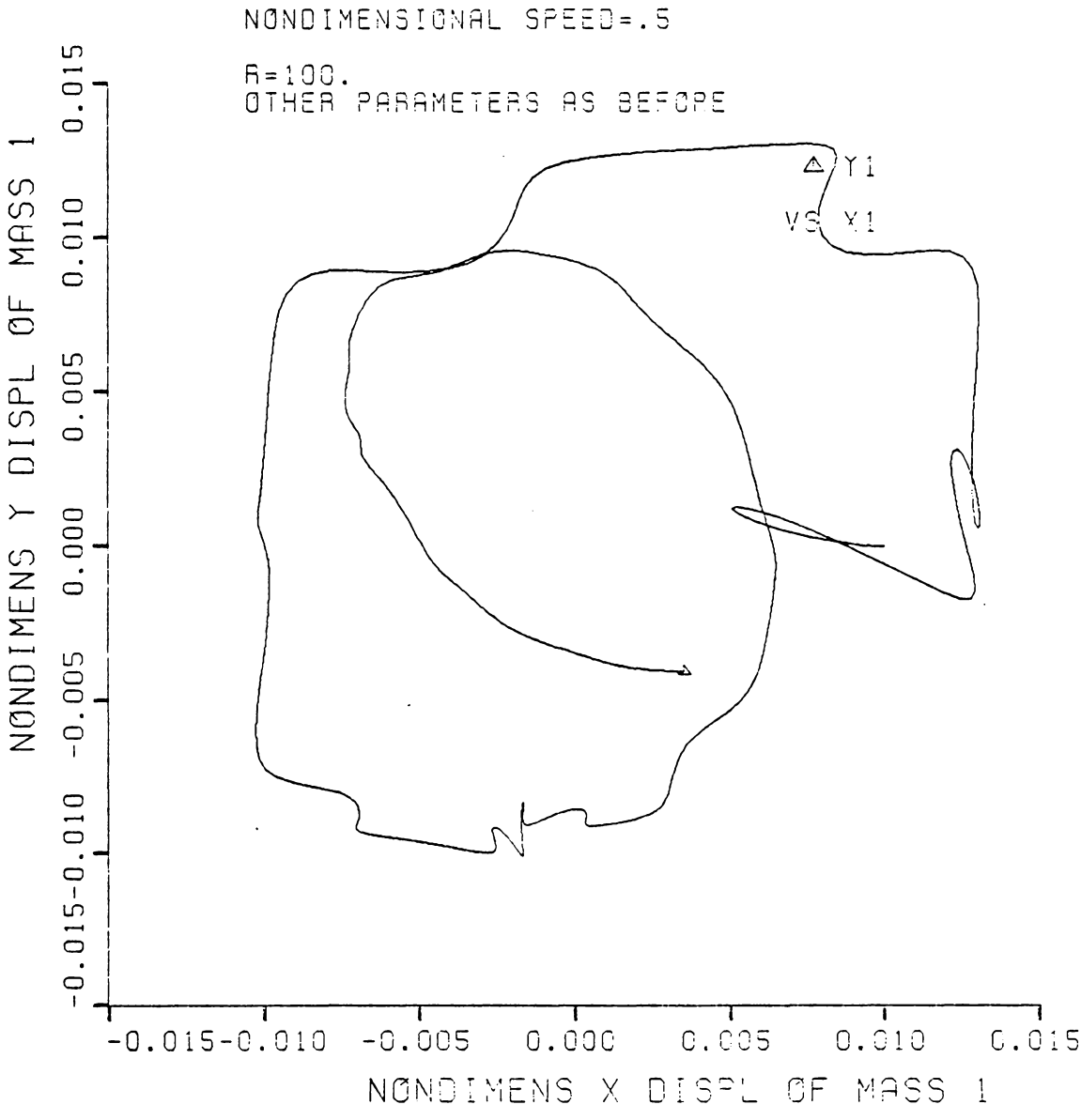

FIGURE 2.26 CONTROLLED TWO MASS SYSTEM:
POLAR PLOT OF MASS1 DISPLACEMENTS

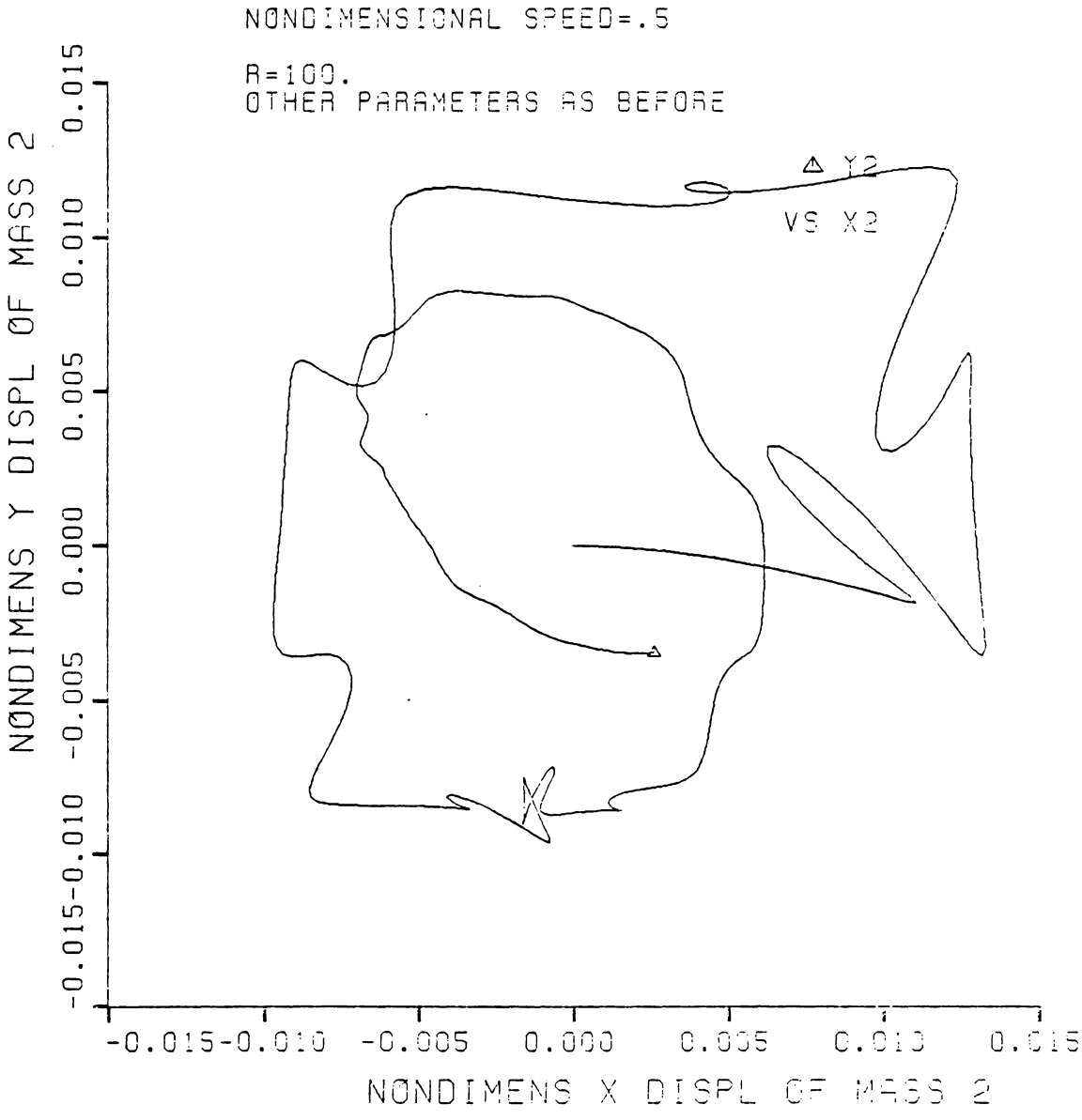

FIGURE 2.27 CONTROLLED TWO MASS SYSTEM:
POLAR PLOT OF MASS2 DISPLACEMENTS

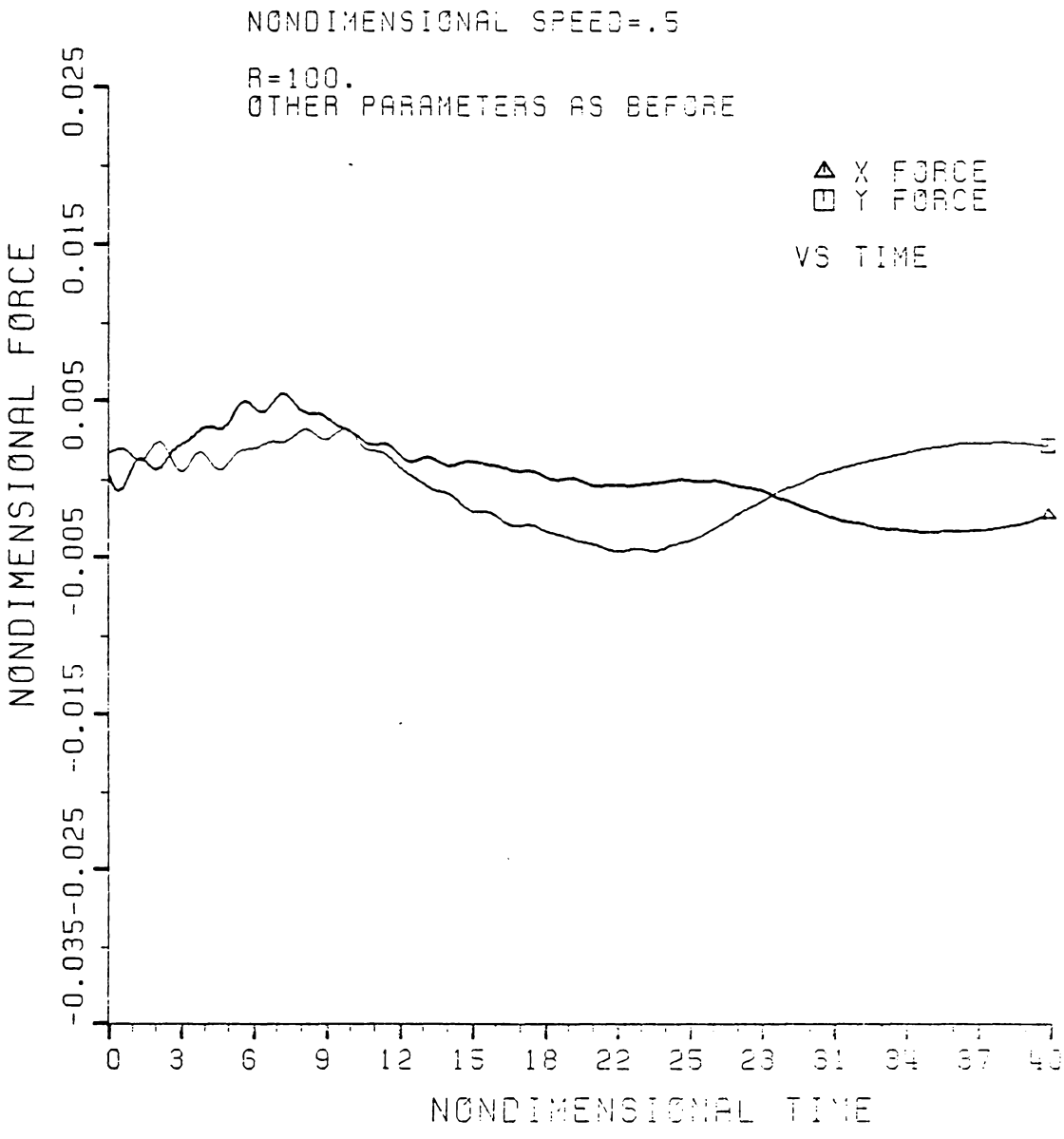

FIGURE 2.28 CONTROLLED TWO MASS SYSTEM: NONDIMENSIONAL FORCE

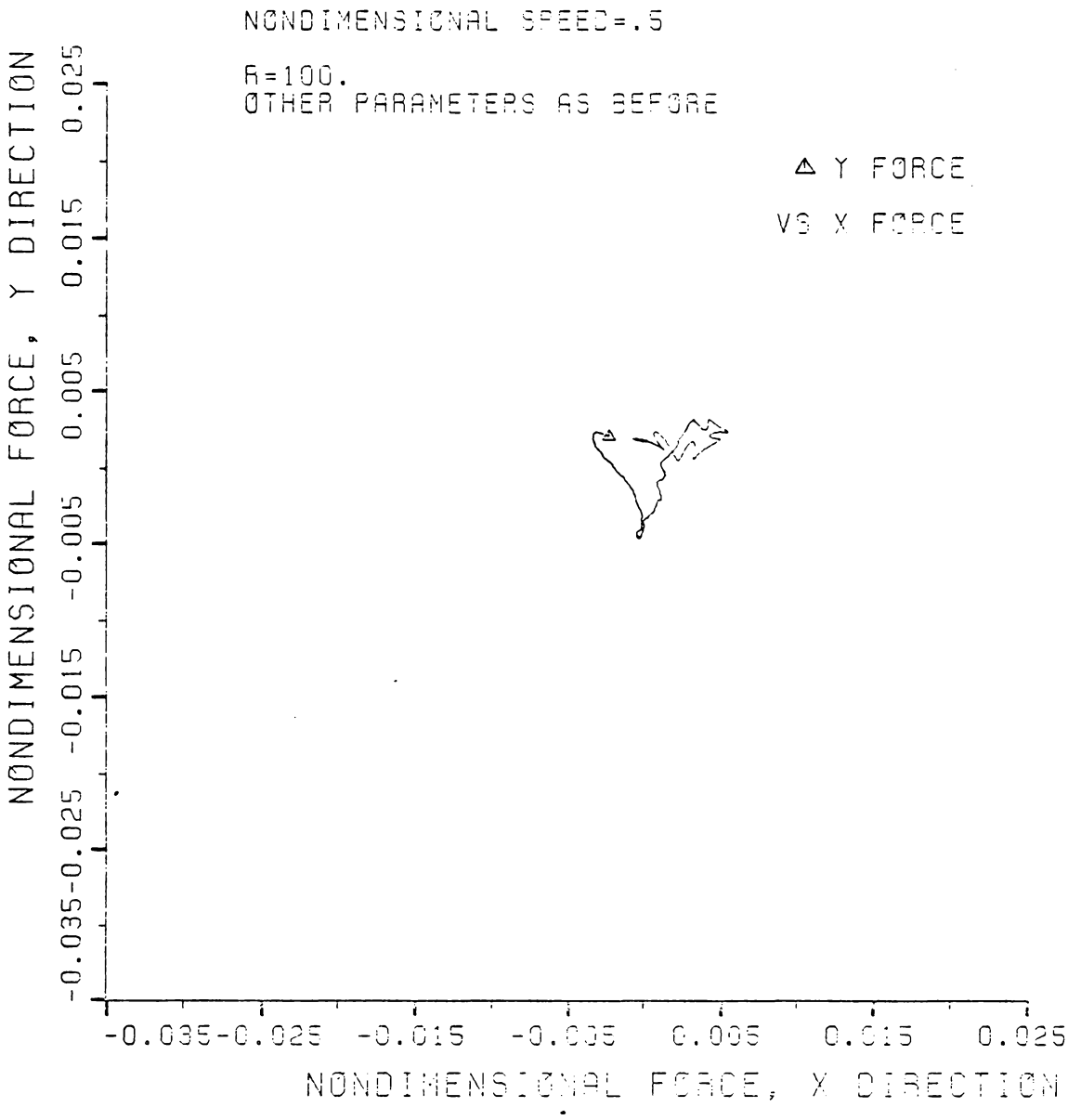

FIGURE 2.29 CONTROLLED TWO MASS SYSTEM:
POLAR PLOT OF FORCE

2.3.5 INFLUENCE OF PERFORMANCE INDEX WEIGHTING FACTORS

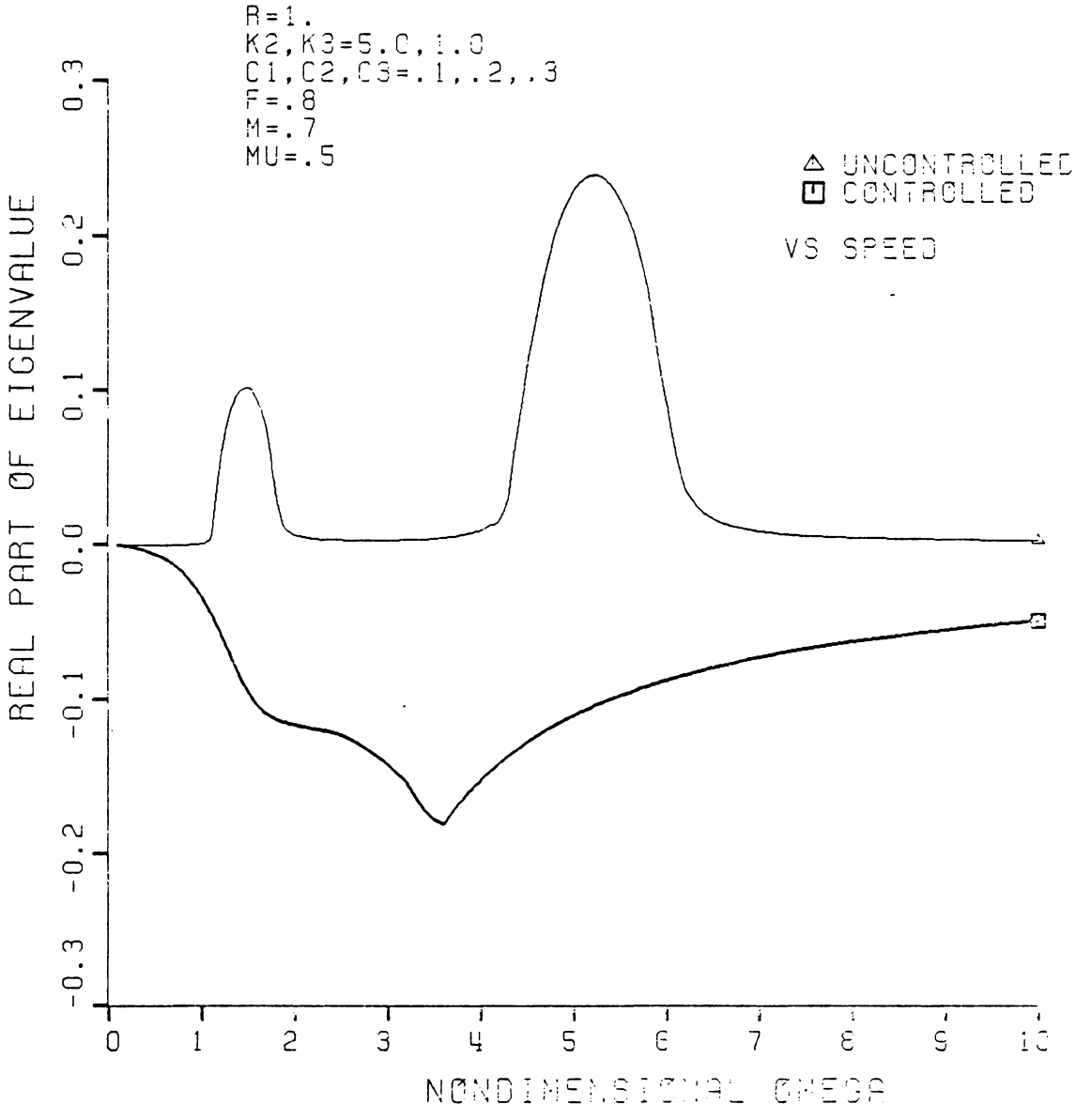

FIGURE 2.30 TWO MASS SYSTEM STABILITY: MAXIMUM REAL PART OF EIGENVALUES

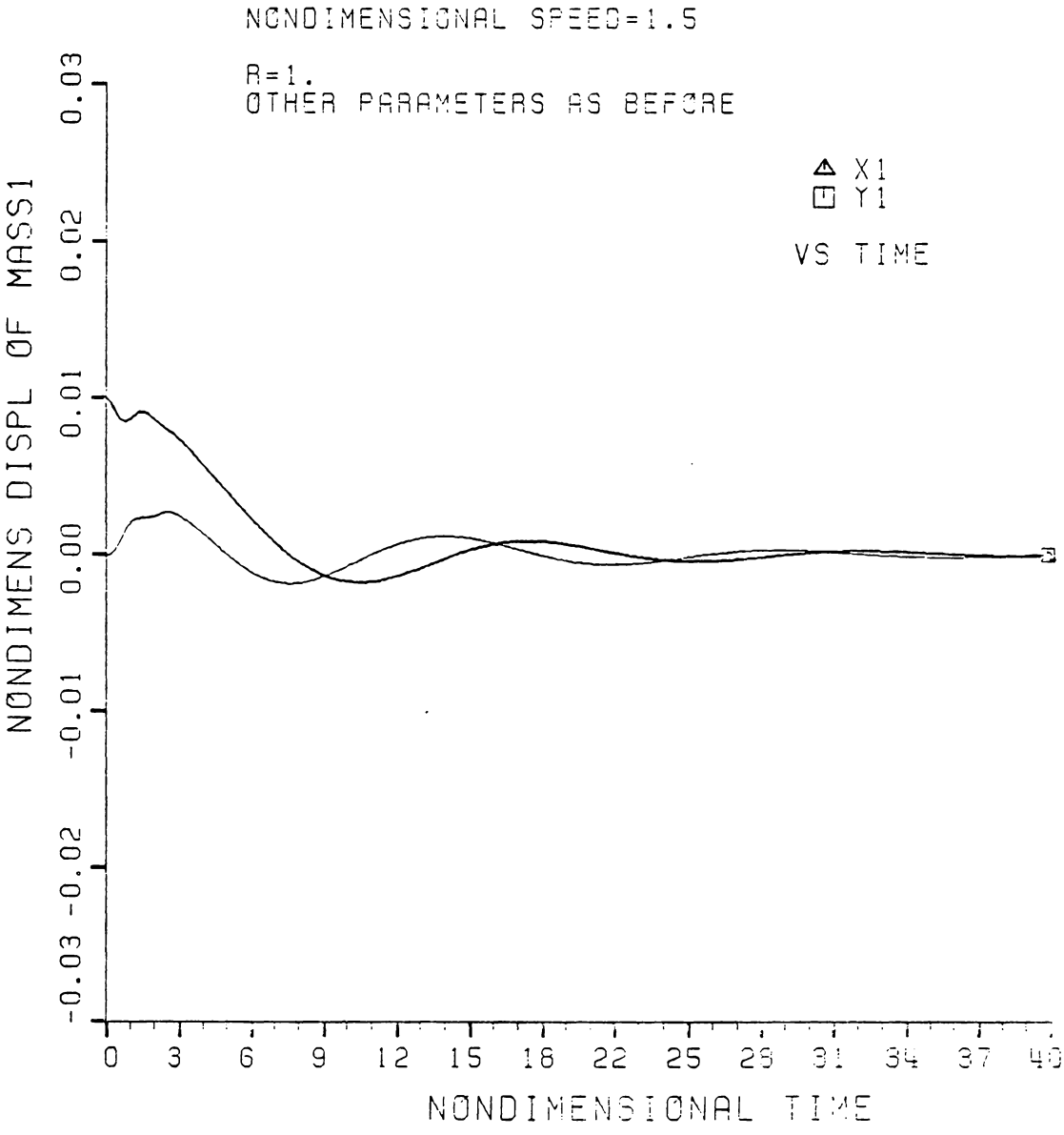

FIGURE 2.31 CONTROLLED TWO MASS SYSTEM:
MASS 1 DISPLACEMENTS

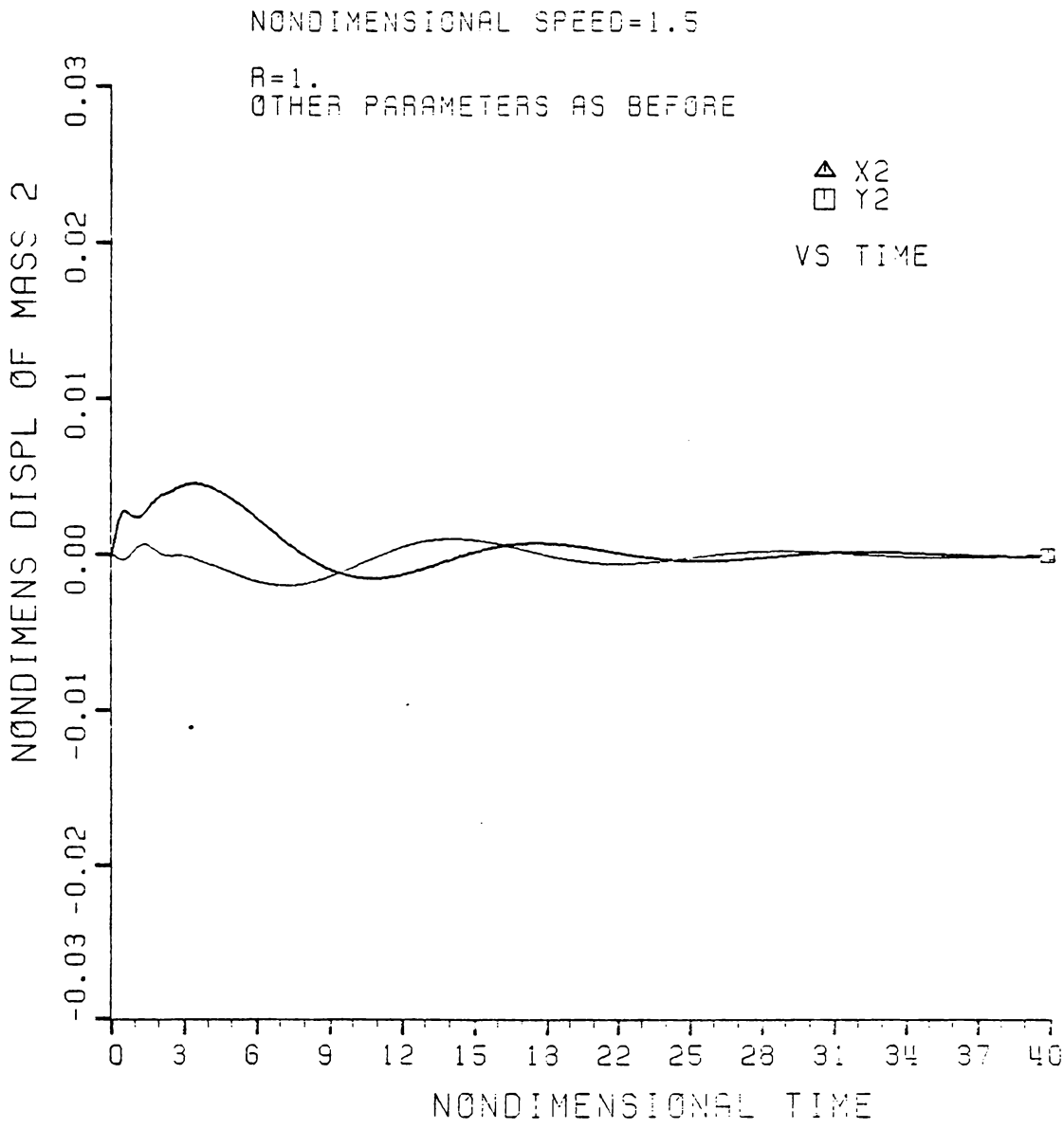

FIGURE 2.32 CONTROLLED TWO MASS SYSTEM: MASS 2 DISPLACEMENTS

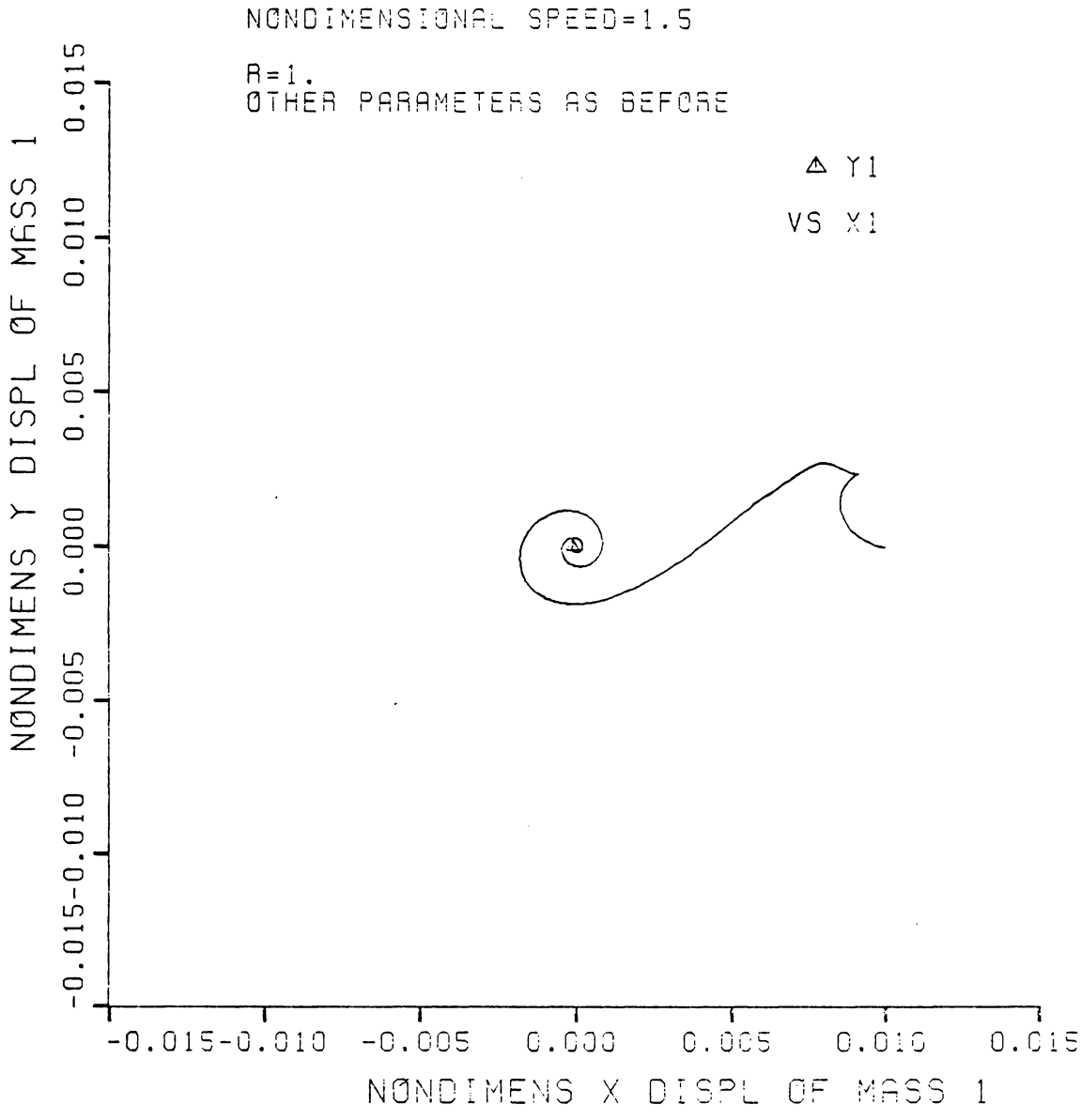

FIGURE 2.33 CONTROLLED TWO MASS SYSTEM:
POLAR PLOT OF MASS1 DISPLACEMENTS

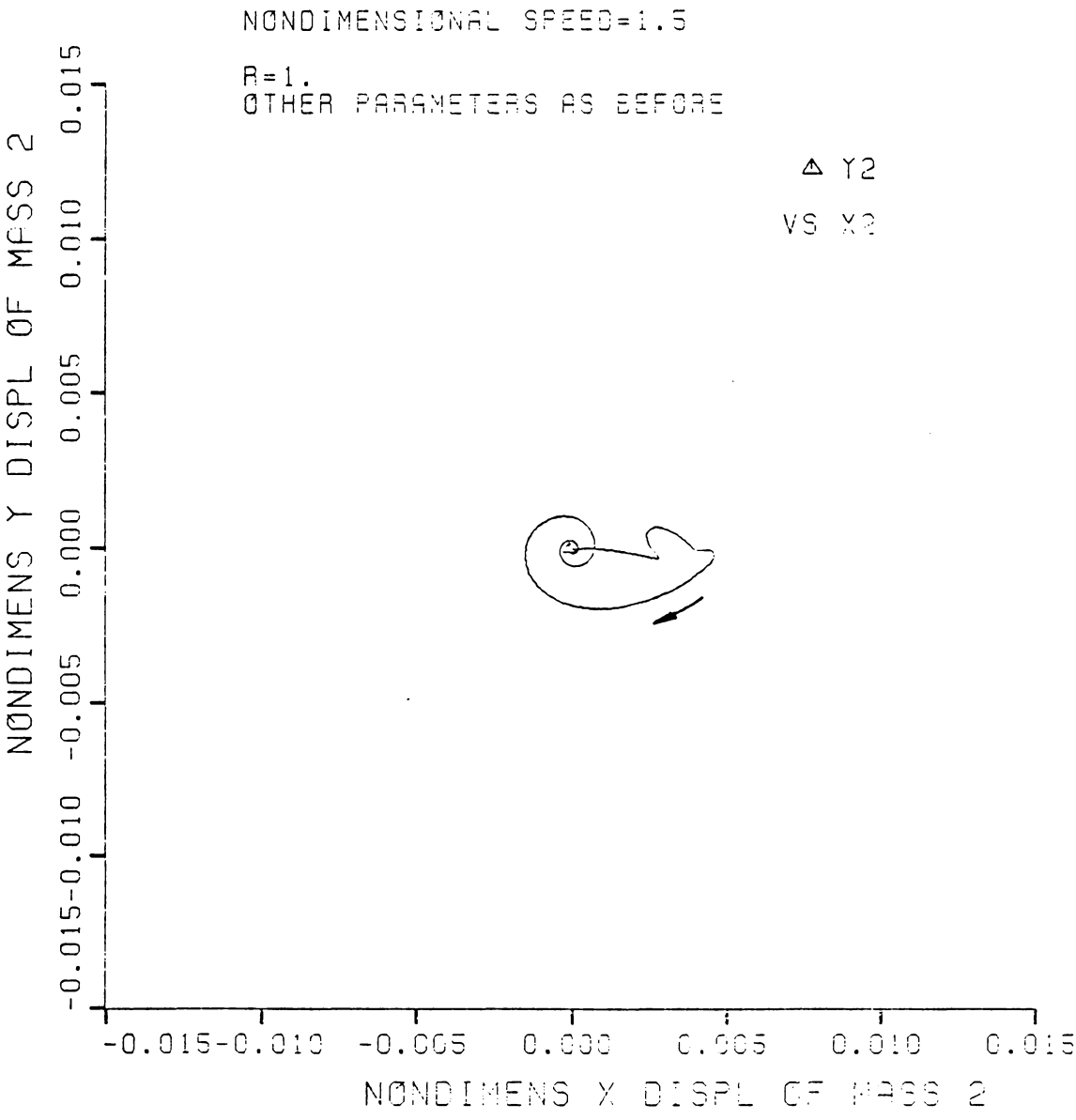

FIGURE 2.34 CONTROLLED TWO MASS SYSTEM:
POLAR PLOT OF MASS2 DISPLACEMENTS

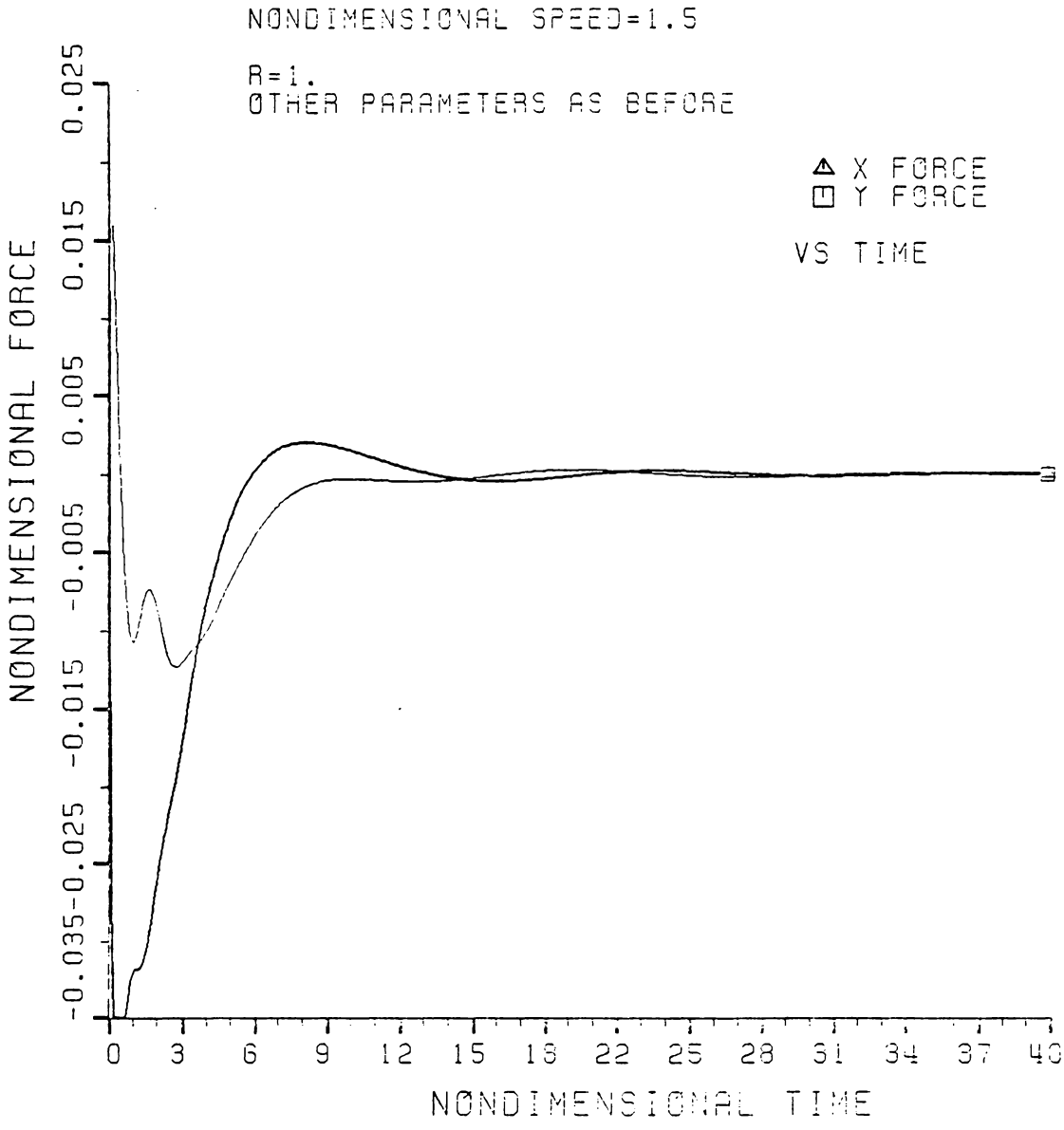

FIGURE 2.35 CONTROLLED TWO MASS SYSTEM: NONDIMENSIONAL FORCE

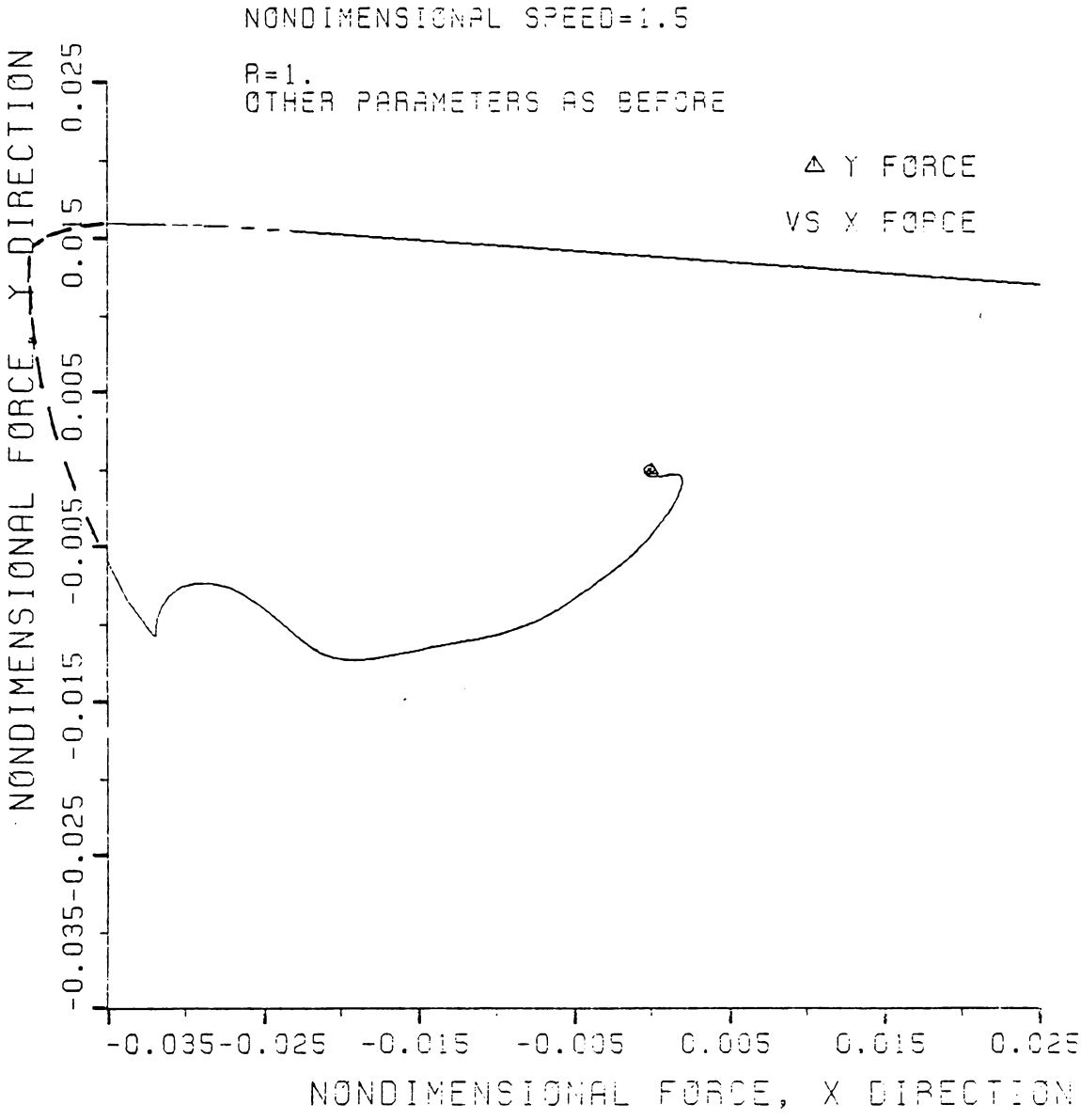

FIGURE 2.36 CONTROLLED TWO MASS SYSTEM:
POLAR PLOT OF FORCE

2.4 DISCUSSION

The following discussion follows the same general subheadings utilized in Section 2.3.

System Stability

From Figure 2.3 it can be gleaned that, at all operating speeds, at least one free system eigenvalue has a positive real part.[1] Consistent with the results mentioned earlier (see reference [9]), this indicates that the uncontrolled rotor has no regimes over which it is stable. Note that the degree of instability is greatly exacerbated at system resonances (Ω = 1.5 and Ω = 5.2)[2]. Application of the feedback force changes the maximum real part of all system eigenvalues from positive to negative at all values of Ω, demonstrating that the controlled system is asymptotically stable.

The peculiar shape of the controlled curve can be readily explained with the aid of Figure 2.37. Since the system has n (n = 3 here) complex degrees of freedom, these are 2n distinct complex eigenvalues.[3] Figure 2.3 is not a plot of any single one of these.

---

[1]Actually, one and only one eigenvalue had a positive real part.

[2]There are two critical frequencies, since the system as modeled has two discrete masses.

[3]Actually, since each dimension in complex space represents two real degrees of freedom, there are 2n = 6 sets of double roots, i.e., 4n = 12 eigenvalues in all (see Appendix E).

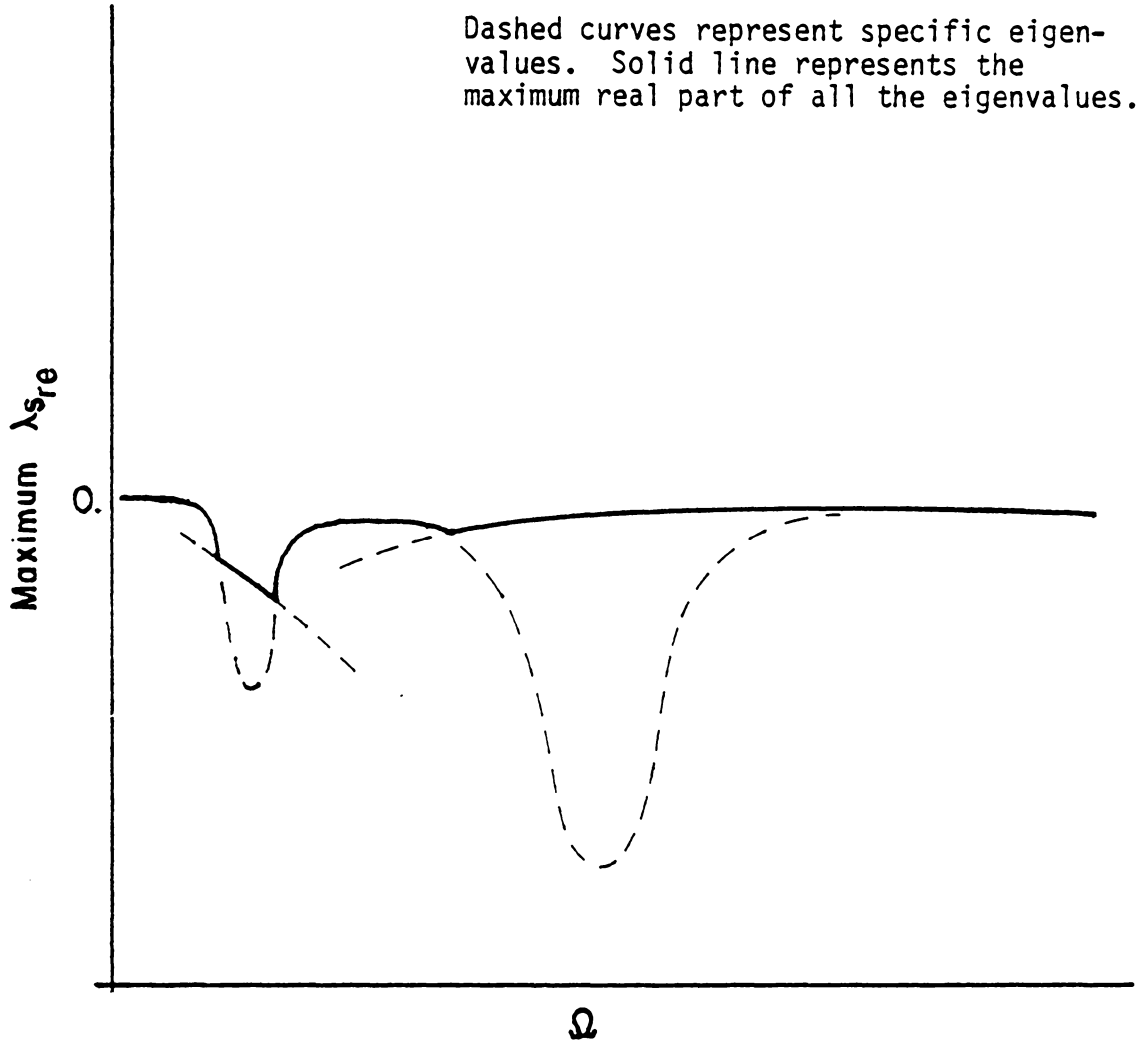

FIGURE 2.37. OBTAINING DOMINANT EIGENVALUE PLOT

Rather, it is a graph in which the maximum $\lambda_{s_{re}}$ (out of all of the n $\lambda_{s_{re}}$'s) is picked out and plotted at each value of Ω.

Figures 2.4-2.6 and 2.7-2.8 display the time histories of the exponentially exploding mass displacements and fluid surface velocity for the uncontrolled system. Figures 2.9-2.13 show similar histories for the controlled system. Note that the latter are unquestionably asymptotically stable, though the polar plots (Figures 2.12 and 2.13) make it clear that the motion is far from simple.

System Gains

Figures 2.14-2.19 represent the respective complex components of the $\{G\}$ vector of equation (2.50). For any given spin speed, greater value of gain on a particular plot (for example gain 2) indicates a greater response by the control force ϕ to a disturbance in the corresponding state vector component (for example, $Y_2(t) = \eta_2(t)$). In short, the gains indicate relative sensitivity of ϕ to individual system disturbances.

Since both the gains and the state vector are complex, some care must be exercised in interpretation. Note particularly that while

$$G_j = G_{re_j} + iG_{im_j}, \quad (j = 1,\ldots n)$$

$$Y_j = Y_{re_j} + iY_{imj},$$

$$\text{and } \phi = \phi_{re} + i\phi_{im}$$

have, by definition, positive signs before their imaginary parts, Y_{im_j}

and ϕ_{im} represent real physical quantities measured in the negative y axis direction.

For instance, since

$$\phi = \phi_x - i\phi_y$$

$$\text{and } Y_1 = \eta_1 = (x_1 - iy_1)/a,$$

$$\phi_y = -\phi_{im} \text{ and } y_1/a = -Y_{im_1}.$$

The gains effectively maximize at system resonances. The slight shifting of real and imaginary peaks results (after the appropriate complex algebraic multiplication) in maximum influence on ϕ at critical speeds.

The behavior of gains 1 and 2 for high spin speed (Ω) results from the fact that the inertial force is directly proportional to the square of the whirl speed (ω), i.e., $F_{inertial} = ma = m\omega^2 R$, where R here can represent either R_1 or R_2. At high speeds ω approaches Ω so that $F_{inertial} \rightarrow m\Omega^2 R$.

Since R reflects displacement from the axis of bearing centers (either of the first two components of the state vector), a control force proportional to R that can "overcome" the given centrifugal force will have to increase with the second power of Ω as Ω gets large. This is the general behavior shown in Figures 2.14 and 2.15.

The feedback force also depends on system velocities. The velocity dependent parts of the control force are proportional to Ω. The third, fourth, and fifth components of the state vector are velocity terms and

as expected, their corresponding gains can be seen to be linearly dependent (albeit slightly) on spin speed.

Feedback Control Force

If the system is being controlled, the state vector must get progressively smaller in time. As the feedback force is directly related to $\{Y(t)\}$ (see equation (2.36)), this means the control force must die out as well. Figures 2.20 and 2.21 illustrate this quite clearly, though once again it is noteworthy that the trajectory is not a simple one.

Influence of Operating Speed

From Figure 2.3, it is obvious that λ_{re} at $\Omega = .5$ is barely greater than zero for the uncontrolled case and barely less than zero for the controlled one. This implies motion that will grow almost imperceptibly in the former case and decay almost as slowly in the latter. Figures 2.22-2.27, when compared to Figures 2.4-2.5, 2.9-2.10, and 2.12-2.13, bear this out.

Control force can be expected to behave in a manner qualitatively similar to that of any given state vector component. Figures 2.28 and 2.29 attest to this, showing a control force which shows little sign of dying out quickly.

Influence of Performance Index Weighting Factors

Changing the value of R in the performance index from 100 to 1 considerably reduces the penalty placed on the control ψ. Increased

weighting will be given to minimization of the state vector which will, at the expense of greater feedback force, decay more rapidly.

Figure 2.30 indicates that this is indeed the case. Maximum λ_{re} for the controlled system is more negative at every spin speed than the corresponding values of Figure 2.3. Figures 2.31-2.34 further corroborate this, showing clearly that the state vector components die out more quickly than in the earlier case. As expected, the control force likewise goes to zero in a very short time (Figures 2.35-2.36).

2.5 DIMENSIONAL EXAMPLE

To obtain some feeling for the magnitudes of the physical gains and forces, the following typical values are used to dimensionalize the two mass model problem.

$\hat{k}_1$ = 20,000 newtons/meter

cup mass, m_1 = 2.5 kilograms

radius to cup inner wall, a = .1 meter

The characteristic values of mass, length, and frequency (inverse of time) are then 2.5 kilograms, .1 meter, and $\sqrt{\hat{k}_1/m_1}$ = 89.44 radians/second, respectively.

This results in the following conversion factors, each of which can be multiplied by the corresponding nondimensional quantity in order to obtain its dimensional equivalent.

Nondimensional Quantity	Multiplying Factor
Displacement	.1 meter
Gains 1,2 (force per unit displacement)	20,000 nwts/meter
Velocity	8.94 meter/sec
Gains 3,4,5 (force per unit velocity)	223.6 nwt-sec/meter
Acceleration	800 meter/sec^2
Gain 6 (force per unit acceleration)	2.5 nwt-sec^2/meter
Force	2,000 newtons

Note that force depends, in general, on the state vector (the displacements, velocities, and fluid acceleration) at each point in time. From the above chart it may at first appear that because physical gains 1 and 2 are much larger than gains 3-6, mass displacements should be almost the sole dictators over feedback force. It should be observed, however, that the multiplying factors for displacements, velocities, and accelerations are inversely proportional to those for their associated gains, so that in effect each component in the state vector makes a significant contribution to the determination of the control force.

In the plots of Section 2.3 the only initial disturbance was taken to be .01 nondimensional displacement in the x direction of the cup. This converts to .1 cm physically, large by control standards. The actual force needed will be considerably less than that shown of course, limited only by the sensitivity of the instrumentation used to measure the state vector components.

For the example at hand, with Ω = 1.5 and R = 100., Figures 2.14-2.21 yield the following results.

Gains	Nondimensional Value	Dimensional Value
1	-.608 + .991i	-12,160 + 19,820i nwts/m
2	.656 + .204i	13,120 + 4080i nwts/m
3	.197 + .615i	44.0 + 137.5i nwt-sec/m
4	-.294 + .121i	-65.7 + 27.1i nwt-sec/m
5	-.269 - .003i	-60.1 - .7i nwt-sec/m
6	.419 - .200i	1.05 - .50i nwt-sec^2/m

Force	Maximum Nondimensional Value	Maximum Dimensional Value
F_x	-.0115	23.0 nwts
F_y	-.0100	20.0 nwts

Since the forces shown are for an initial mass 1 displacement at .1 cm, the maximum values might be better expressed as 23.0 and 20.0 newtons per millimeter initial disturbance.

It is possible to get some feel for the system dynamics by noting that $m_1 R_{1_{max}} \omega^2$, where $R_{1_{max}}$ is the largest displacement the first mass sees, yields a value of approximately 21 newtons. This compares favorably with the control force values F_x and F_y listed above.

2.6 CONCLUSIONS

The rotor system modelled by two discrete cylindrical masses, the first of which is partially filled with ideal fluid, is inherently unstable over all operating speeds. The system has been shown to be

controllable and can be stabilized by introducing a feedback force on the second (fluid free) mass. This latter conclusion is an important one, since, as mentioned in the introduction, it is not at all obvious that this must be the case. It has further been shown that this force can be optimized, i.e., for any given weighting, the performance index can be minimized.

It is also significant that the control force is not a simple function of any one or more of the state vector components. It cannot be determined by a more elementary approach and the extensive analysis and numerical evaluation presented herein are both justifiable and necessary for a complete solution.

CHAPTER III

CONTINUOUS MASS ROTOR

3.1 GOVERNING EQUATIONS

This section generates the differential equations needed to analyze a flexible rotor with a suspension system at each end. The rotor is partially filled with an inviscid incompressible fluid and a control force is applied to the lower suspension mass. The model is similar to that used in Ref. [9] but the development is repeated here for completeness. The equations will again be put in state space form by eliminating the spatial dependence of the fluid variables.

3.1.1 ROTOR EQUATIONS OF MOTION

Consider a long flexible cylinder (mass M, radius a, length L), with rigid masses mounted on the top and bottom ends. Each end of the rotor is supported by a suspension system consisting of linear springs, linear dampers, and a suspension mass (Figure 3.1).

Let $(\hat{\underline{I}}, \hat{\underline{J}}, \hat{\underline{K}})$ be a cartesian coordinate system fixed in space, $(\hat{\underline{i}}, \hat{\underline{j}}, \hat{\underline{k}})$ a cartesian coordinate system spinning about a fixed origin with nondimensional angular velocity $\Omega\hat{\underline{k}}$, $(\hat{\underline{n}}_1, \hat{\underline{n}}_2, \hat{\underline{n}}_3)$ a cartesian coordinate system spinning with nondimensional angular velocity Ω in the $\hat{\underline{k}}$ direction and oriented so that $\hat{\underline{n}}_3$ is along the line joining the centers of the two end masses, $(\hat{\underline{d}}_1, \hat{\underline{d}}_2, \hat{\underline{d}}_3)$ a coordinate system fixed in an arbitrary disk located at a point ζ along the rotor (see

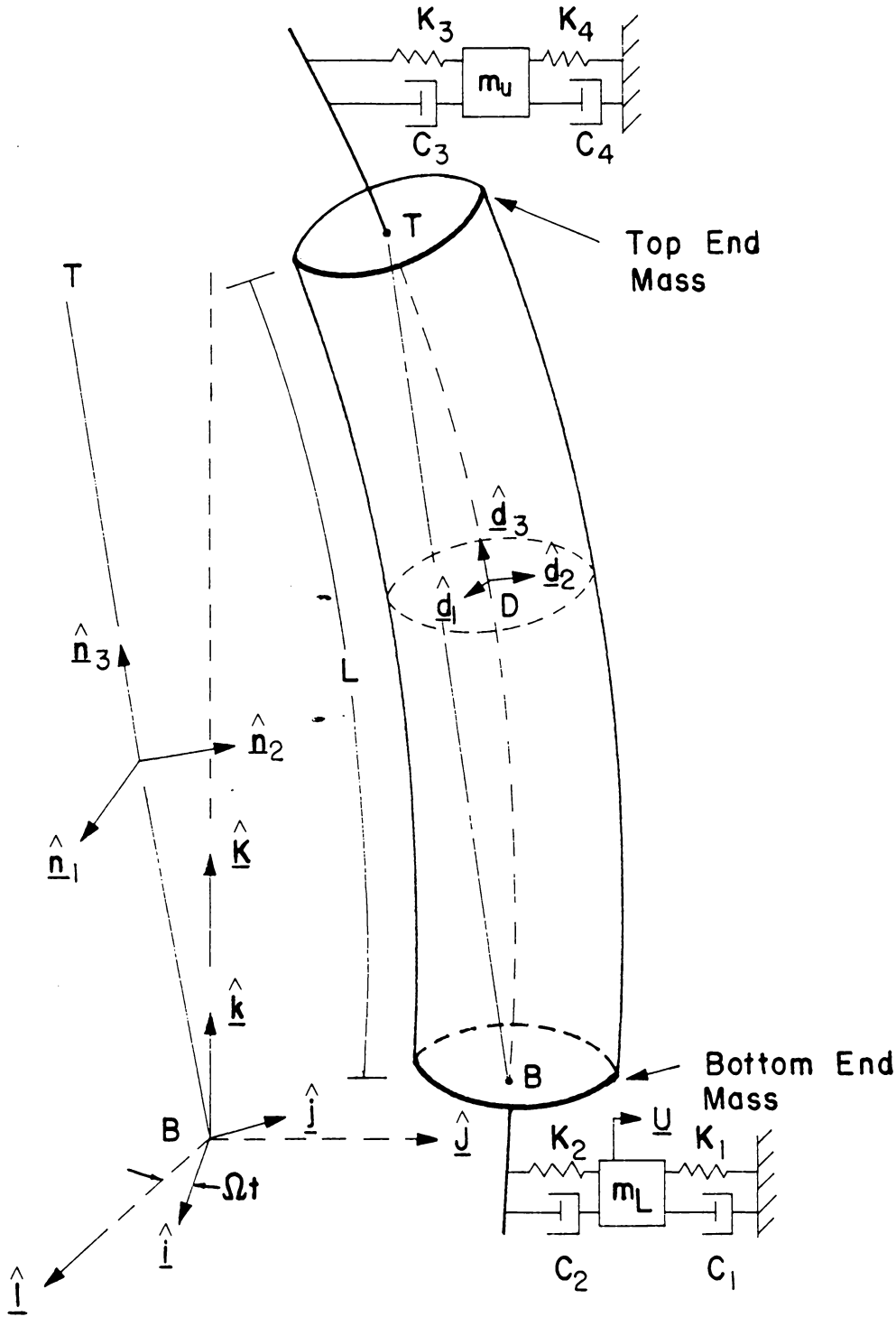

FIGURE 3.1 FLEXIBLE ROTOR MODEL AND COORDINATE SYSTEMS

Figure 3.1), and $(\hat{r}, \hat{\theta}, \hat{z})$ a cylindrical coordinate system fixed to $(\hat{d}_1, \hat{d}_2, \hat{d}_3)$.

ϕ_2, ϕ_1, α, and β are the 3-2-1 Euler angles which orient the $(\hat{n}_1,\hat{n}_2,\hat{n}_3)$ to $(\hat{i}, \hat{j}, \hat{k})$ and $(\hat{d}_1,\hat{d}_2,\hat{d}_3)$ to $(\hat{n}_1,\hat{n}_2,\hat{n}_3)$ systems respectively. Note that in each case the first rotation (i.e., "3" in the 3-2-1 sequence) is zero (see Figure 3.2)

The following relationships exist:

$$\begin{Bmatrix} \hat{r} \\ \hat{\theta} \\ \hat{z} \end{Bmatrix} = \begin{bmatrix} \cos\theta & \sin\theta & 0 \\ -\sin\theta & \cos\theta & 0 \\ 0 & 0 & 1 \end{bmatrix} \begin{Bmatrix} \hat{d}_1 \\ \hat{d}_2 \\ \hat{d}_3 \end{Bmatrix} ; \begin{Bmatrix} \hat{i} \\ \hat{j} \\ \hat{k} \end{Bmatrix} = \begin{bmatrix} \cos\Omega t & \sin\Omega t & 0 \\ -\sin\Omega t & \cos\Omega t & 0 \\ 0 & 0 & 1 \end{bmatrix} \begin{Bmatrix} \hat{I} \\ \hat{J} \\ \hat{K} \end{Bmatrix} \tag{3.1a,b}$$

$$\begin{Bmatrix} \hat{n}_1 \\ \hat{n}_2 \\ \hat{n}_3 \end{Bmatrix} = \begin{bmatrix} 1 & 0 & 0 \\ 0 & \cos\phi_1 & \sin\phi_1 \\ 0 & -\sin\phi_1 & \cos\phi_2 \end{bmatrix} \begin{bmatrix} \cos\phi_2 & 0 & -\sin\phi_2 \\ 0 & 1 & 0 \\ \sin\phi_2 & 0 & \cos\phi_2 \end{bmatrix} \begin{matrix} \hat{i} \\ \hat{j} \\ \hat{k} \end{matrix}$$

$$= \begin{bmatrix} \cos\phi_2 & 0 & -\sin\phi_2 \\ \sin\phi_1\sin\phi_2 & \cos\phi_1 & \sin\phi_1\cos\phi_2 \\ \cos\phi_1\sin\phi_2 & -\sin\phi_1 & \cos\phi_1\cos\phi_2 \end{bmatrix} \begin{Bmatrix} \hat{i} \\ \hat{j} \\ \hat{k} \end{Bmatrix} \tag{3.1c}$$

$$\begin{Bmatrix} \hat{d}_1 \\ \hat{d}_2 \\ \hat{d}_3 \end{Bmatrix} = \begin{bmatrix} 1 & 0 & 0 \\ 0 & \cos\beta & \sin\beta \\ 0 & -\sin\beta & \cos\beta \end{bmatrix} \begin{bmatrix} \cos\alpha & 0 & -\sin\alpha \\ 0 & 1 & 0 \\ \sin\alpha & 0 & \cos\alpha \end{bmatrix} \begin{Bmatrix} \hat{n}_1 \\ \hat{n}_2 \\ \hat{n}_3 \end{Bmatrix}$$

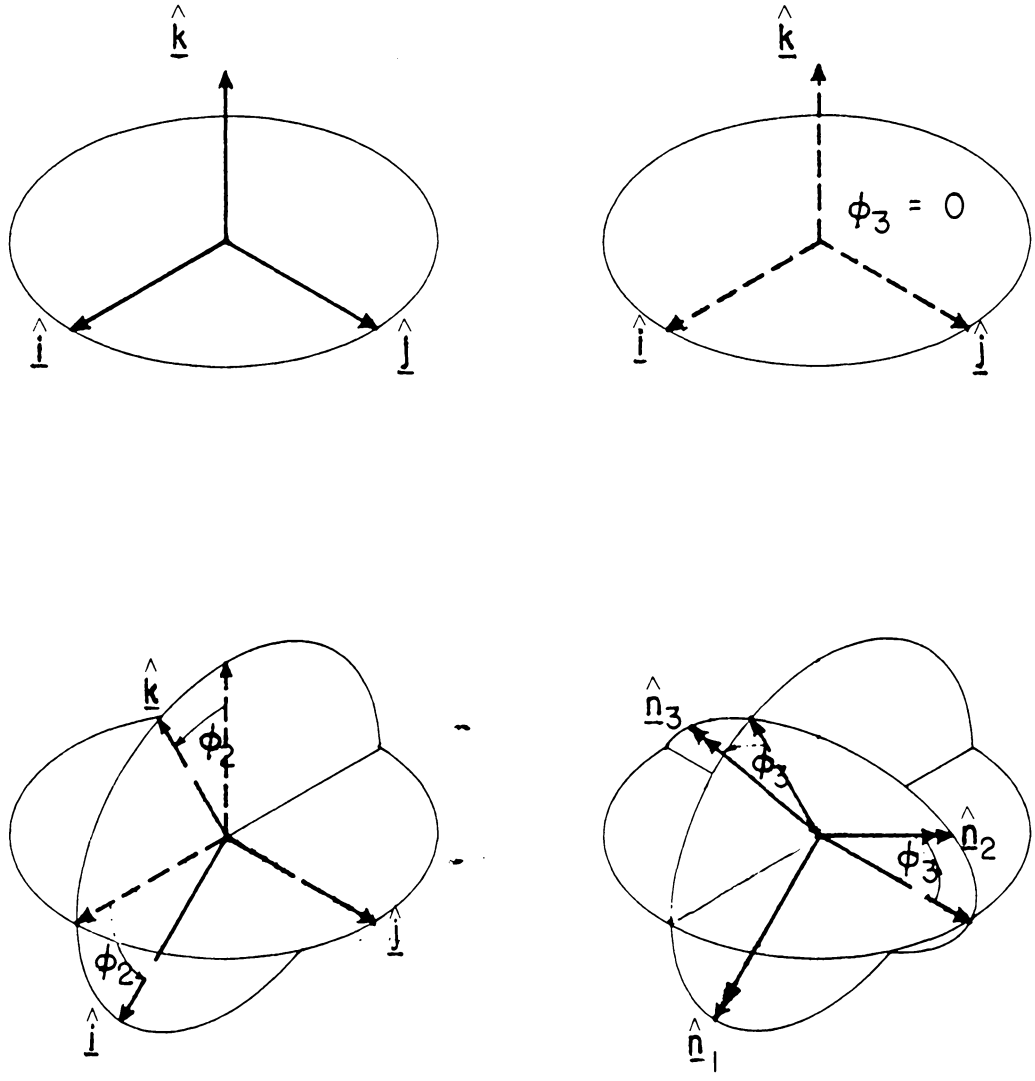

To relate $(\hat{d}_1, \hat{d}_2, \hat{d}_3)$ to $(\hat{n}_1, \hat{n}_2, \hat{n}_3)$ make the following substitutions:

$(\hat{i}, \hat{j}, \hat{k})$ above to $(\hat{n}_1, \hat{n}_2, \hat{n}_3)$

$(\hat{n}_1, \hat{n}_2, \hat{n}_3)$ above to $(\hat{d}_1, \hat{d}_2, \hat{d}_3)$

ϕ_2 to α

ϕ_1 to β

FIGURE 3.2. EULER ANGLE ORIENTATIONS

$$= \begin{bmatrix} \cos\alpha & 0 & -\sin\alpha \\ \sin\alpha\sin\beta & \cos\beta & \sin\beta\cos\alpha \\ \sin\alpha\cos\beta & -\sin\beta & \cos\alpha\cos\beta \end{bmatrix} \begin{Bmatrix} \hat{\underline{n}}_1 \\ \hat{\underline{n}}_2 \\ \hat{\underline{n}}_3 \end{Bmatrix} \qquad (3.1d)$$

The rotor is made up of the following elements nondimensionalized by M (the mass of the rotor), a (the rotor radius), and $\omega_o = [Ea/M]^{1/2}$ (E is the Young's Modulus of the rotor).

m_L = nondimensional mass of lower suspension (i.e., = [dimensional m_L]/M)

m_u = nondimensional mass of upper suspension

m_{bot} = nondimensional mass of bottom end mass

m_{top} = nondimensional mass of the top end mass

I_{bot} = nondimensional transverse moment of inertia of bottom end mass [dimensional I_{bot}]/Ma^2)

I_{top} = nondimensional transverse moment of inertia of top end mass

J_{bot} = nondimensional polar moment of inertia of bottom end mass

J_{top} = nondimensional polar moment of inertia of top end mass

J_{rot} = nondimensional polar moment of inertia of rotor

EI = Young's Modulus times the area moment of inertia [dimensional EI]/$\omega_o^2 Ma^3$)

k'GA = shear shape factor times the shear modulus times the cross-sectional area ([dimensional k'GA]/$\omega_o^2 Ma$)

K_1-K_4 = suspension stiffness coefficients (e.g., [dimensional K_1]/$\omega_o^2 M$)

C_1-C_4 = suspension damping coefficients (e.g. [dimensional C_1]$\omega_o M$)

The other nondimensional inputs important in the problem are

$$\Omega = \Omega^*/\omega_0 \; ; \; f = b/a \; ; \; z_0 = L/a \; ; \; \mu = \pi\rho a^2 L/M. \qquad (3.2a\text{-}b)$$

The nondimensional independent spatial variables are

$$r = r^*/a \; ; \; \zeta = z/a.$$

There are twelve nondimensional coordinates associated with the model (see Figure 3.1). These are expressed in terms of the $(\hat{i},\hat{j},\hat{k})$ system, since that is the system in which the equations of motion will be written. They describe the position of the lower suspension mass, the position of the upper suspension mass, the position of the bottom of the rotor, the rotational orientation of the rotor fixed coordinate system $(\hat{n}_1,\hat{n}_2,\hat{n}_3)$, and the translation and rotation of the rotor as a function of ζ due to bending and shear deformation. The coordinates are:

$x_L(t)$, $y_L(t)$ — translation of the lower suspension mass

$x_u(t)$, $y_u(t)$ — translation of the upper suspension mass

$x_B(t)$, $y_B(t)$ — translation of the rotor base point

$\phi_2(t)$, $\phi_1(t)$ — Euler angles orienting the rotor fixed coordinate system

$x(\zeta,t)$, $y(\zeta,t)$ — deflection of the rotor due to bending and shear deformation (with respect to $\hat{n}_3$ but in terms of $(\hat{i},\hat{j},\hat{k})$)

$\alpha(\zeta,t)$, $\beta(\zeta,t)$ — rotation of the rotor due to bending and shear deformation (note that bending and shear take place in two directions, i.e., not plane beam bending, and each angle includes both bending and shear effects)

The position and velocity of the lower suspension mass relative to the

inertial frame $(\hat{I},\hat{J},\hat{K})$ but measured in the $(\hat{i},\hat{j},\hat{k})$ coordinate system are:

$$\underline{R}_L = x_L\hat{i} + y_L\hat{j} \tag{3.3a}$$

$$\dot{\underline{R}}_L = (\dot{x}_L - \Omega y_L)\hat{i} + (\dot{y}_L + \Omega x_L)\hat{j}. \tag{3.3b}$$

The position and velocity of the upper suspension mass are:

$$\underline{R}_u = x_u\hat{i} + y_u\hat{j} \tag{3.4a}$$

$$\dot{\underline{R}}_u = (\dot{x}_u - \Omega y_u)\hat{i} + (\dot{y}_u + \Omega x_u)\hat{j}. \tag{3.4b}$$

The position and velocity of the bottom end mass are:

$$\underline{R}_B = x_B\hat{i} + y_B\hat{j} \tag{3.5a}$$

$$\dot{\underline{R}}_B = (\dot{x}_B - \Omega y_B)\hat{i} + (\dot{y}_B + \Omega x_B)\hat{j}. \tag{3.5b}$$

The position and velocity of the top end mass are (using (3.1c) to express $\hat{n}_3$ and linearizing for small ϕ_1,ϕ_2):

$$\underline{R}_T = \underline{R}_B + z_o\hat{n}_3$$

$$= (x_B + z_o\phi_2)\hat{i} + (y_B - z_o\phi_1)\hat{j} + z_o\hat{k} \tag{3.6a}$$

$$\dot{\underline{R}}_T = (\dot{x}_B + z_o\dot{\phi}_2 - \Omega[y_B - z_o\phi_1])\hat{i} + (\dot{y}_B - z_o\dot{\phi}_1 + \Omega[x_B + z_o\phi_2])\hat{j}. \tag{3.6b}$$

The position and velocity of an arbitrary disk located at point ζ along the rotor are (again using (3.1c) and linearizing for small x,y as well as ϕ_1,ϕ_2):

$$\underline{R}_D = \underline{R}_B + x\hat{\underline{n}}_1 + y\hat{\underline{n}}_2 + \zeta\hat{\underline{n}}_3$$

$$= (x_B+x+\zeta\phi_2)\hat{\underline{i}} + (y_B+y-\zeta\phi_1)\hat{\underline{j}} + \zeta\hat{\underline{k}} \tag{3.7a}$$

$$\dot{\underline{R}}_D = (\dot{x}_B+\dot{x}+\zeta\dot{\phi}_2-\Omega[y_B+y-\zeta\phi_1])\hat{\underline{i}} + (\dot{y}_B+\dot{y}-\zeta\dot{\phi}_1+\Omega[x_B+x+\zeta\phi_2])\hat{\underline{j}}. \tag{3.7b}$$

To incorporate the discrete springs and dampers, the following position and velocity vectors will also be needed:

$$\underline{R}_1 = \underline{R}_L = x_L\hat{\underline{i}} + y_L\hat{\underline{j}} \tag{3.8a}$$

$$\underline{R}_2 = \underline{R}_B - \underline{R}_L = (x_B-x_L)\hat{\underline{i}} + (y_B-y_L)\hat{\underline{j}} \tag{3.8b}$$

$$\underline{R}_3 = \underline{R}_T - \underline{R}_u = \underline{R}_B + z_o\hat{\underline{n}}_3 - z_o\hat{\underline{k}} - \underline{R}_u \tag{3.8c}$$

$$= (x_B+z_o\phi_2-x_u)\hat{\underline{i}} + (y_B-z_o\phi_1-y_u)\hat{\underline{j}} \tag{3.8d}$$

$$\underline{R}_4 = \underline{R}_u = x_u\hat{\underline{i}} + y_u\hat{\underline{j}} \tag{3.8e}$$

$$\dot{\underline{R}}_1 = (\dot{x}_L-\Omega y_L)\hat{\underline{i}} + (\dot{y}_L + \Omega x_L)\hat{\underline{j}} \tag{3.8f}$$

$$\dot{\underline{R}}_2 = (\dot{x}_B-\dot{x}_L-\Omega[y_B-y_L])\hat{\underline{i}} + (\dot{y}_B-\dot{y}_L+\Omega[x_B-x_L])\hat{\underline{j}} \tag{3.8g}$$

$$\dot{\underline{R}}_3 = (\dot{x}_B+z_o\dot{\phi}_2-\dot{x}_u-\Omega[y_B-z_o\phi_1-y_u])\hat{\underline{i}} + (\dot{y}_B-z_o\dot{\phi}_1-\dot{y}_u+\Omega[x_B+z_o\phi_2-x_u])\hat{\underline{j}} \tag{3.8h}$$

$$\dot{\underline{R}}_4 = (\dot{x}_u-\Omega y_u)\hat{\underline{i}} + (\dot{y}_u+\Omega x_u)\hat{\underline{j}}. \tag{3.8i}$$

Using the vector time differentiation law again, this time on $\dot{\underline{R}}_D$ (3.7b), the acceleration of point D is found to be

$$\ddot{\underline{R}}_D = (\ddot{x}_B+\ddot{x}+\zeta\ddot{\phi}_2-2\Omega[\dot{y}_B+\dot{y}-\zeta\dot{\phi}_1]-\Omega^2[x_B+x+\zeta\phi_2])\hat{\underline{i}}$$

$$+ (\ddot{y}_B+\ddot{y}-\zeta\ddot{\phi}_1+2\Omega[\dot{x}_B+\dot{x}+\zeta\dot{\phi}_2]-\Omega^2[y_B+y-\zeta\phi_1])\hat{\underline{j}}. \qquad (3.9)$$

The position vector which locates a point in the fluid on the disk formed by $\hat{\underline{d}}_1$ and $\hat{\underline{d}}_2$ with respect to point D is

$$\underline{r} = r\hat{\underline{r}} = r\cos\theta\hat{\underline{d}}_1 + r\sin\theta\hat{\underline{d}}_2.$$

With (3.1d) and the appropriate linearization this becomes

$$\underline{r} = r\hat{\underline{r}} = r\cos\theta\ \hat{\underline{n}}_1 + r\sin\theta\ \hat{\underline{n}}_2 + r[\beta\sin\theta-\alpha\cos\theta]\hat{\underline{n}}_3. \qquad (3.10)$$

Since angular velocities are additive from frame to frame, the angular velocity of $(\hat{\underline{n}}_1,\hat{\underline{n}}_2,\hat{\underline{n}}_3)$ relative to $(\hat{\underline{I}},\hat{\underline{J}},\hat{\underline{K}})$ is

$$\underline{\omega}^n = \Omega\hat{\underline{k}} + \dot{\phi}_2\hat{\underline{j}} + \dot{\phi}_1\hat{\underline{n}}_1. \qquad (3.11)$$

Similarly the angular velocity of $(\hat{\underline{d}}_1,\hat{\underline{d}}_2,\hat{\underline{d}}_3)$ is

$$\underline{\omega}^d = \underline{\omega}^n + \dot{\alpha}\hat{\underline{n}}_2 + \dot{\beta}\hat{\underline{d}}_1. \qquad (3.12)$$

In converting $\underline{\omega}_d$ to $(\hat{\underline{d}}_1,\hat{\underline{d}}_2,\hat{\underline{d}}_3)$ system components, it is necessary to retain terms up to second order. The reason for this becomes more apparent later when $\underline{\omega}_d$ is used in Lagrange's equation.

$$\underline{\omega}^d = (\dot{\phi}_1+\dot{\beta}-\Omega[\phi_2+\alpha])\hat{\underline{d}}_1 + (\dot{\phi}_2+\dot{\alpha}+\Omega[\phi_1+\beta])\hat{\underline{d}}_2$$

$$+ (\Omega+\alpha\dot{\phi}_1-\beta\dot{\phi}_2-\beta\dot{\alpha}-\dot{\phi}_2\phi_1-\Omega[\alpha\phi_2+\beta\phi_1] - \frac{\Omega}{2}[\alpha^2+\beta^2+\phi_2^2+\phi_1^2])\hat{\underline{d}}_3.$$

To first order

$$\underline{\omega}^d = (\dot{\phi}_1+\dot{\beta}-\Omega[\phi_2+\alpha])\hat{\underline{d}}_1 + [\dot{\phi}_2+\dot{\alpha}+\Omega[\phi_1+\beta])\hat{\underline{d}}_2 + \Omega\hat{\underline{d}}_3 \tag{3.14}$$

$$\dot{\underline{\omega}}^d = (\ddot{\phi}_1+\ddot{\beta}-\Omega[\dot{\phi}_2+\dot{\alpha}])\hat{\underline{d}}_2 + (\ddot{\phi}_2+\ddot{\alpha}+\Omega[\dot{\phi}_1+\dot{\beta}])\hat{\underline{d}}_2 \tag{3.15}$$

where $\dot{\underline{\omega}}^d$ was found using the vector differentiation rule again.

The rotor deflection and rotation coordinates are expanded in a complete set of functions,

$$x(\zeta,\tau) = \sum_{j=1}^{N} x_j(\tau)\phi_j(\zeta) \; ; \quad y(\zeta,\tau) = \sum_{j=1}^{N} y_j(\tau)\phi_j(\zeta) \tag{3.16a,b}$$

$$\alpha(\zeta,\tau) = \sum_{j=1}^{N} \alpha_j(\tau)\phi_j'(\zeta) \; ; \quad \beta(\zeta,\tau) = \sum_{j=1}^{N} \beta_j(\tau)\phi_j'(\zeta) \tag{3.16c,d}$$

where

$$\phi_j(\zeta) = \sqrt{2/z_o}\,\sin(j\pi\zeta/z_o) \; ; \; \phi_j'(\zeta) = \frac{d}{d\zeta}\,\phi_j(\zeta).$$

The constant term $\sqrt{2/z_o}$ was selected so that

$$\int_o^{z_o} \phi_j^2 d\zeta = 1.$$

The kinetic energy, T, the dissipation function D, and the potential energy V are written as functions of x_L, y_L, x_u, y_u, x_B, y_B, ϕ_2, ϕ_1, $x_j(j=1,N)$, $y_j(j=1,N)$, $\alpha_j(j=1,N)$, and $\beta_j(j=1,N)$.

$$T = \frac{1}{2}\,m_L\dot{\underline{R}}_L\cdot\dot{\underline{R}}_L + \frac{1}{2}\,m_u\dot{\underline{R}}_u\cdot\dot{\underline{R}}_u + \frac{1}{2}\,m_{bot}\dot{\underline{R}}_B\cdot\dot{\underline{R}}_B$$

$$+ \frac{1}{2}\,m_{top}\dot{\underline{R}}_T\cdot\dot{\underline{R}}_T + \frac{1}{2z_o}\int_o^{z_o} \dot{\underline{R}}_D\cdot\dot{\underline{R}}_D d\zeta + \frac{1}{2}\,\underline{\omega}^d(\zeta=0)\cdot\underline{\underline{I}}_{bot}\cdot\underline{\omega}^d(\zeta=0)$$

$$+ \frac{1}{2}\,\underline{\omega}^{d}(\zeta=z_o)\cdot\underline{I}_{top}\cdot\underline{\omega}^{d}(\zeta=z_o) + \frac{1}{2}\int_{o}^{z_o}\underline{\omega}^{d}(\zeta)\cdot\underline{\underline{I}}_{rot}\cdot\underline{\omega}^{d}(\zeta)d\zeta \quad (3.17)$$

where

$$\underline{\underline{I}}_{bot} = \begin{bmatrix} I_{bot} & 0 & 0 \\ 0 & I_{bot} & 0 \\ 0 & 0 & J_{bot} \end{bmatrix} ; \quad \underline{\underline{I}}_{top} = \begin{bmatrix} I_{top} & 0 & 0 \\ 0 & I_{top} & 0 \\ 0 & 0 & J_{top} \end{bmatrix} \quad (3.18a,b)$$

$$\underline{\underline{I}}_{rot} = \begin{bmatrix} J_{rot}/2z_o & 0 & 0 \\ 0 & J_{rot}/2z_o & 0 \\ 0 & 0 & J_{rot}/z_o \end{bmatrix} \quad (3.18c)$$

$$D = \frac{1}{2}\,C_1\dot{\underline{R}}_1\cdot\dot{\underline{R}}_1 + \frac{1}{2}\,C_2\dot{\underline{R}}_2\cdot\dot{\underline{R}}_2 + \frac{1}{2}\,C_3\dot{\underline{R}}_3\cdot\dot{\underline{R}}_3 + \frac{1}{2}\,C_4\dot{\underline{R}}_4\cdot\dot{\underline{R}}_4 \quad (3.19)$$

$$V = \frac{1}{2}\,K_1\underline{R}_1\cdot\underline{R}_1 + \frac{1}{2}\,K_2\underline{R}_2\cdot\underline{R}_2 + \frac{1}{2}\,K_3\underline{R}_3\cdot\underline{R}_3 + \frac{1}{2}\,K_4\underline{R}_4\cdot\underline{R}_4$$

$$+ \frac{1}{2}\int_{o}^{z_o} EI\left[\left(\frac{\partial\alpha}{\partial\zeta}\right)^2 + \left(\frac{\partial\beta}{\partial\zeta}\right)^2\right]d\zeta + \frac{1}{2}\int_{o}^{z_o} k'GA\left[\left(\frac{\partial x}{\partial\zeta} - \alpha\right)^2 + \left(\frac{\partial y}{\partial\zeta} + \beta\right)^2\right]d\zeta. \quad (3.20)$$

The 5th and 6th terms in (3.20) are due to bending and shear respectively.

The equations of motion follow from Lagrange's Equations, where it is noted that, as before, all $P_n e^{in\theta}$ terms in the pressure expansion where $n \neq 1$ drop out during integration, and P_1 is taken as simply P.

$$\frac{d}{dt}\left[\frac{\partial T}{\partial \dot{q}}\right] + \frac{\partial D}{\partial \dot{q}} - \frac{\partial T}{\partial q} + \frac{\partial V}{\partial q} = \int_0^{z_o}\int_0^{2\pi} \frac{\partial}{\partial q}\,(\underline{R}_D+\underline{r})\cdot \mathrm{Re}\{P(r=1,t)e^{i\theta}\}\,d\theta d\zeta\,[\cos\theta\,\hat{\underline{d}}_1 + \sin\theta\,\hat{\underline{d}}_2] + \frac{\partial \underline{R}_L}{\partial q}\cdot\underline{U} \tag{3.21}$$

q represents any of the 4N+8 coordinates. The nondimensional entrapped fluid pressure $\mathrm{Re}\{Pe^{i\theta}\}$ and control force $\underline{U}=U_x\hat{\underline{i}}+U_y\hat{\underline{j}}$ are generalized forces acting on the system.

These 4N+8 second-order differential equations are written as 2N+4 complex equations (see Appendix F). Define the (2N+4)x1 vectors $\{X\}$, $\{Q\}$, and $\{E''\}$ such that:

$$X = \begin{Bmatrix} \eta_L \\ \eta_u \\ \eta_B \\ \phi \\ \eta_j \quad j=1,N \\ \xi_j \quad j=1,N \end{Bmatrix} = \begin{Bmatrix} x_L - iy_L \\ x_u - iy_u \\ x_B - iy_B \\ \phi_1 - i\phi_2 \\ x_j - iy_j \quad j=1,N \\ \beta_j - i\alpha_j \quad j=1,N \end{Bmatrix}; \tag{3.22a}$$

$$\{Q\} = \begin{Bmatrix} 0 \\ 0 \\ 1 \\ -iz_o/2 \\ \frac{1}{j\pi}\sqrt{\frac{2}{z_o}}\,[1-(-1)^j] \quad j=1,N \\ 0 \quad j=1,N \end{Bmatrix} \tag{3.22b}$$

$$\{E''\} = \begin{Bmatrix} 1 \\ 0 \\ 0 \\ 0 \\ 0 \quad j=1,N \\ 0 \quad j=1,N \end{Bmatrix} \tag{3.22c}$$

where the index j runs from 1 to N.

Then the equations of motion for the rotor are written as

$$[M]\{\ddot{X}\} + [C]\{\dot{X}\} + [K]\{X\} = \underset{\sim}{\pi} z_0 P(r=1,t)\{Q\} + \psi\{E''\} \tag{3.23}$$

where [M], [C], and [K] are (2N+4) by (2N+4) matrices (see Appendix F), and $\psi = U_x - iU_y$ is the nondimensional control force (equation (2.8)) to be determined.

3.1.2 FLUID EQUATIONS OF MOTION

The nondimensional acceleration vector relative to ground of any point p in the fluid is

$$\underline{A}^p = \ddot{\underline{R}}_D + \dot{\underline{\omega}}^d x \underline{r} + \underline{\omega}^d x (\underline{\omega}^d x \underline{r}) + \Omega^2 \underline{r} + \dot{\underline{q}} + (\underline{\nabla} \cdot \underline{q})\underline{q} \tag{3.24}$$

where, similar to Chapter II, the last two terms are the Eulerian representation of the acceleration relative to the $(\hat{\underline{d}}_1, \hat{\underline{d}}_2, \hat{\underline{d}}_3)$ frame. If second and higher order terms are dropped, (3.9), (3.10), (3.14), (3.15) used, and all basis vectors converted to the $(\hat{\underline{d}}_1, \hat{\underline{d}}_2, \hat{\underline{d}}_3)$ system via (3.1c) and (3.1d), the result is

$$\underline{A}^p = (\ddot{x}_B+\ddot{x}+\zeta\ddot{\phi}_2-2\Omega[\dot{y}_B+\dot{y}-\zeta\dot{\phi}_1]-\Omega^2[x_B+x+\zeta\phi_2])\hat{\underline{d}}_1$$

$$+ (\ddot{y}_B+\ddot{y}-\zeta\ddot{\phi}_1+2\Omega[\dot{x}_B+\dot{x}+\zeta\dot{\phi}_2]-\Omega^2[y_B+y-\zeta\phi_1])\hat{\underline{d}}_2 \qquad (3.25)$$

$$+ r(\sin\theta(\ddot{\beta}+\ddot{\phi}_1+\Omega^2(\beta+\phi_1)]-\cos\theta[\ddot{\alpha}+\ddot{\phi}_2+\Omega^2(\alpha+\phi_1)]\hat{\underline{d}}_3 + \dot{\underline{q}}$$

The nondimensional fluid momentum and continuity equations are then

$$\underline{A}^p + \frac{1}{\rho}\underline{\nabla}P(r,\theta,t) = 0. \qquad (3.26a)$$

$$\underline{\nabla}\cdot\underline{q} = 0 \qquad (3.26b)$$

From here the development parallels that of Section 2.1.2. The linearized two dimensional fluid equations reduce, in complex notation to:

$$\dot{u}(r,t) - 2\Omega v(r,t) + \frac{\pi z_o}{\mu}\frac{\partial P(r,t)}{\partial r}[\{\ddot{X}\}^T-2i\Omega\{\dot{X}\}^T-\Omega^2\{X\}^T]\{Q^\dagger\} = 0 \qquad (3.27a)$$

$$\dot{v}(r,t) + 2\Omega u(r,t) + \frac{i\pi z_o}{\mu r}P(r,t) + i[\{\ddot{X}\}^T-2i\Omega\{\dot{X}\}^T-\Omega^2\{X\}^T]\{Q^\dagger\} = 0 \qquad (3.27b)$$

$$\frac{u(r,t)+iv(r,t)}{r} + \frac{\partial u(r,t)}{\partial r} = 0 \qquad (3.27c)$$

with boundary conditions

$$u(r=1,t) = 0 \qquad (3.27d)$$

at the wall, and

$$u(r=f,t) = -\frac{\pi z_o}{\mu\Omega^2 f}\dot{P}(r=f,t) \qquad (3.27e)$$

at the free surface (see equation (2.20) and Appendix B2). $\{Q^\dagger\}$ = complex conjugate of $\{Q\}$ (equation (3.22b)).

In Eqs. (3.27a-e) the θ and ζ dependence has been eliminated by operating on each equation with

$$\int_0^{z_o} \int_0^{2\pi} \frac{1}{2\pi z_o} e^{-i\theta} d\theta d\zeta .$$

As in section 2.1.2, equations (3.27) must be reduced to one fluid equation in u(t) and its time derivatives. In the process a relationship defining pressure at the wall as a function of time will be obtained, and this can be used to eliminate P(r=1,t) from (3.23).

Steps similar to those of Section 2.1.2 are followed: i) eliminate P(r,t) and v(r,t) from (3.27a,b,c) obtaining one differential equation in u(r,t), and find the general solution, ii) apply (3.27d) to determine the precise r dependence of u(r,t), and iii) use (3.27e) to eliminate the r dependence in u(r,t) (i.e., find u(r=f,t), the velocity at the free surface).[1]

i) Finding the general solution u(r,t).

From (3.27c)

$$v = ir \frac{\partial u}{\partial r} + iu \qquad \dot{v} = ir \frac{\partial \dot{u}}{\partial r} + i\dot{u}. \qquad (3.28a,b)$$

With this, (3.27b) can be solved for P(r,t).

---

[1]Note that as in Chapter II, variable arguments are used to distinguish between different quantities (e.g., $u(t) \neq u(r,t)$).

$$P(r,t) = \frac{\mu r}{\pi z_o}\{(-r\frac{\partial \dot{u}}{\partial r} - \dot{u} + i2\Omega u) - r(\{\ddot{X}\}^T - 2i\Omega\{\dot{X}\}^T - \Omega^2\{X\}^T)\{Q^\dagger\} = 0. \quad (3.29)$$

(3.29) in (3.27a) yields

$$\frac{\partial}{\partial t}[3\frac{\partial}{\partial r} + r\frac{\partial^2}{\partial r^2}]u(r,t) = 0. \quad (3.30)$$

This is identical to equation (2.15b) and the general solution is (2.16).

ii) Applying the wall boundary condition.

(3.27d) is the same as (2.17), so

$$u(r,t) = u(t)[1 - 1/r^2], \quad (3.31)$$

and

$$u(r=f,t) = u(t)[1 - 1/f^2]. \quad (3.32)$$

iii) Applying the free surface boundary condition.

Equation (3.32) and the time derivative of (3.29) are used in (3.27e) to yield

$$(1 + \frac{1}{f^2})\ddot{u}(t) - (1 - \frac{1}{f^2})[2i\Omega\dot{u}(t) + \Omega^2 u(t)] + [\{X\}^T - 2i\Omega\{\ddot{X}\}^T - \Omega^2\{\dot{X}\}^T]\{Q^\dagger\} = 0. \quad (3.33)$$

Equation (3.33) is 3rd order in time, but has the spatial dependence eliminated. $\{\dddot{X}\}$ can now be eliminated from the equation in the same way in which $\dddot{\eta}_1$ was eliminated from (2.21). First use equation (3.29) at r = 1 in equations (3.23), then take the time derivative of the result and solve for $\{\dddot{X}\}$. Substitution of this into (3.33) produces

$$(1 + \frac{1}{f^2})\ddot{u} - (1 - \frac{1}{f^2})2i\Omega\dot{u} - (1 - \frac{1}{f^2})\Omega^2 u$$
$$- \{Q^\dagger\}^T \cdot [\hat{M}]^{-1}([C] - 2i\Omega\mu\{Q\}\{Q^\dagger\}^T)\cdot\{\ddot{X}\}$$
$$- \{Q^\dagger\}^T \cdot [\hat{M}]^{-1}([K] - \mu\Omega^2\{Q\}\{Q^\dagger\}^T)\cdot\{\dot{X}\}$$
$$- 2\mu\{Q^\dagger\}^T \cdot [\hat{M}]^{-1}\cdot\{Q\}\ddot{u} - \dot{\phi}\{Q^\dagger\}^T \cdot [\hat{M}]^{-1}\cdot\{E''\}$$
$$- 2i\Omega\{Q^\dagger\}^T \cdot \{\ddot{X}\} - \Omega^2\{Q^\dagger\}^T \cdot \{\dot{X}\} = 0 \qquad (3.34)$$

where

$$[\hat{M}] = [M] + \mu\{Q\}\{Q^\dagger\}^T$$

and for simplicity u(t) has been written as u.

Equation (3.34) is the desired fluid equation, dependent only on u(t) and $\{X\}$ and their time derivatives.

3.1.3 COMBINED ROTOR FLUID EQUATIONS

Equations (3.23) and (3.34) can be combined into a complex matrix relation by using (3.29) at r = 1 in (3.23). The system equations then become

$$[M']\{\ddot{Z}\} + [C']\{\dot{Z}\} + [K']\{Z\} = \phi\{E'\} \qquad (3.35)$$

where

$$\{Z\} = \begin{Bmatrix} u \\ \eta_L \\ \eta_u \\ \eta_B \\ \phi \\ \eta_j \quad j=1,N \\ \xi_j \quad j=1,N \end{Bmatrix} \quad ; \qquad \{E'\} = \begin{Bmatrix} 0 \\ 1 \\ 0 \\ 0 \\ 0 \\ 0 \quad j=1,N \\ 0 \quad j=1,N \end{Bmatrix} \tag{3.36a,b}$$

$$[M'] = \begin{bmatrix} (1 + \frac{1}{f^2}) - 2\mu\{Q^\dagger\}^T[\hat{M}]^{-1}\{Q\} & -\{Q^\dagger\}^T([\hat{M}]^{-1}[\hat{C}] + i2\Omega[I]) \\ [0] & [\hat{M}] \end{bmatrix} \tag{3.36c}$$

$$[C'] = \begin{bmatrix} -2i\Omega(1 - \frac{1}{f^2}) & -\{Q^\dagger\}^T([\hat{M}]^{-1}[\hat{K}] + \Omega^2[I]) \\ 2\mu\{Q\} & [\hat{C}] \end{bmatrix} \tag{3.36d}$$

$$[K'] = \begin{bmatrix} -\Omega^2(1 - \frac{2}{f^2}) & \{0\}^T \\ [0] & [\hat{K}] \end{bmatrix} \tag{3.36e}$$

and

$$[\hat{M}] = [M] + \mu\{Q\}\{Q^\dagger\}^T$$

$$[\hat{C}] = [C] - 2i\Omega\mu\{Q\}\{Q^\dagger\}^T$$

$$[\hat{K}] = [K] - \mu\Omega^2\{Q\}\{Q^\dagger\}^T$$

and use has been made of the fact that

$$\dot{\phi}\{Q^{\dagger}\}^{T}[\hat{M}]^{-1}\{E''\} = 0 \tag{3.37}$$

because the control force is applied to the lower suspension mass. If a control force were applied at some other point along the rotor then (3.37) may not be satisfied and (3.35) would involve both ϕ and $\dot{\phi}$, that is the system would be sensitive to both the control force and the time rate of change of the control force.

3.1.4 STATE SPACE FORMULATION

Analogous to Section 2.1.4, the 2N+5 equations (3.35) can be expressed in terms of 4N+10 first order equations by

$$\{\dot{Y}\} = [\hat{A}]\{Y\} + \phi\{E\} \tag{3.37}$$

where

$$\{Y\} = \begin{Bmatrix} Z \\ \dot{Z} \end{Bmatrix} \; ; \; [A] = \begin{bmatrix} [0] & [I] \\ -[M']^{-1}[K'] & [-M']^{-1}[C'] \end{bmatrix} \; ; \; \{E\} = \begin{Bmatrix} \{0\} \\ [-M']^{-1}\{E'\} \end{Bmatrix}. \tag{3.38}$$

3.2 OPTIMAL CONTROL PROBLEM

The optimal control problem for the continuous mass system is virtually identical to that for the two mass system. The primary difference is in the dimension of the respective matrices ([A], [K],

etc.) and vectors ($\{Y\}$,$\{E\}$, etc.). For the two mass case this was six, while here it is $4N + 10$.

The results of Section 2.2 are, therefore, applied directly to the continuous mass model. N, the number of terms in the expansions (3.16), is taken here to be four, so that the order of the system in state space is then 26.[1]

Except for the generation of the [A] matrix, the software package of the two mass case can be taken over directly to the present one, providing only that all summations range from 1 to 26 instead of from 1 to 6 and that proper care be taken to insure that the feedback force is applied at the correct location (i.e., the lower suspension mass such that $\{E'(2)\} = 1.0$).

3.3 NONDIMENSIONAL NUMERICAL RESULTS

The nondimensional optimal control analysis was carried out for a specific continuous mass system with the following nondimensional parameter values:

$R = 100., 1.0, .01$

$[Q] = [I]$

$\mu = .30$

$z_0 = 75.$

$EI = 3.19$

---

[1] In actual application, the degree of accuracy desired may be higher than that attained here for N = 4. The total system order might then be closer to 50 or 60 rather than 26.

$k'GA = 0.76$

$K_1 = K_2 = .00143$

$K_3, K_4 = .00036$

$C_1 = C_2 = .00133$

$C_3 = C_4 = .00053$

$m_{top} = m_{bot} = .018$

$m_L = .005$

$m_u = .015$

$I_{top} = I_{bot} = .011$

$J_{top} = J_{bot} = .020$

$J_{rot} = 1.63$

System Stability

The real parts of the dominant system eigenvalues are plotted as a function of spin speed in Figure 3.3. Only the first three criticals are shown.

Dominant System Modes

The uppermost two parts of Figure 3.4 display the shapes of the dominant uncontrolled and controlled rotor mode shapes at the first critical ($\Omega = .0195$).

Influence of Performance Index Weighting Factors

It was found that changes in the weighting factor R had very little influence on the dominant eigenvalue of the controlled system. Varying

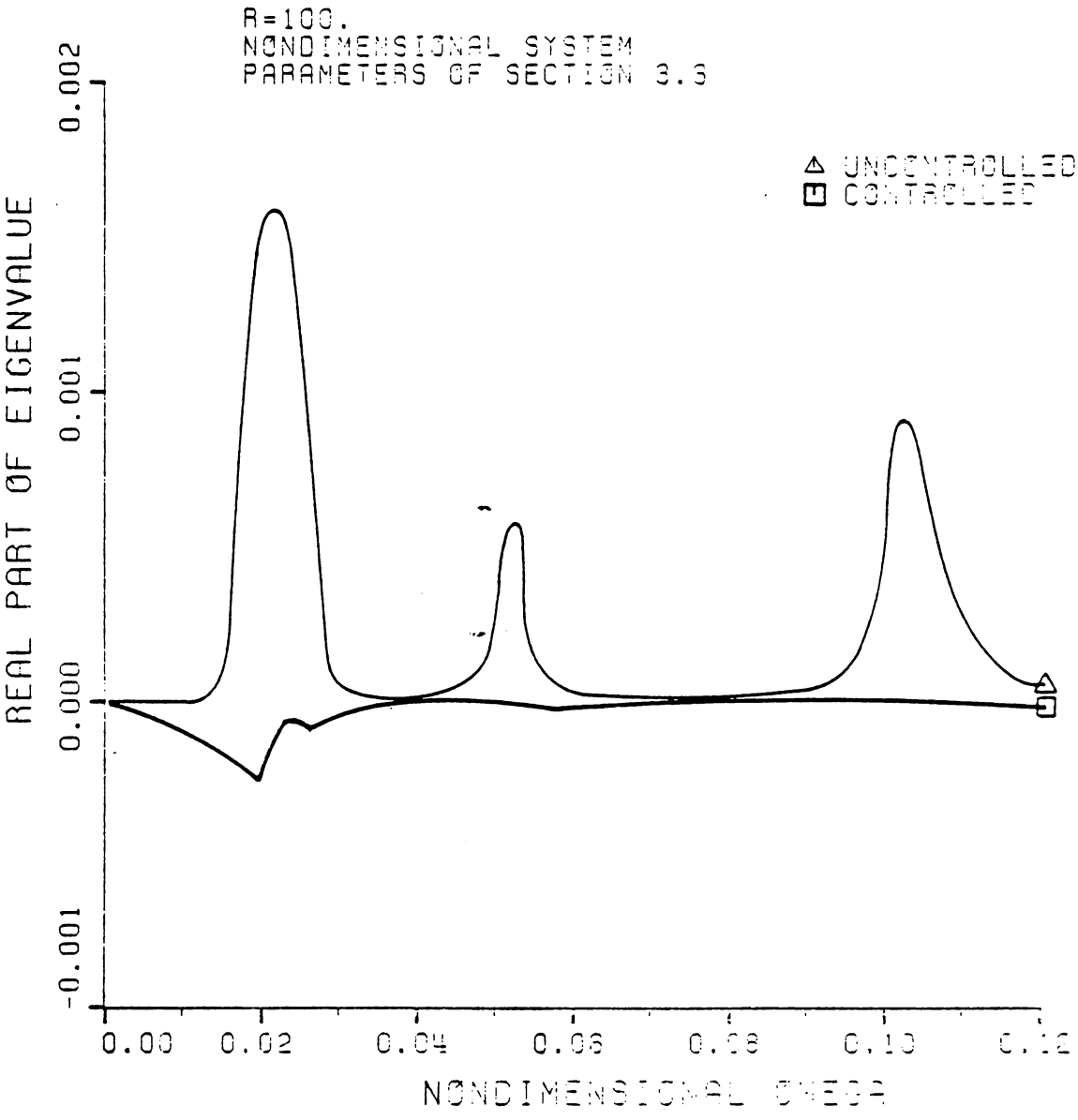

FIGURE 3.3 CONTINUOUS SYSTEM STABILITY: MAXIMUM REAL PART OF EIGENVALUES

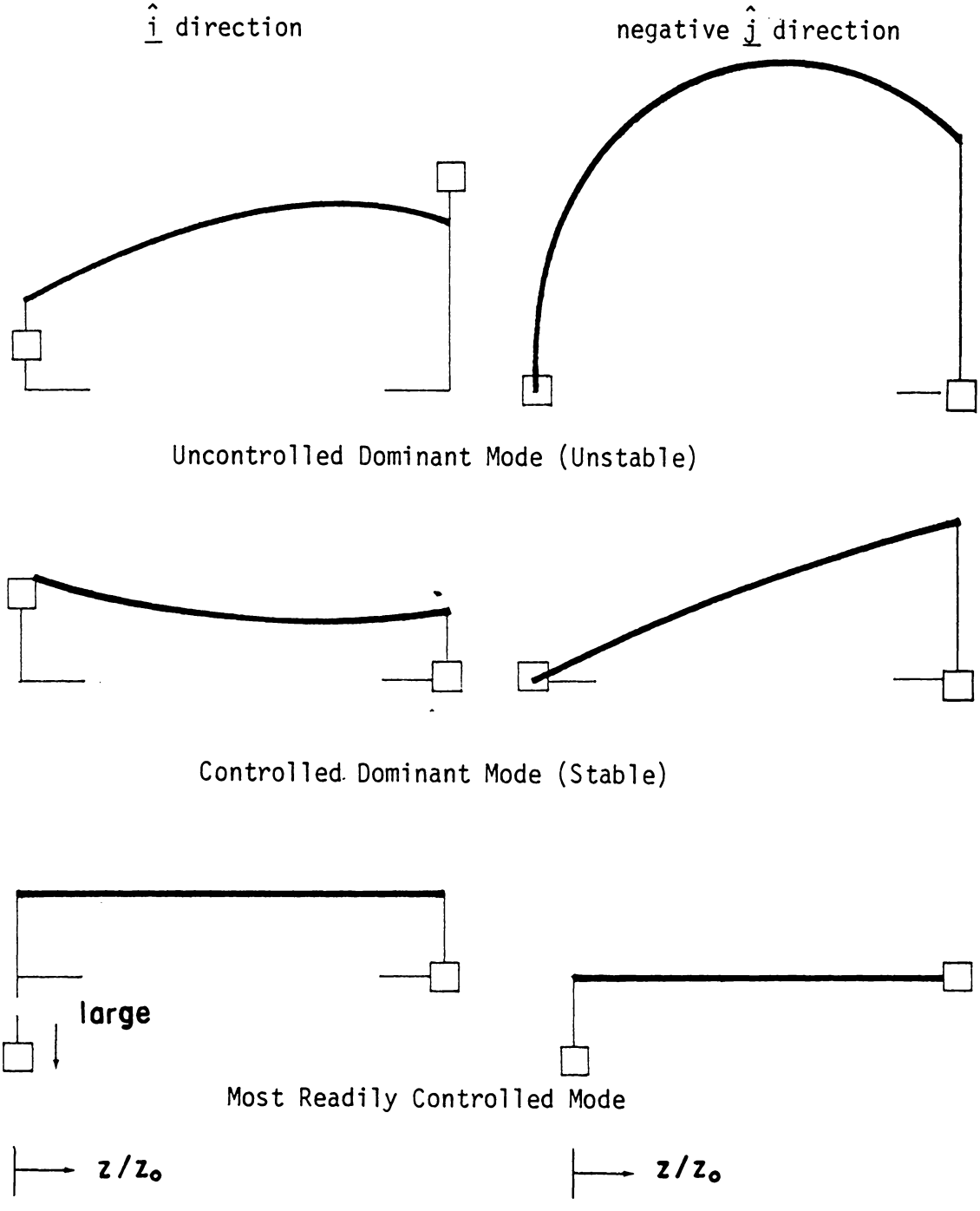

FIGURE 3.4. CONTINUOUS SYSTEM MODE SHAPES - FIRST CRITICAL

R did, however, have a significant effect on the real part of the eigenvalue associated with the particular mode depicted at the bottom of Figure 3.4 (henceforth called the "most readily controlled mode").

Quantitatively, for Ω = .0195, these changes were:

	R = 100.	R = 1.0
λ_{Re} of Dominant Mode	-.000245	-.000245
λ_{Re} of Most Readily Controlled Mode	-19.95	-200.0

Time dependent plots, such as those utilized in Chapter II to elaborate on certain controllability concepts, express little more information than that depicted already in Figure 3.3. Since they are expensive to generate for systems of present order and dominant eigenvalue magnitudes, they have not been produced here.

3.4 DISCUSSION

From Figure 3.4 it can be seen that the destabilizing effect of the fluid on the dominant uncontrolled mode was effectively neutralized by the feedback force. The dominant controlled mode displays considerably less deflection (cylinder bending) due to fluid pressure.

Figure 3.3 can be interpreted in much the same manner as were Figures 2.3 and 2.30. There is one significant difference, however.

Unlike the two mass case, the controlled continuous system dominant eigenvalue exhibits little sensitivity to changes in R. The eigenvalue plots for R = 100., R = 1.0, and R = .01 all look virtually identical. The reason for this can be seen with the aid of Figure 3.4.

The most readily controlled mode has an extremely large deflection at the lower suspension mass. Since this is the location of the feedback control force, such behavior is not unreasonable. The deflection of the lower mass becomes, therefore, the dominating factor in the performance index J (equation (2.26)). Decreasing R (increasing control) places more emphasis on the reduction of $\{Y^{\dagger}\}^{T}[Q]\{Y\}$. Hence, the mode which will be most readily damped out is the one which contributes most significantly to this term, i.e., the lowermost mode of Figure 3.4.

Not unexpectedly, higher values for R (decreased control force) result in smaller deflection at the lower mass.

3.5 CONCLUSIONS

It has been shown in this chapter that an optimal feedback force can be determined which will cause the free (unstable) continuous mass modelled centrifuge system to become asymptotically stable.

For the system parameters chosen, the degree of control (as measured by the real part of the dominant eigenvalue) is relatively unaffected by variations in the weighting factor R. The λ_{re} of the mode shape in which the deflection of the lower suspension mass is large, does, however, become less negative with increase of R. Higher R also results in reduced deflection of the lower suspension mass.

It is suggested, therefore, that a large value for R be used in actual implementation of the control. This will have the twofold effect of increasing fatigue life of the lower bearing and saving in energy

expenditure, while keeping the system damping characteristics relatively unchanged. The actual choice for R is a design decision which can only be made with respect to a large number of interacting factors, only a few of which are mentioned here.

CHAPTER IV

CONTROL WITH INCOMPLETE STATE MEASUREMENTS

The developments of Chapters II and III were carried out under the assumption that all components of the respective state vectors were available (i.e., were physically measurable). In practice this will probably not be the case.

Measurement of the fluid surface displacement in the rapidly rotating closed cup could, for example, prove infeasible. At best it would be a formidable design problem. Almost as impractical would be the determination of modal displacement and angular amplitudes for the continuous mass rotor. In all cases n (6 or 26)[1] sensors would be needed, since the state vector itself has n components, each of which is used in the feedback control.

To avoid severe limitations on availability and to reduce hardware expense for sensors, controllability of the system(s) with fewer than n feedback inputs is investigated. The present chapter demonstrates that this can in fact be done.

4.1 POLE PLACEMENT LUENBERGER OBSERVER

An "observer" is a device which approximates the entire state vector from knowledge of only some of its components. It is itself a

---

[1]As the state vector is complex, each component will need a pickup in both the x and y directions. "n" here actually refers then to n pairs of sensors.

linear dynamic system ("an electronic box" in practice) with input equal to those values of the measured output from the original system. From these it estimates all of the state vector components of the original system.[1] This estimation (the observer output) is then used as the state vector input to the feedback control.

If a system which is controllable (in the sense that it could be controlled if all state vector components were available), can be controlled using the observer estimation, then the system is said to be "observable". This is not necessarily true for any controllable system and each must be investigated separately to determine observability.

4.1.1 LUENBERGER IDENTITY OBSERVER - TWO MASS SYSTEM

There are several types of observers. One of the simplest, the Luenberger Identity Observer (see reference [21] pages 300-304), is employed for the two mass system.

Consider an nth order system analogous to those treated earlier.

$$\{\dot{Y}(t)\} = [A]\{Y(t)\} + \{E\}\phi \tag{4.1}$$

where the symbols are the same as those used in Chapters II and III.

Since [A] represents the physical system, independent of any measurements made, the contribution of $[A]\{Y(t)\}$ to $\{\dot{Y}(t)\}$ is independent of state vector availability. The control force ϕ was in

---

[1] For this reason, an observer is sometimes referred to as an "estimator".

the earlier cases a linear function of $\{Y(t)\}$, the assumption being that $\{Y(t)\}$ was completely available. When that assumption is no longer valid, ϕ must of necessity become a function of the observer estimate for $\{Y(t)\}$ (henceforth called $\{Z(t)\}$).

To determine $\{Z(t)\}$, consider that p components of the n dimensional $\{Y(t)\}$ are available. These components form a vector $\{V(t)\}$ which is related to $\{Y(t)\}$ by

$$\{V(t)\} = [C]\{Y(t)\} \tag{4.2}$$

where $[C]$ is the suitable pxn matrix with components C_{ij} such that $C_{ij} = 1$ when the jth component of $\{Y(t)\}$ is available and is equal to the ith component of $\{V(t)\}$, and $C_{ij} = 0$ for all other i and j.

For reasons which will become apparent, the following observer is constructed.

$$\{\dot{Z}(t)\} = [A]\{Z(t)\} + [B](\{V(t)\} - [C]\{Z(t)\}) + \{E\}\phi \tag{4.3}$$

The nxp matrix $[B]$ is yet to be determined. Note again that ϕ is now a function of $\{Z(t)\}$ (i.e., replace $\{Y(t)\}$ by $\{Z(t)\}$ in equation 2.36).

It is claimed that proper choice of $[B]$ makes $\{Z(t)\}$ an accurate estimation of $\{Y(t)\}$. The objective is then to determine $\{Z(t)\}$ by integrating (4.3) and use this to determine ϕ in (4.1). Given initial conditions for $\{Z(t)\}$ (chosen arbitrarily but judiciously) and with $\{V(t)\}$ readily measurable at every point in time, this is

straightforward. This integration process is in fact what the observer does. $\{V(t)\}$ is input and $\{Z(t)\}$ is output.

To prove that $\{Z(t)\}$ can in fact be made to approximate $\{Y(t)\}$, substitute (4.2) into (4.3) and subtract (4.1) from the result. This yields

$$\{\dot{Z}(t)\} - \{\dot{Y}(t)\} = ([A] - [B][C])(\{Z(t)\} - \{Y(t)\}) \tag{4.4}$$

Note that if the observer is initiated with

$$\{Z(0)\} = \{Y(0)\}, \text{ then } \{Z(t)\} = \{Y(t)\}$$

for all time and the estimation tracks the state vector exactly.

If $\{Z(0)\} \neq \{Y(0)\}$, then the time history of the error $\{e(t)\} = \{Z(t)\} - \{Y(t)\}$ is determined by the system

$$\{\dot{e}(t)\} = ([A] - [B][C])\{e(t)\}. \tag{4.5}$$

If [B] is selected such that the dominant eigenvalue of [A] - [B][C] has a negative real part, then the error tends to zero and $\{Z(t)\}$ approaches $\{Y(t)\}$. The problem then becomes simply one of pole placement. Correct choice of [B] assures that $\{Z(t)\}$ approximates $\{Y(t)\}$. Equation (4.3), integrated, (the "electronic box") determines $\{Z(t)\}$ which is then used in ϕ in (4.1) to control $\{Y(t)\}$.

Placing the poles in (4.5) can, of course, be accomplished by finding the appropriate characteristic equation (Det ([A] - [B][C] - λ[I]) = 0) algebraically, picking the n desired λ's, and solving the

resulting n equations for specific components of [B]. For systems of order greater than 2 or 3, however, this becomes very tedious. A more direct numerical method, derived by the author, is presented in Appendix G. It is assumed there that control can be achieved by using a single sensor pair (i.e., $\{V(t)\}$ has only one complex component and [C] is 1 x n). For n less than 9 or 10, this is a valid assumption, and the results for the two mass systems bear this out (see Section 4.2).

4.1.2 REDUCED ORDER OBSERVER - CONTINUOUS MASS SYSTEM

While the results of the previous section are, in theory, directly applicable to matrices of any size, in actual practice difficulties arise for large systems. For systems of order greater than 9 or 10, the coefficients of the characteristic equation become extremely sensitive to choices for λ.[1] The effect is so severe that numerical solutions are simply not possible.

To observe the larger order continuous mass model system a slightly different approach is needed. In effect it must be an approach which observes a larger order system, but is only required to pole place a low order characteristic equation. The Luenberger Reduced Order Observer described below (see [21], page 304-307) is such an approach.

Consider a large order system where it is possible to measure p components of the n dimensional state vector $\{Y\}$. Equations (4.1) and (4.2) of Section 4.1.1 are carried over directly.

---

[1]See reference [23], page 135.

For reasons which will become apparent, (4.1) and (4.2) will be transformed to a new space by the matrix

$$[P] = \begin{bmatrix} [S] \\ \hline [C] \end{bmatrix} \tag{4.6}$$

where [S] is any arbitrary (n - p) x n matrix chosen such that the p x p matrix [P] is nonsingular.

After transformation, the new state vector becomes

$$\{\bar{Y}(t)\} = [P]\{Y(t)\} = \begin{Bmatrix} \{W(t)\} \\ \hline \{V(t)\} \end{Bmatrix} \tag{4.7}$$

where $\{W(t)\}$ is n - p dimensional and $\{V(t)\}$ is, as before, the p dimensional vector of measurable quantities.

Transformation and partitioning of (4.1) yields

$$\begin{Bmatrix} \dot{\{W(t)\}} \\ \hline \dot{\{V(t)\}} \end{Bmatrix} = \begin{bmatrix} [\bar{A}_{11}] & [\bar{A}_{12}] \\ \hline [\bar{A}_{21}] & [\bar{A}_{22}] \end{bmatrix} \begin{Bmatrix} \{W(t)\} \\ \hline \{V(t)\} \end{Bmatrix} + \begin{Bmatrix} \{\bar{E}_1\} \\ \hline \{\bar{E}_2\} \end{Bmatrix} \phi(t) \tag{4.8}$$

A subsystem of order n - p, with known inputs $\phi(t)$ and $\{V(t)\}$, will now be constructed. Premultiply the bottom of (4.8) by a yet to be determined (n - p) x p matrix [B] and subtract from the top part. This results in

$$\dot{\{W(t)\}} - [B]\dot{\{V(t)\}} = ([\bar{A}_{11}] - [B][\bar{A}_{21}])\{W(t)\}$$

$$+ ([\bar{A}_{12}] - [B][\bar{A}_{22}])\{V(t)\} + (\{\bar{E}_1\} - [B]\{\bar{E}_2\})\phi(t) \qquad (4.9)$$

Rewritten this becomes

$$\begin{aligned}\{\dot{W}(t)\} - [B]\{\dot{V}(t)\} &= ([\bar{A}_{11}] - [B][\bar{A}_{21}])(\{W(t)\} - [B]\{V(t)\}) \\ &+ ([\bar{A}_{11}][B] - [B][\bar{A}_{21}][B] + [\bar{A}_{12}] - [B][\bar{A}_{22}])\{V(t)\} \\ &+ (\{\bar{E}_1\} - [B]\{\bar{E}_2\})\phi(t) \qquad (4.10)\end{aligned}$$

Introducing the change of variables

$$\{X(t)\} = \{W(t)\} - [B]\{V(t)\} \qquad (4.11)$$

(4.10) becomes

$$\begin{aligned}\{\dot{X}(t)\} &= ([\bar{A}_{11}] - [B][\bar{A}_{21}])\{X(t)\} \\ &+ ([\bar{A}_{11}][B] - [B][\bar{A}_{21}][B] + [\bar{A}_{12}] - [B][\bar{A}_{22}])\{V(t)\} \\ &+ (\{\bar{E}_1\} - [B]\{\bar{E}_2\})\phi(t). \qquad (4.12)\end{aligned}$$

Note that no determination can be made of the n - p dimensional vector $\{X(t)\}$ since $\{W(t)\}$ is not available.

The observer is found by simply copying the system (4.12), i.e.,

$$\begin{aligned}\{\dot{Z}(t)\} &= ([\bar{A}_{11}] - [B][\bar{A}_{21}])\{\dot{Z}(t)\} \\ &+ ([\bar{A}_{11}][B] - [B][\bar{A}_{21}][B] + [\bar{A}_{12}] - [B][\bar{A}_{22}])\{V(t)\} \\ &+ (\{\bar{E}_1\} - [B]\{\bar{E}_2\})\phi(t). \qquad (4.13)\end{aligned}$$

(4.13) is the observer for (4.8). Note that subtracting (4.12) from (4.13) yields

$$\{\dot{Z}(t)\} - \{\dot{X}(t)\} = ([\bar{A}_{11}] - [B][\bar{A}_{21}])(\{Z(t)\} - \{X(t)\}) \qquad (4.14)$$

As before, $\{Z(t)\}$ will approach $\{X(t)\}$ if the matrix in (4.14) has all negative real parts of its eigenvalues. Since [B] is arbitrary, pole placement can once again be used.

The method of Appendix G can be employed if $[B][\bar{A}_{21}]$ can be made to take a form where only one column is non-zero, and each component of that column is a linear function of one of the n unspecified components of [B]. This is easily accomplished by choosing the arbitrary [S] matrix of (4.6) such that $[\bar{A}_{21}]$ has a row with all but one component equal to zero. If the corresponding column of [B] is the only non-zero column of [B], $[B][\bar{A}_{21}]$ will have the desired form.

Once the poles are placed, $\{Z(t)\}$ can be found from (4.13). As this is an estimate of $\{X(t)\}$, the estimate for $\{W(t)\}$ can be found from (4.11). This is used in (4.7) to estimate $\{\bar{Y}(t)\}$, and the estimate for $\{Y(t)\}$ can be obtained by

$$\{Y(t)\}_{est} = [P]^{-1}\{\bar{Y}(t)\}_{est}. \qquad (4.15)$$

$\{Y(t)\}_{est}$ is then used in the feedback force

$$\phi(t) = \{GAIN\} \times \{Y(t)\}_{est}.$$

The key point is that, unlike the identity observer case, the poles were placed in an n - p order matrix (see (4.14)) rather than one of nth order. If n - p is less than 9 or so, all of the numerical methodology previously presented is applicable.

4.2 RESULTS

4.2.1 TWO MASS SYSTEM

Figures 4.1 to 4.4 display time histories of selected components of

(1) the actual state vector for the case where all quantities could be measured (i.e., the optimal curves of Chapter II superimposed here.)

(2) the actual state vector (in practice not fully measured, but monitored in the computer simulation for comparison purposes), labeled "for estim" in the legend

(3) the state vector estimation, labeled "estimator" in the legend.

The only component measured is the displacement of the first (liquid filled) cylinder. From this all six state vector components are estimated.

Figure 4.5 is a polar plot of the control force for the estimator (compare with Figure 2.21).

4.2.2 CONTINUOUS MASS SYSTEM

To demonstrate, as simply as possible, that the continuous mass system could in fact be observed, a model with n = 14 (N = 1) was

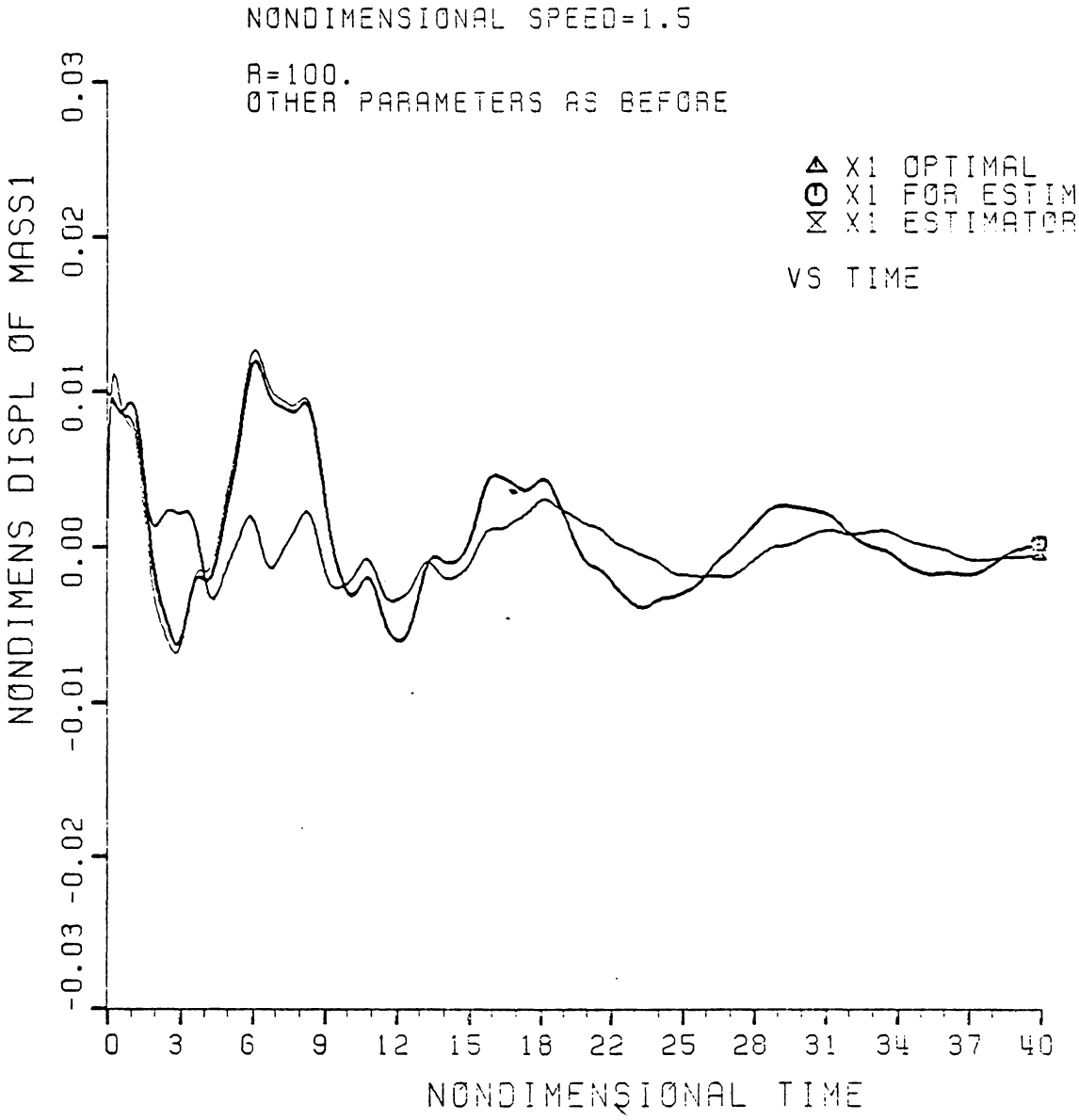

FIGURE 4.1 CONTROLLED TWO MASS SYSTEM:
MASS 1 DISPLACEMENTS
ESTIMATED VS OPTIMAL

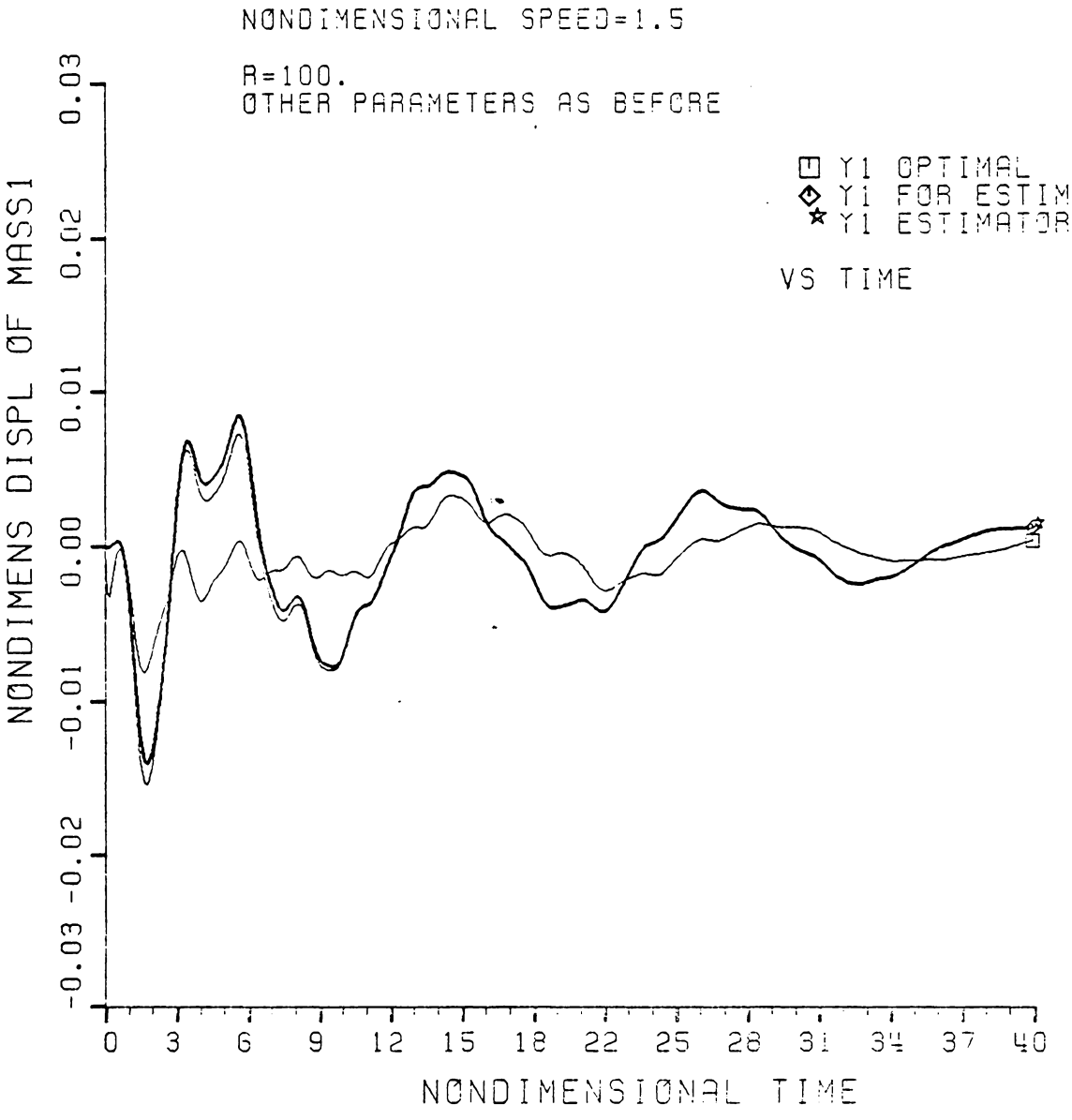

FIGURE 4.2 CONTROLLED TWO MASS SYSTEM:
MASS 1 DISPLACEMENTS
ESTIMATED VS OPTIMAL

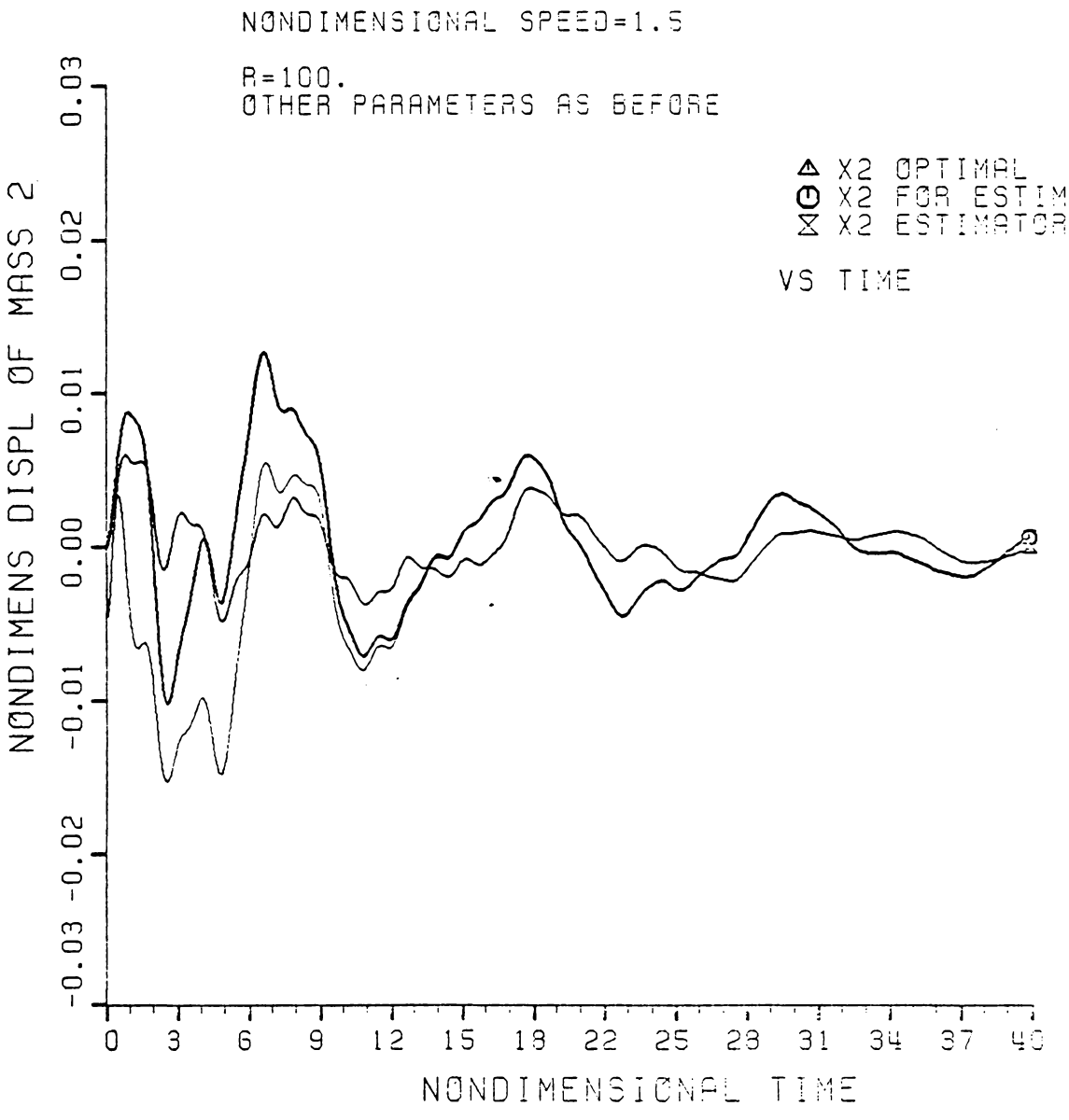

FIGURE 4.3 CONTROLLED TWO MASS SYSTEM
MASS 2 DISPLACEMENTS
ESTIMATED VS OPTIMAL

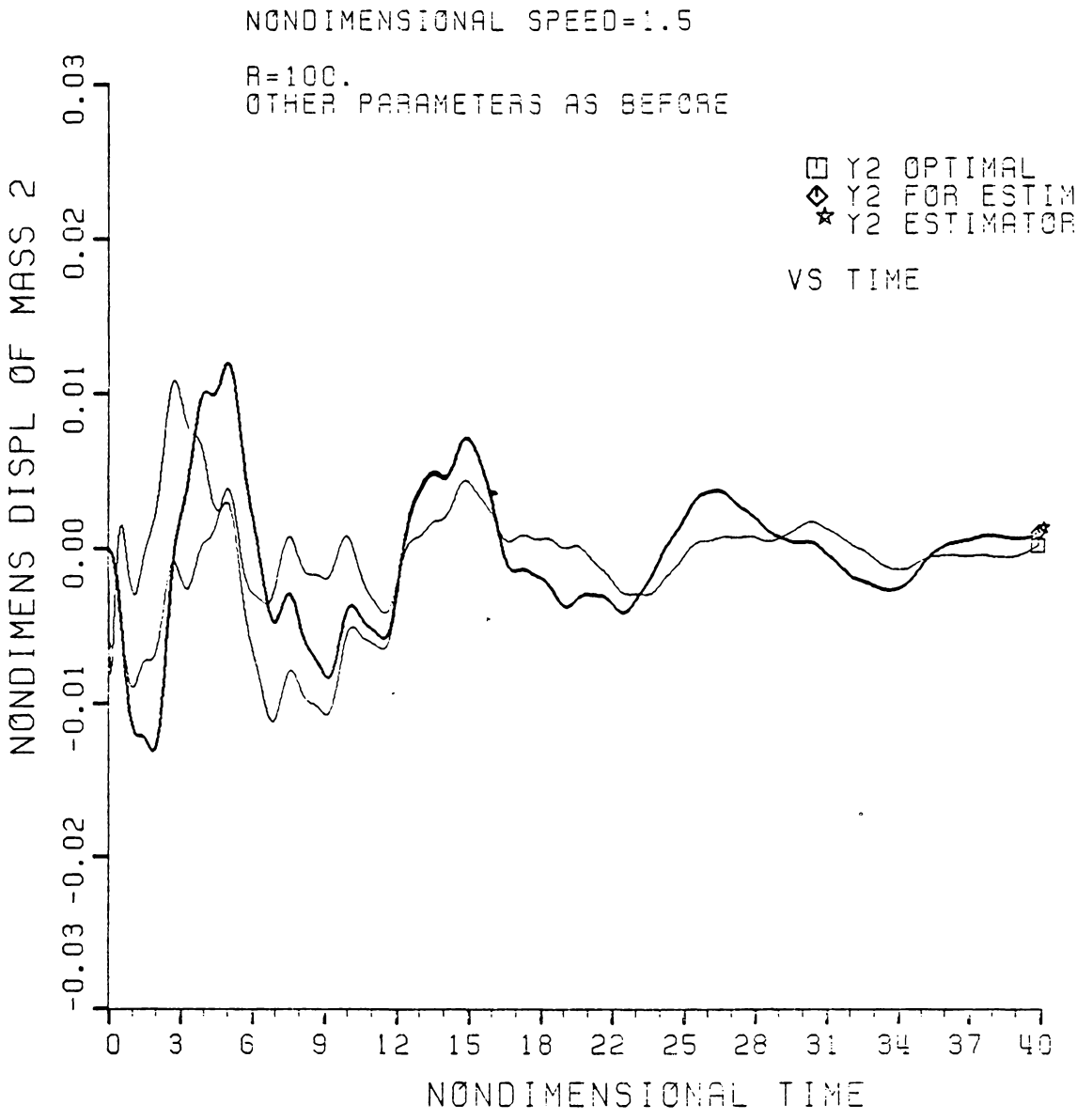

FIGURE 4.4 CONTROLLED TWO MASS SYSTEM: MASS 2 DISPLACEMENTS ESTIMATED VS OPTIMAL

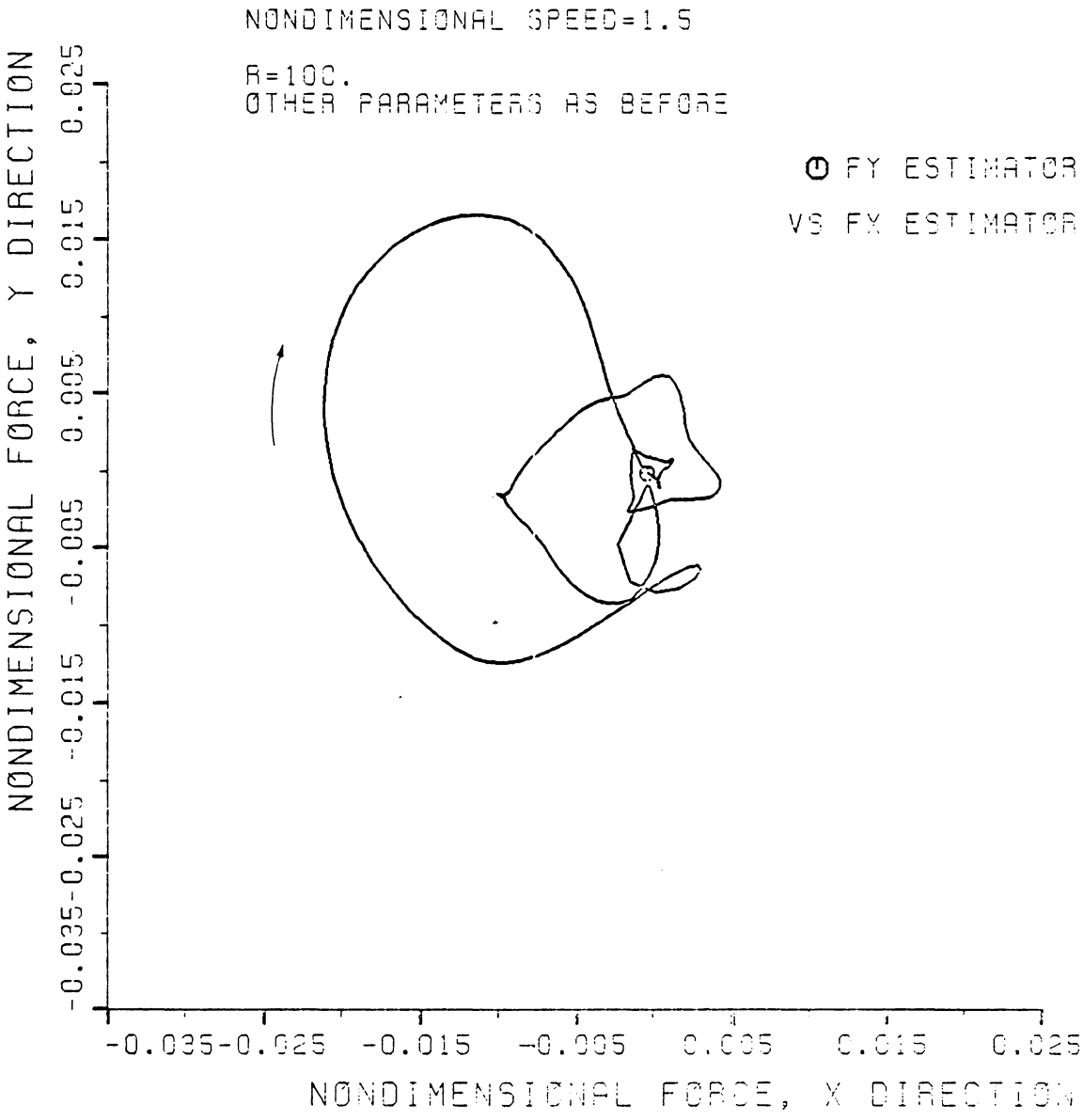

FIGURE 4.5 CONTROLLED TWO MASS SYSTEM
POLAR PLOT OF FORCE
ESTIMATED STATE VECTOR

selected. All components of the state vector were assumed measurable except for the expansion terms and the fluid velocity and acceleration. Hence p = 8 and the characteristic equation was of degree 14 - 8 = 6.

The software was written and the poles placed using the methodology of Section 4.1 and Appendix G. Actual integration of the equations of motion was at that point considered a meaningless exercise and is not included.

4.3 DISCUSSION

Figures 4.1 to 4.4 demonstrate quite graphically that the state vector estimate does indeed approach the actual state vector asymptotically. The response is not the same as that of the fully observable case, nor can it be expected to be.

Figure 4.5 shows that the control force starts at zero, varies from the fully available case for a time and then approaches the behavior of Figure 2.21. This is to be expected since the control force in Figure 4.5 is linearly related to the state vector estimate $\{Z(t)\}$ by the same gains used in the fully available case. The initial condition on $\{Z(t)\}$ was taken as $\{0\}$ and thereafter $\{Z(t)\}$ approaches the actual state vector $\{Y(t)\}$ asymptotically. The observed control force time history is consistent with this.

For a higher order continuous mass system ($N > 1$), numerical problems will arise in trying to place the poles as long as n-p is 8 or

more. Additional pickups on the cylinder itself will then be needed in order to determine the coefficients in the expansion terms.

The author is aware that more sophisticated procedures for state vector estimation exist (see Chapter V recommendations). The intention here was simply to demonstrate that the system can in fact be controlled without having to measure the fluid wave velocity inside the cylinder.

4.4 CONCLUSIONS

Both the two mass and the continuous mass system models can be observed, i.e., the entire state vector can be estimated from knowledge of only some of its components.

Further, both systems can be stabilized by using the state vector estimate in the feedback control. Since the input to the control is, of necessity, only an estimation, the observer itself must, in this sense, be considered sub-optimal.

CHAPTER V

RECOMMENDATIONS

A number of simplifying assumptions were made in the course of this research in order to obtain a preliminary analysis of the feasibility for active control of an unstable centrifuge.

Further research should study the effect of relaxing some of these restrictions. In particular, the following areas should be investigated in greater depth:

(1) The influence of fluid viscosity

(2) Axial acceleration effects in the fluid

(3) State estimation via Kalman filtering or some other estimation procedure

The estimation technique of (3) should consider the problem of observation from a somewhat more practical perspective than that of the Luenberger observers. It should be more suited to making allowances for system noise, slight inaccuracies in system modeling, etc. It may also possess economic advantages over the method of Chapter IV. In any event, it is the next logical step on the path to complete understanding of the system treated herein.

REFERENCES

1. Pedersen, P. T. "On Self Excited Whirl of Rotors," Ingenieur-Archiv, Vol. 42, 1973, pp. 267-284.

2. Herrmann, G. and Tong, I. C. "On the Destabilizing Effect of Damping in Non-conservative Elastic Systems," Journal of Applied Mechanics, Vol. 32, No. 3, 1965.

3. Lund, J. W. "Self Excited Stationary Whirl Orbits of a Journal in a Sleeve Bearing," Ph.D. Thesis, Rensselaer Polytechnic Institute, 1966.

4. Kollman, F. G., "Experimentelle und theoretische Untersuchungen uber die Kritischen Drehzahlen flussigkeitsgefulter Hohlkorper," Forschund auf dem Gebiete des Ingenieurwessens, Ausgabe B, vol. 28, 1962, pp. 115-123 and 147-153.

5. Kuipers, M., "On the Stability of a Flexible Mounted Rotating Cylinder Partially Filled with Liquid," Applied Scientific Research, Section A, Vol. 13, 1964, pp. 121-137.

6. Philips, O. M., "Centrifugal Waves," Journal of Fluid Mechanics, vol. 7, 1960, pp. 340-352.

7. Miles, J. W. and Troesch, B. A., "Surface Oscillations of a Rotating Liquid," ASME Journal of Applied Mechanics, vol. 28, 1961, pp. 491-496.

8. Wolfe, J. A., Jr., "Whirl Dynamics of a Rotor Partially Filled with Liquid," ASME Journal of Applied Mechanics, vol. 35, 1968, pp. 676-682.

9. Hendricks, S. L., "Dynamics of Flexible Rotors Partially Filled with a Viscous Incompressible Fluid," Ph.D. Dissertation, University of Virginia, May 1979.

10. Hendricks, S. L., and Morton, J. B., "Stability of a Rotor Partially Filled with a Viscous Incompressible Fluid," ASME Journal of Applied Mechanics, vol. 46, No. 4, 1979, pp. 913-918.

11. Taylor, M., "Active Optimal Control for Suppression of Whirl of a Flexible Centrifuge," Ph.D. Dissertation, University of Virginia, January 1979.

12. Zubov, V. I., et al., Control of the Rotational Motion of a Solid Body, Izdatel' stvo Leningrads Kogo Universiteta, 1978, In Russian, NASA #79A43616.

13. Auziak, A. G., "Optimal Control Synthesis in the Case of Incomplete Measurement for a Solid Body with a Cavity Partially Filled by a Liquid," Dynamics of Controllable Systems, Novosibirsk, Izdatel' stvo Nauka, 1979, In Russian, NASA #80A33878.

14. Meirovitch, L., Computational Methods in Structural Dynamics, Sijthoff & Noordhoff, Rockville, Maryland, 1980.

15. Meirovitch, L., and Öz, H., "Modal-Space Control of Distributed Gyroscopic Systems," Journal of Guidance and Control, Vol. 3, March-April 1980, pp. 140-150.

16. Meirovitch, L., and Baruh, H., "Optimal Control of Damped Flexible Gyroscopic Systems," Journal of Guidance and Control, vol. 4, March-April 1981, pp. 157-163.

17. Kirk, D. E. Optimal Control Theory: An Introduction, Prentice-Hall, Englewood Cliffs, New Jersey 1970.

18. Kalman, R. E., "Contributions of the Theory of Optimal Control," Bol. Soc. Mat. Mex., 1960, pp. 102-119.

19. Kalman, R. E., "On the General Theory of Control Systems," Proceedings of First IFAC Congress, Moscow, 1960, pp. 481-492.

20. Potter, J. E., "Matrix Quadratic Solutions", Siam Journal of Applied Mathematics, vol. 14, No. 3, May 1966, pp. 496-501.

21. Luenberger, D. G., Introduction of Dynamic Systems: Theory, Models, and Applications, John Wiley & Sons, NY 1979.

22. Brogan, William, L., Modern Control Theory, Quantum Publishers, Inc., NY, 1974.

23. I. Saacson, Eugene and Keller, H. B., Analysis of Numerical Methods, John Wiley & Sons, NY, 1966.

APPENDIX A

TWO MASS ROTOR ADDENDA

A1 Pressure Force Derivation

With equations (2.6a) and (2.5), the generalized force in Lagrange's equation (2.7) for x_1 becomes

$$\int_0^L \int_0^{2\pi} \frac{\partial \underline{R}_1^*}{\partial x_1} \cdot \hat{P}(r^*=a,\theta,t)[\cos\theta\,\underline{\hat{i}}+\sin\theta\,\underline{\hat{j}}]a\,d\theta\,dz + \frac{\partial \underline{R}_2^*}{\partial x_1} \cdot [U_x^*\underline{\hat{i}} + U_y^*\underline{\hat{j}}].$$

Use of equations (2.2a), (2.3a), and (2.10a) results in

$$\mathrm{Re}\{aL \int_0^{2\pi} \underline{\hat{i}} \cdot [\cos\theta\,\underline{\hat{i}}+\sin\theta\,\underline{\hat{j}}](\sum_{n=0}^{\infty} \hat{P}_n(a,t)[\cos(n\theta)+i\sin(n\theta)]d\theta\}.$$

After inner product multiplication and subsequent integration, all terms where $n \neq 1$ vanish, leaving

$$\mathrm{Re}\{\pi aL\hat{P}_1(a,t)\} = \pi aL\hat{P}_{1_{re}}(a,t).$$

For $q = x_2$ in (2.7) the physical force is similarly found to be

$$-\mathrm{Im}\{\pi aL\hat{P}_1(a,t)\} = -\pi aL\hat{P}_{1_{im}}(a,t).$$

A2 Physical Justification for Loss of $n \neq 1$ Terms

Equation (2.10a) (and (2.10c)) can be interpreted physically with the aid of Figure A1. Since any arbitrary wave shape can be expanded in

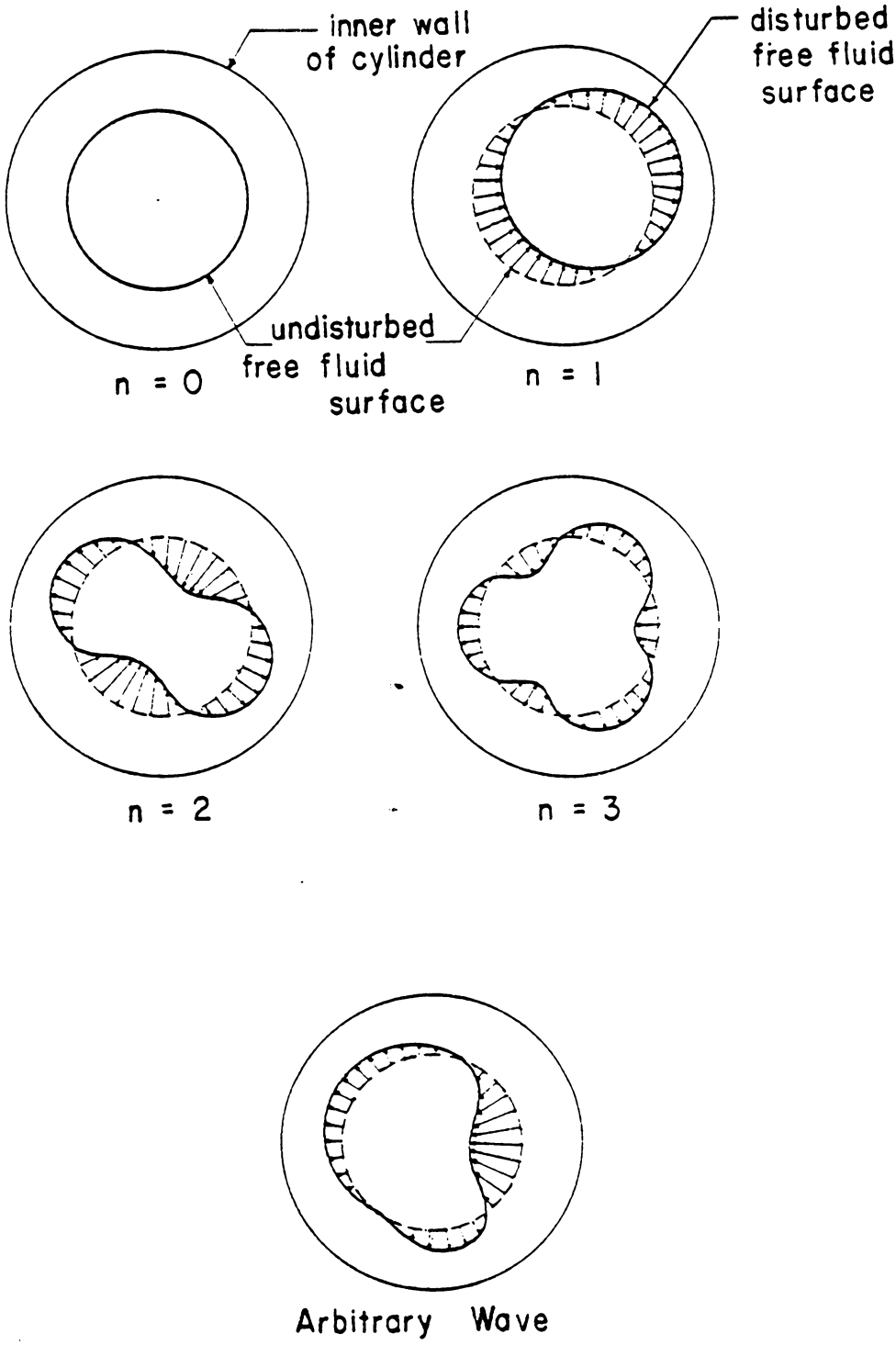

Note: Arrows represent fluid surface (or pressure) perturbations

FIGURE A1. WAVE, WAVE MODE, AND PRESSURE VARIATIONS

a Fourier series, the physical fluid surface can be considered to be the superposition of an infinite number of wave modes, the first four of which are depicted in the figure. Associated with each mode is a corresponding "partial" pressure whose variation in θ and time at $r^* = a$ parallels that of the sinusoidal wave generating it. It is evident from the figure that only in the second ($n = 1$) case will a pressure integration around the circumference make any contribution to the total force felt by the cylinder center of mass.

A3 Interpretation of P_{re} and P_{im}

From equation (2.10d) the real nondimensional pressure is

$$P(r,\theta,t) = Re\{P(r,t)e^{i\theta}\} = P_{re}(r,t)\cos\theta - P_{im}(r,t)\sin\theta.$$

Necessarily, at $\theta = 0^0$, $P(r,\theta,t) = P_{re}(r,t)$; and at $\theta = -90°$, $P(r,\theta,t) = P_{im}(r,t)$.

So, though the components of complex variables like η_1 and η_2 represent perpendicularly directed quantities at the same point, $P_{re}(r,t)$ and $P_{im}(r,t)$ refer to different values of the same real scalar variable measured at two separate locations 90° removed from one another about a given arc.

A4 Derivation of Complex Dimensionless Equations of Motion

Substituting the kinetic energy, potential energy, dissipation function, and control force of equations (2.4) and (2.5) into the Lagrangian equation (2.7), incorporating the results of part A1 above,

and carrying out some fairly straightforward manipulations, one can derive the following equations of motion for x_1 and y_1 (in real physical quantities):

$$m_1\ddot{x}_1 + (\hat{c}_1+\hat{c}_2)\dot{x}_1 - 2m_1\Omega^*\dot{y}_1 - \hat{c}_2\dot{x}_2 + (\hat{k}_1 + \hat{k}_2 - m(\Omega^*)^2)x_1 - (\hat{c}_1+\hat{c}_2)\Omega^*y_1$$

$$- \hat{k}_2x_2 + \hat{c}_2\Omega^*y_2 = aL\pi\hat{P}_{re}(r^*=a,t)$$

and

$$m_1\ddot{y}_1 + (\hat{c}_1+\hat{c}_2)\dot{y}_1 + 2m_1\Omega^*\dot{x}_1 - \hat{c}_2\dot{y}_2 + (\hat{k}_1+\hat{k}_2-m_1(\Omega^*)^2)y_1 + (\hat{c}_1+\hat{c}_2)\Omega^*x_1$$

$$- \hat{k}_2y_2 - \hat{c}_2\Omega^*x_2 = -aL\pi\hat{P}_{im}(r^*=a,t)$$

Note that, for simplicity, the subscripts "1" have been dropped from $\hat{P}_{1_{re}}$ and $\hat{P}_{1_{im}}$.

Dividing each of the above relations by $am_1\omega_o^2$, multiplying the second by -i, and working through some lengthy but elementary algebra, one arrives at the first row equation in the matrix representation of (2.11). A parallel procedure for x_2 and y_2 yields the second row.

APPENDIX B

TWO MASS FLUID EQUATIONS ADDENDA

B1. Derivation of Fluid Equations (2.14)

The continuity equation is simplest and is treated first. Substitution of (2.13b) in (2.12b) yields[1]

$$\nabla\cdot\underline{q} = (\hat{\underline{r}}\,\frac{\partial}{a\partial r} + \hat{\underline{\theta}}\,\frac{1}{ar}\,\frac{\partial}{\partial\theta}) \cdot [\mathrm{Re}\{\sum_{r=0}^{\infty} (u_n(r,t)\hat{\underline{r}} + v_n(r,t)\hat{\underline{\theta}})e^{in\theta}a\omega_o\}] = 0$$

or

$$\sum_{n=0}^{\infty} \mathrm{Re}\{e^{in\theta}(\hat{\underline{r}}\cdot\frac{\partial u_n(r,t)}{\partial r}\,\hat{\underline{r}} + \hat{\underline{\theta}}\cdot\frac{u_n(r,t)\partial\hat{\underline{r}}}{r\quad\partial\theta} + \hat{\underline{\theta}}\,\frac{in}{r}\cdot[u_n(r,t)\hat{\underline{r}}$$

$$+ v_n(r,t)\hat{\underline{\theta}}]) + \text{vanishing terms}\} = 0$$

or, more succinctly

$$\mathrm{Re}\{\sum_{n=0}^{\infty} e^{in\theta}\,(\frac{\partial u_n(r,t)}{\partial r} + \frac{u_n(r,t)}{r} + \frac{inv_n(r,t)}{r})\} = 0.$$

Multiplication by $\cos\theta$, use of $e^{i\theta} = \cos\theta + i\sin\theta$, and integration from $\theta = 0$ to $\theta = 2\pi$ cause all terms where $n\neq 1$ to vanish. The result is

$$\mathrm{Re}\{\frac{\partial u_1(r,t)}{\partial r} + \frac{u_1(r,t)}{r} + \frac{iv_1(r,t)}{r}\} = 0.$$

---

[1]Note that since $r^*/a = r$, $\frac{\partial}{\partial r^*} = \frac{\partial}{a\partial r}$.

Since no generality is lost by dealing with the entire complex quantity, the "Re" restriction can be removed. Dropping the "1" subscript for simplicity yields equation (2.14c), i.e.,

$$\frac{\partial u(r,t)}{\partial r} + \frac{u(r,t)}{r} + \frac{iv(r,t)}{r} = 0.$$

Similar treatment of the Euler equation begins with substitution of (2.13b) into (2.12a).[1] This is shown below where, for the reader's benefit, each line represents a corresponding equivalent term in (2.12a).[2]

$$\begin{aligned}
&\mathrm{Re}\Big\{ \sum_{n=0}^{\infty} (\dot{u}_n(r,t)\hat{\underline{r}} + \dot{v}_n(r,t)\hat{\underline{\theta}})e^{in\theta} a\omega_o^2 \Big\} \\
&\quad - (\Omega^*)^2 r^* \hat{\underline{r}} \\
&\quad + 2\Omega^* a\omega_o \mathrm{Re}\Big\{ \sum_{n=0}^{\infty} e^{in\theta}[u_n(r,t)\hat{\underline{\theta}} - v_n(r,t)\hat{\underline{r}}]\Big\} \qquad \text{(B.1)} \\
&\quad + (\ddot{x}_1 - 2\Omega^*\dot{y}_1 - (\Omega)^{*2} x_1)\hat{\underline{i}} + (\ddot{y}_1 + 2\Omega^*\dot{x}_1 - (\Omega^*)^2 y_1)\hat{\underline{j}} \\
&\quad + \frac{1}{\rho}\frac{\partial \hat{P}(r^*,\theta,t)}{\partial r^*}\hat{\underline{r}} + \frac{1}{\rho}\frac{\partial}{r^*\partial\theta}\hat{P}(r^*,\theta,t)\hat{\underline{\theta}} = 0
\end{aligned}$$

---

[1] As in Appendix A, time derivatives of nondimensional quantities must be divided by ω_o to remain nondimensional.

[2] Note that $(\underline{\nabla}\cdot\underline{q})\underline{q}$ is second order and has been dropped.

When (see 2.13a)

$$\frac{1}{\rho}\frac{\partial \hat{P}(r^*,\theta,t)}{\partial r^*}\hat{\underline{r}} = (\Omega^*)^2 r^* \hat{\underline{r}} + \mathrm{Re}\{\sum_{n=0}^{\infty}\frac{\partial P_n(r,t)}{a\partial r}e^{in\theta}\frac{m_1\omega_o^2}{\rho a}\}\hat{\underline{r}} \quad (B.2)$$

and

$$\frac{1}{\rho}\frac{\partial \hat{P}(r^*,\theta,t)}{r^*\partial\theta} = \mathrm{Re}\{\sum_{n=o}^{\infty}\frac{inP_n(r,t)}{ar}\frac{m_1\omega_o^2}{\rho a}\} \quad (B.3)$$

are employed, the second line in (B.1) cancels with the first term in (B.2).

The fourth line in (B.1) can be expressed as

$$\mathrm{Re}\{\ddot{\eta}_1 a\omega_o^2 - i2\Omega^*\dot{\eta}_1 a\omega_o - (\Omega^*)^2\eta_1 a\}\hat{\underline{i}}$$

$$+ \mathrm{Re}\{i(\ddot{\eta}_1 a\omega_o^2 - i2\Omega^*\dot{\eta}_1 a\omega_o - (\Omega^*)^2\eta_1 a)\}\hat{\underline{j}}. \quad (B.4)$$

Utilization of (B.2), (B.3), (B.4), ignoring of the "Re" restriction, and division by $a\omega_o^2$ converts (B.1) to

$$\begin{aligned}
&\sum_{n=0}^{\infty} e^{in\theta}(\dot{u}_n(r,t)\hat{\underline{r}} + \dot{v}_n(r,t)\hat{\underline{\theta}}) \\
&+ \sum_{n=0}^{\infty} 2\Omega e^{in\theta}(-v_n(r,t)\hat{\underline{r}} + u_n(r,t)\hat{\underline{\theta}}) \\
&+ (\ddot{\eta}_1 - i2\Omega\dot{\eta}_1 - \Omega^2\eta_1)(\hat{\underline{i}} + i\hat{\underline{j}}) \\
&+ \sum_{n=o}^{\infty} e^{in\theta}\left(\frac{\pi m_1}{\pi\rho a^2 L}\frac{L}{a}\frac{\partial P_n(r,t)}{\partial r}\hat{\underline{r}} + \frac{in\pi m_1}{\pi\rho a^2 L}\frac{L}{a}\frac{P_n(r,t)}{r}\hat{\underline{\theta}}\right) = 0
\end{aligned} \quad (B.5)$$

The seemingly superfluous "π" and "L" terms in the last line are included in order to reduce the coefficients by incorporating nondimensional fluid density $\mu = \pi\rho a^2 L/m_1$ and nondimensional rotor length $z_0 = L/a$.

Substitution of

$$\hat{i} = \cos\theta\hat{r} - \sin\theta\hat{\theta},$$

and

$$\hat{j} = \sin\theta\hat{r} + \cos\theta\hat{\theta}$$

into the third line of (B.5) produces two scalar equations (the coefficients of $\hat{r}$ and $\hat{\theta}$) each of which must equal zero separately for all θ and r. Multiplication of each of these equations by $\cos\theta$ and integration from 0 to 2π eliminates all but the $n = 1$ term, culminating in

$\hat{r}$ equation:

$$\dot{u}_1(r,t) - 2\Omega v_1(r,t) + (\ddot{\eta}_1 - i2\Omega\dot{\eta}_1 - \Omega^2\eta_1) + \frac{\pi z_o}{\mu}\frac{\partial P_1(r,t)}{\partial r} = 0$$

$\hat{\theta}$ equation:

$$\dot{v}_1(r,t) + 2\Omega u_1(r,t) + i(\ddot{\eta}_1 - i2\Omega\dot{\eta}_1 - \Omega^2\eta_1) + \frac{i\pi z_o}{\mu r} P_1(r,t) = 0.$$

Once again notation is streamlined by discarding the subscript "1", the result being equations (2.14a,b).

B2. The Free Surface Boundary Condition

Since, as shown earlier, only the first term in the velocity and pressure expansions is relevant, it is appropriate to i) drop all other terms in (2.13a) and ii) consider $\lambda(\theta,t)$ as representing only the n = 1 wave mode. Division of (2.13a) by $m_1\omega_o^2/a$ then produces the nondimensional equation

$$P(r,\theta,t) = \frac{1}{2}\frac{\pi}{\pi}\frac{\rho a^2 L}{m_1}\left(\frac{a}{L}\right)\left(\frac{\Omega^*}{\omega_o}\right)^2\left[\left(\frac{r^*}{a}\right)^2 - \left(\frac{b}{a}\right)^2\right] + \mathrm{Re}\{\hat{P}(r,t)e^{i\theta}\}.$$

Setting this equal to zero at $r = f + \lambda(\theta,t)$ results in

$$\frac{1}{2}\frac{\mu}{\pi z_o}\Omega^2\left[(f+\lambda)^2 - f^2\right] + \mathrm{Re}\{P(r\approx f,t)e^{i\theta}\} = 0.$$

After dropping the second order term (i.e., λ^2), this yields

$$\lambda = -\frac{\pi z_o}{\mu\Omega^2 f}\,\mathrm{Re}\{P(r\approx f,t)e^{i\theta}\}. \qquad (B.6)$$

The nondimensional time derivative of λ (where $\frac{\partial P}{\omega_o \partial t} = \dot{P}$) is equal to the nondimensional normal fluid velocity at the free surface. Hence

$$\mathrm{Re}\{u(r=f,t)e^{i\theta}\} = -\frac{\pi z_o}{\mu\Omega^2 f}\,\mathrm{Re}\{\dot{P}(r=f,t)e^{i\theta}\}$$

where from here on the notation r =f will refer to the free surface. After dropping the "Re" nomenclature, one is left with equation (2.20).

B3. The Single Second Order Time Dependent Fluid Equation

The time derivative of the first of equations (2.11) is

$$\dddot{\eta}_1 + 2(c_1+c_2-i\Omega)\ddot{\eta}_1 - 2c_2\ddot{\eta}_2 + (1+k_2 - \Omega^2 - 2i\Omega[c_1+c_2])\dot{\eta}_1$$

$$+ (-k_2 + 2i\Omega c_2)\dot{\eta}_2 = \pi z_0 \dot{P}(r=1,t) \qquad (B.7)$$

The right hand side is evaluated using (2.15a) at r = 1, i.e.,

$$P(r=1,t) = \frac{\mu}{\pi z_0}\left[(2i\Omega r - r^2 \frac{\partial^2}{\partial r \partial t} - r\frac{\partial}{\partial t})u(t)(1 - \frac{1}{r^2})\right.$$

$$\left. - r\,(\frac{\partial^2}{\partial t^2} - 2i\Omega\frac{\partial}{\partial t} - \Omega^2)\eta_1\right]_{r=1}$$

or, after taking the appropriate derivatives,

$$P(r=1,t) = \frac{\mu}{\pi z_0}\left[-2\dot{u}(t) - \ddot{\eta}_1 + 2i\Omega\dot{\eta}_1 + \Omega^2\eta_1\right] \qquad (B.8)$$

Substituting the time derivative of (B.8) into (B.7) and solving the resulting equation for $\dddot{\eta}_1$ yields

$$\dddot{\eta}_1 = \frac{1}{1+\mu}\left[(2i\mu\Omega - 2(c_1+c_2-i\Omega)\right]\ddot{\eta}_1 + 2c_2\ddot{\eta}_2$$

$$+ (\mu\Omega^2 - 1 - k_2 + \Omega^2 + 2i\Omega(c_1 + c_2)\left]\dot{\eta}_1\right. \qquad (B.9)$$

$$+ (k_2 - 2i\Omega c_2)\dot{\eta}_2 - 2\mu\ddot{u}(t)\left].\right.$$

Insertion of (B.9) into (2.21) produces (2.22).

APPENDIX C

OPTIMAL CONTROL THEORY

Performance Index Minimization

The development of Section 2.2.1 assumes that the admissible state and control regions are not bounded, and that the initial conditions [Y(t=0)] and the initial time (t=0) are specified.

For the reader's convenience, the constraint equations (the equations of motion (2.25)) are reproduced here

$$\{\dot{Y}\} = [A]\{Y\} + \phi\{E\} \tag{C.1}$$

For methodological reasons the performance index (2.26) will be temporarily expanded to include a weighting on the final system state.

$$J = \frac{1}{2}\{Y^{\dagger}(t_f)\}^{T}[V]\{Y(t_f)\} - \frac{1}{2}\{Y^{\dagger}(0)\}[V]\{Y(0)\}$$
$$+ \frac{1}{2}\int_{0}^{t_f}(\{Y^{\dagger}(t)\}^{T}[Q]\{Y(t)\} + \phi^{\dagger}R\phi)dt \tag{C.2}$$

Once the desired relations have been determined, [V] can be set equal to zero, and the resulting equations will be directly applicable to section 2.2.1. The second term on the right hand side of (C.2) is constant (since Y(0) is given) and will not affect the extremization of J. It is used to bring J into suitable form by expressing both [V] matrix terms as

$$\int_o^{t_f} \frac{d}{dt} \left(\frac{1}{2}\{Y^\dagger(t)\}^T[V]\{Y(t)\}\right)dt.$$

Employing the chain rule and substituting into (C.2) results in

$$J = \frac{1}{2}\int_o^{t_f} \left(\{\dot{Y}(t)\} \frac{\partial}{\partial\{Y(t)\}} [\{Y^\dagger(t)\}^T[V]\{Y(t)\}]+\{Y^\dagger(t)\}^T[Q]\{Y(t)\}+\phi^\dagger R\phi\right)dt$$

The augmented form of the functional J is

$$J_a = J + \int_o^{t_f} \{\lambda^\dagger(t)\}^T([A]\{Y(t)\} + \phi(t)\{E\} - \{\dot{Y}(t)\})dt. \quad (C.3)$$

This can be expressed more compactly as

$$J_a = \int_o^{t_f} M(\{Y\},\{\dot{Y}\},\phi,\{\lambda^\dagger\})dt$$

$$= \int_o^{t_f} \{\dot{Y}\} \frac{\partial}{\partial\{Y\}} [Y^\dagger\}^T[V]\{Y\}] - \{\lambda^\dagger\}^T\{\dot{Y}\} + H)dt \quad (C.4)$$

where H is the Hamiltonian defined by equation (2.27).

Extremization of J_a requires $\delta J_a = 0$ or

$$\frac{1}{2}\int_o^{t_f} \delta M dt = 0.$$

Reexpressed, this is

$$\frac{1}{2}\int_o^{t_f} \left(\frac{\partial M}{\partial\{Y\}} \delta\{Y\} + \frac{\partial M}{\partial\{\dot{Y}\}} \delta\{\dot{Y}\} + \frac{\partial M}{\partial\phi} \delta\phi + \frac{\partial M}{\partial\{\lambda^\dagger\}^T} \delta(\lambda^\dagger)^T\right)dt. \quad (C.5)$$

Carrying out the indicated partial differentiations, integrating (by parts where necessary), and collecting coefficients of independently varying quantities results in the following relationships

$$\frac{d}{dt}\frac{\partial M}{\partial \dot{q}} - \frac{\partial M}{\partial q} = 0 \quad \text{(Euler-Lagrange Equations)} \tag{C.6a}$$

and

$$\frac{\partial M}{\partial \dot{q}}\,\delta q\Big|_0^{t_f} = 0 \quad \text{(Boundary or Transversality Conditions)} \tag{C.6b}$$

where q is successively $\{Y(t)\}$, $\psi(t)$, and $\{\lambda^{\dagger}(t)\}^T$. The intermediate steps in this development can be found in Chapters 4 and 5 of reference [17] or in any textbook on variational calculus.

Equations (C.6a) yield in turn, for the various values of q, equations (2.28a), (2.28b), and (2.25). Since M is not a function of $\dot{\psi}$ or $\{\dot{\lambda}^{\dagger}\}^T$, only the $q = \{Y\}$ equation (C.6b) is nontrivial. It is

$$\frac{\partial M}{\partial\{\dot{Y}(t_f)\}}\,\delta\{Y(t_f)\} - \frac{\partial M}{\partial\{\dot{Y}(0)\}}\,\delta\{Y(0)\} = 0 \tag{C.7}$$

For this problem $\{Y(0)\}$ is specified and hence fixed. Therefore $\delta\{Y(0)\} = 0$. $\{Y(t_f)\}$ is not fixed, however, so by necessity

$$\frac{\partial M}{\partial\{\dot{Y}(t_f)\}} = 0. \tag{C.8}$$

(C.8) readily reduces to

$$\frac{\partial}{\partial\{Y(t_f)\}}\left(\{Y^{\dagger}(t_f)\}^T[V]\{Y(t_f)\}\right) = 2\{Y^{\dagger}(t_f)\}^T[V] = \{\lambda^{\dagger}(t_f)\}^T. \tag{C.9}$$

In Section 2.2.1 [V] is taken as zero, so that the complex

conjugate transpose of (C.9) is then simply equation (2.34), i.e., the final boundary condition on $\{\lambda\}$.

APPENDIX D

JUSTIFICATION FOR RICCATI EQUATION SOLUTION METHOD

D1 Riccati Equation Solution Properties

i) Steady State $[K(t)]$

In reference [18], Kalman proves the following theorem, restated here in the language of this paper. Note that, to aid in the following discussion, $[K(t)]$ is sometimes written as $[K(t,t_f)]$.

Stability Theorem: Given the Riccati Equation

$$\frac{d[K(t)]}{dt} = -[K(t)][A] - [A^{\dagger}]^{T}[K(t)] - [Q] + [K(t)]\{E\}\{E^{\dagger}\}^{T}[K(t)]/R \qquad (D.1)$$

derived from the optimal control problem of Section 2.2.1 and subject to the assumptions delineated there, all solutions to (D.1), i.e., $[K(t,t_f)]$, approach a constant value as $t \to -\infty$.

Corollary: for fixed t_f defined such that $[K(t,t_f)]_{t=t_f} = 0$ (see equation (2.39)), $[K(t,t_f)]$ is unstable for $t \to \infty$.

For fixed t_f, the behavior of matrix components of solutions to (D.1) is qualitatively similar to that of Figure D.1a. The situation can be viewed slightly differently by fixing t and letting t_f vary. This is depicted in Figure D.1b and clearly illustrates that for t_f approaching infinity, $[K(t)]$ is constant for all time. By

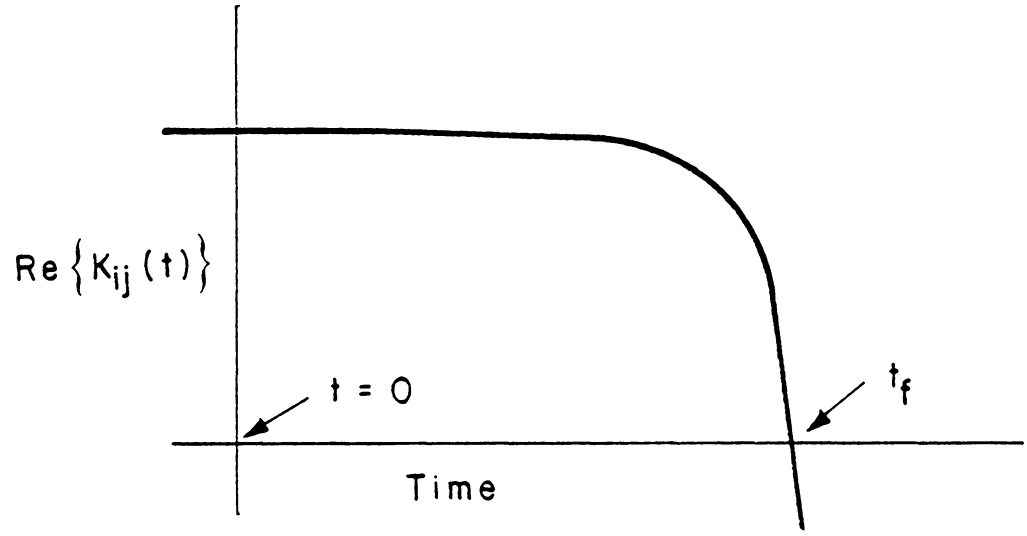

FIGURE D.1a. TYPICAL COMPONENT OF $[K(t,t_f)]$ FOR GIVEN t_f

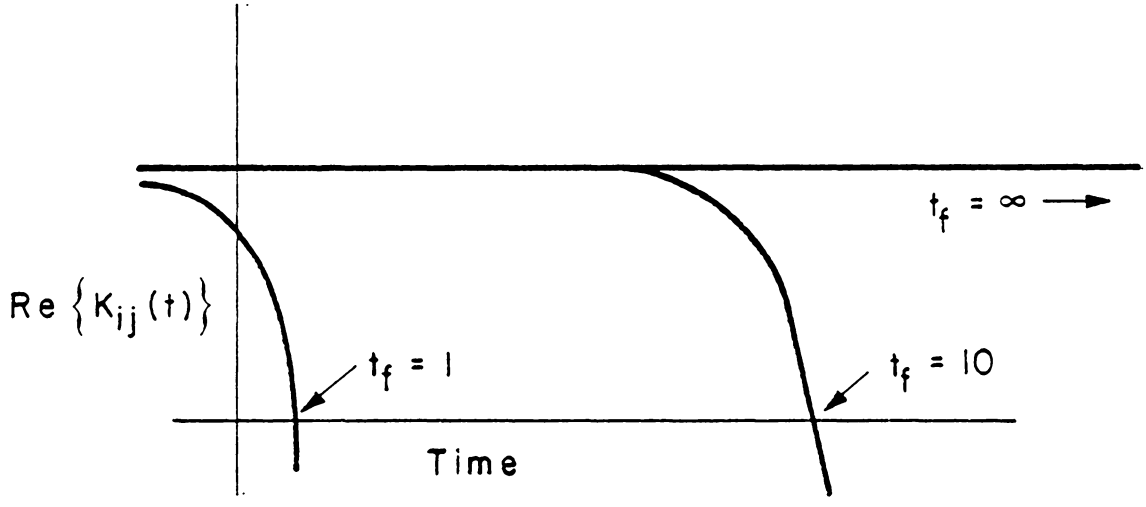

FIGURE D.2a. TYPICAL COMPONENT OF $[K(t,t_f)]$ FOR DIFFERENT t_f

taking $t_f \to \infty$ in the performance index (2.26), the differential Riccati equation (D.1) reduces to the algebraic (steady state) equation (2.40).

ii) [K(t)] Hermitian

From (D.1), boundary condition (2.39), i.e.,

$$[K(t_f)] = [0],$$

and the hermitian nature of [Q], $\frac{d}{dt}[K(t)]|_{t=t_f}$ must be hermitian. At time $t_f - dt$, therefore, [K(t)] must be hermitian also. It is then demonstrable that the first two terms on the right hand side of (D.1) taken together and the fourth term are hermitian as well. As a result, integration backward in time will always produce an hermitian [K(t)].

iii) [K(t)] Positive Definite

Kalman [19] has shown that if the system is controllable by ϕ (as determined in Section 2.2.1), then [K(t)] must be positive definite.

D2 Main Proof of Solution Method

Except for notation,[1] the following theorems are reproduced directly from reference [20]. Only the first and most enlightening is proven (Section D3 following). For the other two, see reference [20].

Theorem 1. Every solution of (2.40) has the form

$$[K] = [\{b_1\},\{b_2\},\ldots,\{b_n\}][\{c_1\},\{c_2\},\ldots,\{c_n\}]^{-1}$$

---

[1]Symbols used here are explained in the solution steps outline of Section 2.2.2.

where the column vectors $\{b_i\}$ and $\{c_i\}$ are the upper and lower halves of an eigenvector $\{a_i\}$ of [M]. Conversely, if $\{a_1\},\ldots,\{a_n\}$ are eigenvectors of [M] and $[\{c_1\},\ldots,\{c_n\}]$ is nonsingular, then

$$[K] = [\{b_1\},\ldots,\{b_n\}][\{c_1\},\ldots,\{c_n\}]^{-1}$$

satisfies (2.40).

Theorem 2. If [Q] and $\{E\}\{E^\dagger\}^T/R$ are hermitian, $\{a_1\},\ldots,\{a_n\}$ are eigenvectors of [M] corresponding to eigenvalues $\Lambda_1,\ldots,\Lambda_n$, and $\Lambda_i \neq -\Lambda_j^\dagger$ for $1 \leq i, j \leq n$, and if $[\{c_1\},\ldots,\{c_n\}]$ is nonsingular, then

$$[\{b_1\},\ldots,\{b_n\}][\{c_1\},\ldots,\{c_n\}]^{-1}$$

is hermitian.[1]

Theorem 3. Assume that [Q] and $\{E\}\{E^\dagger\}^T/R$ are positive definite hermitian and let $\{a_1\},\ldots,\{a_n\}$ be eigenvectors of [M] corresponding to eigenvalues $\Lambda_1,\ldots,\Lambda_n$. In this case,

(a) if [Q] or $\{E\}\{E^\dagger\}^T/R$ is nonsingular and

$$[K] = [\{b_1\},\ldots,\{b_n\}][\{c_1\},\ldots,\{c_n\}]^{-1}$$

is positive definite, then $\Lambda_1,\ldots,\Lambda_n$ have positive real parts, and

---

[1]Implicit in this (Potter's) statement is the interesting and unexpected fact that in this case for every Λ_i associated with [M], there exists another Λ_j ($j \neq i$) such that $\Lambda_i = -\Lambda_j^\dagger$.

(b) if $\Lambda_1,\ldots,\Lambda_n$ have positive real parts and $[\{c_1\},\ldots,\{c_n\}]$ is nonsingular, then $[\{b_1\},\ldots,\{b_n\}][\{c_1\},\ldots,\{c_n\}]^{-1}$ is positive semidefinite.

Theorem (1) provides justification for working with the eigenvectors of the [M] matrix in the manner prescribed in Section 2.2.2. Theorems(2) and (3) validate the procedure for selecting which unique set of n eigenvectors (of the total 2n eigenvectors) are to be utilized in order to produce a positive definite hermitian solution [K].

D3. Proof of Theorem 1

For the reader's benefit the steady state matrix Riccatti equation (2.40) is reproduced here.

$$[0] = [K][A] + [A^{\dagger}]^{T}[K] + [Q] - [K]\{E\}\{E^{\dagger}\}^{T}[K]/R \qquad (2.40)$$

Step 1: Define a matrix [G] as follows:

$$[G] = \{E\}\{E^{\dagger}\}^{T}[K]/R - [A] \qquad (D.3)$$

Then from (2.40)

$$[K][G] = [Q] + [A^{\dagger}]^{T}[K] \qquad (D.4)$$

Step 2: Assume[G] can be transformed into Jordon Canonical Form [J] by a new matrix [C].

$$[C]^{-1}[G][C] = [J]$$

Premultiplication by $[C]^{-1}$ yields

$$[G][C] = [C][J] \tag{D.5}$$

Step 3: Define another new matrix [B] such that

$$[B] = [K][C] \tag{D.6}$$

Postmultiplication of (D.4) by [C] produces

$$[K][G][C] = [Q][C] + [A^{\dagger}]^{T}[K][C]$$

From (D.5), $[K][C][J] = [Q][C] + [A^{\dagger}]^{T}[K][C]$ or from (D.6)

$$[B][J] = [Q][C] + [A^{\dagger}]^{T}[B] \tag{D.7}$$

Step 4: Postmultiplication of (D.3) by [C] results in

$$[G][C] = \{E\}\{E^{\dagger}\}^{T}[K][C]/R - [A][C]$$

From (D.5) and (D.6)

$$[C][J] = \{E\}\{E^{\dagger}\}^{T}[B]/R - [A][C] \tag{D.8}$$

Step 5: (D.7) and (D.8) are the essence of the proof. They can be written in matrix form as:

$$\begin{Bmatrix} [B] \\ \hline [C] \end{Bmatrix}[J] = \left[\begin{array}{c|c} [A^{\dagger}]^{T} & [Q] \\ \hline \{E\}\{E^{\dagger}\}/R & -[A] \end{array}\right] \begin{Bmatrix} [B] \\ \hline [C] \end{Bmatrix}$$

$2n \times n \quad n \times n \qquad 2n \times 2n \qquad 2n \times n$

Note that the 2n x 2n matrix on the right hand side is identical to the [M] matrix (2.41) of the first solution step in section 2.2.2. Since [J] is Jordon Canonical, its n diagonal components are then eigenvalues Λ_j (j = 1,...,n) of [M]. If [B] and [C] are rewritten in terms of column vectors as

$$[B] = [\{b_1\},\{b_2\},\ldots,\{b_n\}]$$

$$[C] = [\{c_1\},\{c_2\},\ldots,\{c_n\}]$$

then each column vector $\begin{Bmatrix}\{b_j\}\\ ----\\ \{c_j\}\end{Bmatrix} = \{a_j\}$ is an eigenvector of [M].

From (D.6) the solution [K] to (2.40) is then

$$[K] = [B][C]^{-1} = [\{b_1\},\ldots,\{b_n\}][\{c_1\},\ldots,\{c_n\}]^{-1}$$

and the theorem is proven.

Note that this solution is not unique since there are 2n possible eigenvectors of [M] and only n are used to find [K]. Thorems 2 and 3 provide criteria for selecting a unique (i.e., positive definite hermitian) solution.

APPENDIX E

SUMMARY OF NUMBER OF EIGENVALUES

E1. Two Mass Model

	Degrees of Freedom (Number of Independent Equations)	
	Real Equations	Complex Equations
Configuration space (2nd order differential equation)	6[1]	3
State space (1st order differential equation)	12	6

	Number of Eigenvalues (Complex)	
	Real Equations	Complex Equations
	12 (6 distinct)[2]	6 (distinct)

If there were no damping or driving force, each ith independent modal displacement would have the two pure imaginary eigenvalues = ω_i. Since i = 1,2,3 (corresponding to the first mass, second mass, and fluid displacements), there would then be only three distinct eigenvalues.

---

[1]Two directions each for the first mass, the second mass, and the fluid.

[2]Six pairs of repeated roots since x,y directions have the same stiffnesses, damping, etc.

E2. Continuous Mass Model Case

As described in Section 3.1.4, the eigenproblem complex matrix [A] is of order 4N + 10. From reasoning parallel to that of the above section, it can be concluded that the system will then have 4N + 10 distinct eigenvalues.

APPENDIX F

DERIVATION OF [M], [C], [K] MATRICES FOR CONTINUOUS MASS ROTOR

F1 Needed Relationships

The following relationships will be needed repeated by anyone wishing to track the extremely lengthy algebraic computations which lie enroute to the expressions for [M], [C], and [K] at the end of this appendix.

$$\int_0^{z_o} \phi_j(\zeta)d\zeta = \frac{\sqrt{2z_o}}{j\pi}\left[1 - (-1)^j\right] = \delta_j$$

$$\int_0^{z_o} \frac{d\phi_j(\zeta)}{d\zeta} d\zeta = 0$$

$$\int_0^{z_o} \zeta\phi_j(\zeta)d\zeta = \frac{\sqrt{2z_o^3}}{j\pi}(-1)^{j+1} = \varepsilon_j$$

$$\phi_j(0) = 0 \qquad \phi_j(z_o) = 0$$

$$\frac{d\phi_j}{d\zeta}\Big|_{\zeta=0} = \sqrt{2/z_o}\; j\pi/z_o = j\sigma$$

$$\text{where } \sigma = \sqrt{2\pi^2/z_o^3}$$

$$\frac{d\phi_j}{d\zeta}\Big|_{\zeta=z_o} = j\sigma(-1)^j$$

$$\int_0^{z_o} \phi_j^2(\zeta)d\zeta = 1$$

$$\int_0^{z_o} \left(\frac{d\phi_j}{d\zeta}\right)^2 d\zeta = (j\pi/z_o)^2$$

F.2 Kinetic Energy, Dissipation Function, Potential Energy, And Other Expressions Needed in Lagrange Equation

Second and lower order terms are retained in all expressions where derivatives will be taken in equation (3.21).

$$T = \frac{1}{2} m_L(\dot{x}_L-\Omega y_L)^2 + \frac{1}{2} m_L(\dot{y}_L+\Omega x_L)^2 + \frac{1}{2} m_u(\dot{x}_u-\Omega y_u)^2 + \frac{1}{2} m_u(\dot{y}_u+\Omega x_u)^2$$

$$+ \frac{1}{2} m_{bot}(\dot{x}_B-\Omega y_B)^2 + \frac{1}{2} m_{bot}(\dot{y}_B+\Omega x_B)^2 + \frac{1}{2} m_{top}(\dot{x}_B+z_o\dot{\phi}_2-\Omega[y_B-z_o\phi_1])^2$$

$$+ \frac{1}{2} m_{top}(\dot{y}_B-z_o\dot{\phi}_1+\Omega[x_B+z_o\phi_2])^2$$

$$+\frac{1}{2z_o}\int_0^{z_o}(\dot{x}_B+\dot{x}+\zeta\dot{\phi}_2-\Omega[y_B+y-\zeta\phi_1])^2 d\zeta + \frac{1}{2z_o}\int_0^{z_o}(\dot{y}_B+\dot{y}-\zeta\dot{\phi}_1+\Omega[x_B+x+\zeta\phi_2])^2 d\zeta$$

$$+ \frac{1}{2} I_{bot}(\dot{\phi}_1+\dot{\beta}-\Omega[\phi_2+\alpha])^2_{\zeta=0} + \frac{1}{2} I_{bot}(\dot{\phi}_2+\dot{\alpha}+\Omega[\phi_1+\beta])^2_{\zeta=0} + \frac{1}{2} J_{bot}\Omega^2$$

$$+ J_{bot}\Omega(\alpha\dot{\phi}_1-\beta\dot{\phi}_2-\beta\dot{\alpha}-\dot{\phi}_2\phi_1-\Omega[\alpha\phi_2+\beta\phi_1])_{\zeta=0} - J_{bot}\frac{\Omega^2}{2}(\alpha^2+\beta^2+\phi_2^2+\phi_1^2)_{\zeta=0}$$

$$+ \frac{1}{2} I_{top}(\dot{\phi}_1+\dot{\beta}-\Omega\phi_1-\Omega\alpha)^2_{\zeta=z_o} + \frac{1}{2} I_{top}(\dot{\phi}_2+\dot{\alpha}+\Omega[\phi_1+\beta])^2_{\zeta=0} + \frac{1}{2} J_{top}\Omega^2$$

$$+ J_{top}\Omega(\alpha\dot{\phi}_1-\beta\dot{\phi}_2-\beta\dot{\alpha}-\dot{\phi}_2\phi_1-\Omega[\alpha\phi_2+\beta\phi_1]_{\zeta=z_o} - J_{top}\frac{\Omega^2}{2}(\phi_2^2+\phi_1^2)_{\zeta=z_o}$$

$$+ \frac{J_{rot}}{4z_o}\int_0^{z_o}(\dot{\phi}_1+\dot{\beta}-\Omega[\phi_2+\alpha])^2 d\zeta + \frac{J_{rot}}{4z_o}\int_0^{z_o}(\dot{\phi}_2+\dot{\alpha}+\Omega[\phi_1+\beta])^2 d\zeta$$

$$+ \frac{J_{rot}\Omega^2}{2} + \frac{J_{rot}\Omega}{z_o}\int_0^{z_o}(\alpha\dot{\phi}_1-\beta\dot{\phi}_2-\beta\dot{\alpha}-\dot{\phi}_2\phi_1-\Omega[\alpha\phi_2+\beta\phi_1])d\zeta$$

$$- \frac{J_{rot}\Omega^2}{2z_o}\int_0^{z_o}(\alpha_2+\beta^2+\phi_2^2+\phi_1^2)d\zeta$$

$$D = \frac{1}{2} C_1(\dot{x}_L-\Omega y_L)^2 + \frac{1}{2} C_1(\dot{y}_L+\Omega x_L)^2 + \frac{1}{2} C_2(\dot{x}_B-\dot{x}_L-\Omega[y_B-y_L])^2$$

$$+ \frac{1}{2} C_2(\dot{y}_B-\dot{y}_L+\Omega[x_B-x_L])^2 + \frac{1}{2} C_3(\dot{x}_B+z_o\dot{\phi}_2-\dot{x}_u-\Omega[y_B-z_o\phi_1-y_u])^2$$

$$+ \frac{1}{2} C_3(\dot{y}_B-z_o\dot{\phi}_1-\dot{y}_u+\Omega[x_B+z_o\phi_2-x_u])^2 + \frac{1}{2} C_4(\dot{x}_u-\Omega y_u)^2 + \frac{1}{2} C_4(\dot{y}_u+\Omega x_u)^2$$

$$V = \frac{1}{2} K_1 x_L^2 + \frac{1}{2} K_1 y_L^2 + \frac{1}{2} K_2(x_B-x_L)^2 + \frac{1}{2} K_2(y_B-y_L)^2$$

$$+ \frac{1}{2} K_3(x_B+z_o\phi_2-x_u)^2 + \frac{1}{2} K_3(y_B-z_o\phi_1-y_u)^2 + \frac{1}{2} K_4 x_u^2 + \frac{1}{2} K_4 y_u^2$$

$$+ \frac{1}{2}\int_o^{z_o} EI[(\frac{\partial\alpha}{\partial\zeta})^2 + (\frac{\partial\beta}{\partial\zeta})^2]d\zeta + \frac{1}{2}\int_o^{z_o} k'GA[(\frac{\partial x}{\partial\zeta}) - \alpha)^2 + (\frac{\partial y}{\partial\zeta} + \beta)^2]d\zeta$$

$$\underline{R}_L = x_L\hat{\underline{i}} + y_L\hat{\underline{j}} \qquad \underline{U} = U_x\hat{\underline{i}} + U_y\hat{\underline{j}}$$

With (3.1d) used in (3.1a) to get $\underline{r} = r\hat{\underline{r}} = \cos\theta\hat{\underline{d}}_1 + \sin\theta\hat{\underline{d}}_2$ in terms of $\hat{\underline{i}}$, $\hat{\underline{j}}$, $\hat{\underline{k}}$.

$$\underline{R}_D + \underline{r}_{r=1} = (x_B + xC\phi_2 + \zeta C\phi_1 S\phi_2 + C\theta C\phi_2 + S\theta S\phi_1 S\phi_2 + [S\beta S\theta - S\alpha C\theta]C\phi_1 S\phi_2)\hat{\underline{i}}$$

$$+ (y_B + yC\phi_1 - \zeta S\phi_1 + S\theta C\phi_1 - C\theta S\phi_2 + [S\alpha C\theta - S\beta S\theta]S\phi_1)\hat{\underline{j}}$$

$$+ (\zeta C\phi_1 C\phi_2 - xS\phi_2 + yS\phi_1 C\phi_2 + S\theta S\phi_1 C\phi_2 + [S\beta S\theta - S\alpha C\theta]C\phi_1 C\phi_2)\hat{\underline{k}}$$

where "C"'s and "S"'s have been used for cosine and sine respectively.

To first order,

$$C\theta\hat{\underline{d}}_1 + S\theta\hat{\underline{d}}_2 = C\theta\hat{\underline{i}} + S\theta\hat{\underline{j}} + [S\theta(\phi_1 + \beta) - C\theta(\phi_2 + \alpha)]\hat{\underline{k}}$$

F3 Complex Equation Derivation

Only the first (and simplest) of the equations (3.23) will be derived here. Its development will be representative of that for the other equations.

The first step is to find the equation of motion for $q = x_L$ using (3.21) with all terms real. This is then done for y_L as well. These two real O.D.E.'s are then combined into a single complex equation in terms of the complex independent variables of (3.22a).

$q = x_L$ Equation:

$$\frac{d}{dt}\left(\frac{\partial T}{\partial \dot{x}_L}\right) = m_L\ddot{x}_L - m_L\Omega\dot{y}_L$$

$$\frac{\partial D}{\partial \dot{x}_L} = C_1(\dot{x}_L - \Omega x_L) - C_2(\dot{x}_B - x_L - \Omega[y_B - y_L])$$

$$\frac{\partial V}{\partial x_L} = K_1 x_L - K_2(x_B - x_L)$$

$$\frac{\partial T}{\partial x_L} = m_L\Omega(\dot{y}_L + \Omega x_L)$$

$$\frac{\partial(\underline{R}_0+\underline{r})}{\partial x_L} = 0 \qquad \frac{\partial \underline{R}_L}{\partial x_L} \cdot \underline{U} = U_x$$

Equation (3.21) becomes

$$m_L\ddot{x}_L + (C_1 + C_2)\dot{x}_L + (K_1 + K_2 - m_L\Omega^2)x_L - 2m_L\Omega\dot{y}_L - \Omega(C_1 + C_2)y_L$$

$$- C_2\dot{x}_B - K_2 x_B + C_2\Omega y_B = U_x \qquad (F.1)$$

$q = y_L$ Equation:

Similar steps yield

$$m_L\ddot{y}_L + (C_1 + C_2)\dot{y}_L + (K_1 + K_2 - m_L\Omega^2)y_L + 2m_L\Omega\dot{x}_L + \Omega(C_1 + C_2)x_L$$

$$- C_2\Omega x_B - C_2\dot{y}_B - K_2 y_B = U_y \qquad (F.2)$$

Complex equation:

Multiplying (F.2) by -i and adding it to (F.1) yields

$$m_L(\ddot{x}_L - i\ddot{y}_L) + + (C_1 + C_2 - i2m_L\Omega)(\dot{x}_L - i\dot{y}_L) - C_2(\dot{x}_B - i\dot{y}_B)$$

$$+ (K_1 + K_2 - m_L\Omega^2 - i\Omega[C_1 + C_2])(x_L - iy_L) - (K_2 - iC_2\Omega)(x_B - iy_B)$$

$$= U_x - iU_y. \qquad (F.3)$$

This is the first equation in (3.23) where the complete [M], [C], and [K] are given in the next section of this appendix.

F4 [M], [C], and [K] Matrices for Flexible Rotor

The equations of motion for the empty uncontrolled rotor are

$$[M]\{\ddot{X}\} + [C]\{\dot{X}\} + [K]\{X\} = 0.$$

Let

$$\delta_j = [1 - (-1)^j]\frac{\sqrt{2z_o}}{j\pi} \quad ; \quad \varepsilon_j = (-1)^{j+1}\frac{\sqrt{2z_o^3}}{j\pi}$$

$$\sigma = \sqrt{2\pi^2/z_o^3} \quad ; \quad \delta_{\ell j} = \begin{cases} 0 & \ell \neq j \\ 1 & \ell = j \end{cases}$$

The Mass Matrix [M] is

$$
\begin{array}{c}
\\
\\
\\
\\
\\
\\
\end{array}
\begin{array}{c}
\begin{array}{cccccc} & & & & j=1,N & j=1,N \end{array} \\
\begin{bmatrix}
m_L & 0 & 0 & 0 & 0 & 0 \\
0 & m_u & 0 & 0 & 0 & 0 \\
0 & 0 & m_1 & -m_2 & m_{1j} & 0 \\
0 & 0 & m_2 & m_3 & -m_{2j} & m_{3j} \\
0 & 0 & m_{1\ell} & m_{2\ell} & m_{1\ell j} & 0 \\
0 & 0 & 0 & m_{3\ell} & 0 & m_{2\ell j}
\end{bmatrix}
\end{array}
\begin{array}{l}
\\
\\
\\
\\
\ell = 1,N \\
\ell = 1,N
\end{array}
$$

where

$$m_1 = 1 + m_{bot} + m_{top}$$

$$m_2 = -iz_o(1/2 + m_{top})$$

$$m_3 = z_o^2(1/3 + m_{top}) + I_{bot} + I_{top} + J_{rot}/2$$

$$m_{1\ell} = \delta_\ell / z_o$$

$$m_{2\ell} = i\varepsilon_\ell / z_o$$

$$m_{3\ell} = \ell\sigma(I_{bot} + (-1)^\ell I_{top})$$

$$m_{1\ell j} = \delta_{\ell j} / z_o$$

$$m_{2\ell j} = j^2\sigma^2 J_{rot}\delta_{j\ell}/4 + \ell j\sigma^2(I_{bot} + (-1)^{j+\ell} I_{top}).$$

The Damping Matrix [C] is

$$
\begin{array}{c}
\\
\\
\\
\\
\\
\\
\\
\end{array}
\begin{array}{c}
\qquad\qquad\qquad\qquad\qquad\qquad\qquad\qquad\qquad\qquad\qquad\qquad j=1,N \quad j=1,N \\
\left[\begin{array}{cccccc}
C_a & 0 & -C_2 & 0 & 0 & 0 \\
0 & C_b & -C_3 & -C_c & 0 & 0 \\
-C_2 & -C_3 & C_d & C_e & C_{1j} & 0 \\
0 & C_c & -C_e & C_f & -C_{2j} & C_{3j} \\
0 & 0 & C_{1\ell} & C_{2\ell} & C_{1\ell j} & 0 \\
0 & 0 & 0 & C_{3\ell} & 0 & C_{2\ell j}
\end{array}\right]
\end{array}
\begin{array}{l}
\\
\\
\\
\\
\\
\ell = 1,N \\
\ell = 1,N
\end{array}
$$

$$C_a = C_1 + C_2 - 2i\Omega m_L$$

$$C_b = C_3 + C_4 - 2i\Omega m_u$$

$$C_c = iz_o C_3$$

$$C_d = C_2 + C_3 - 2i\Omega(1 + m_{bot} + m_{top})$$

$$C_e = (1 + 2m_{top})\Omega z_o + iz_o C_3$$

$$C_f = z_o^2 C_3 - 2i\Omega(z_o^2[1/3 + m_{top}] + I_{bot} + I_{top} - [J_{bot} + J_{top}]/2)$$

$$C_{1\ell} = -2i\Omega\delta_\ell / z_o$$

$$C_{2\ell} = 2\Omega\varepsilon_\ell / z_o$$

$$C_{3\ell} = 2i\Omega\ell\sigma(-I_{bot} - (-1)^\ell I_{top} + [J_{bot} + (-1)^\ell J_{top}]/2)$$

$$C_{1\ell j} = -2i\Omega\delta_{\ell j} / z_o$$

$$C_{2\ell j} = -2i\Omega j\ell\sigma^2[I_{bot} + I_{top}(-1)^{\ell+j} - \frac{J_{bot}}{2} - \frac{J_{top}}{2}(-1)^{\ell+j}]$$

The Stiffness Matrix [K] is

$$
\begin{array}{c}
 \\
\begin{bmatrix}
K_a & 0 & K_b & 0 & 0 & 0 \\
0 & K_c & K_d & -K_e & 0 & 0 \\
K_b & K_d & K_f & K_g & K_{ij} & 0 \\
0 & K_e & -K_g & K_h & K_{2j} & K_{3j} \\
0 & 0 & K_{1\ell} & -K_{2\ell} & K_{1\ell j} & -K_{2\ell j} \\
0 & 0 & 0 & K_{3\ell} & K_{2\ell j} & K_{3\ell j}
\end{bmatrix}
\end{array}
\begin{array}{l}
 \\
 \\
 \\
 \\
 \\
 \\
\end{array}
\begin{array}{l}
j=1,N \\
 \\
 \\
 \\
 \\
 \\
\end{array}
\begin{array}{l}
j=1,N \\
 \\
 \\
 \\
 \\
 \\
\end{array}
\qquad
\begin{array}{l}
 \\
 \\
 \\
 \\
\ell = 1,N \\
\ell = 1,N
\end{array}
$$

where

$$K_a = K_1 + K_2 - m_L\Omega^2 - i\Omega(C_1 + C_2)$$

$$K_b = -K_2 + i\Omega C_2$$

$$K_c = K_3 + K_4 - m_u\Omega^2 - i\Omega(C_3 + C_4)$$

$$K_d = -K_3 + i\Omega C_3$$

$$K_e = z_o(\Omega C_3 + iK_3)$$

$$K_f = K_2 + K_3 - (1 + m_{bot} + m_{top})\Omega^2 - i\Omega(C_2 + C_3)$$

$$K_g = z_o(\Omega C_3 + iK_3 - i\Omega^2[m_{top} + 1/2])$$

$$K_h = K_3 z_o^2 + \Omega^2(J_{bot} + J_{top} + J_{rot}/2 - I_{bot} - I_{top} - z_o^2[m_{top} + 1/3])$$

$$- iz_o^3 C_3\Omega$$

$$K_{1\ell} = -\Omega^2 \delta_\ell / z_o$$

$$K_{2\ell} = i\Omega^2 \varepsilon_\ell / z_o$$

$$K_{3\ell} = -\ell\sigma\Omega^2 (I_{bot} + (-1)^\ell I_{top} - J_{bot} - (-1)^\ell J_{top})$$

$$K_{1\ell j} = (k'GA[j\pi/z_o]^2 - \Omega^2/z_o)\delta_{\ell j}$$

$$K_{2\ell j} = ik'GA(\ell\pi/z_o)^2 \delta_{\ell j}$$

$$K_{3\ell j} = (EI[j\pi/z_o]^4 + k'GA[j\pi/z_o]^2 + [j\sigma\Omega/2]^2 J_{rot})\delta_{\ell j}$$
$$+ \ell j\sigma^2\Omega^2 [J_{bot} + (-1)^{j+\ell} J_{top} - I_{bot} - (-1)^{j+\ell} I_{top}]$$

APPENDIX G

POLE PLACEMENT IN THE LUENBERGER OBSERVER

If $\{e(t)\}$ in equation (4.5) is taken equal to $\{e(0)\}e^{\lambda t}$, where symbols and methodology parallel those of Section 2.2.3, then (4.5) becomes

$$([A] - [B][C] - \lambda[I])\{e(t)\} = \{0.\}. \qquad (G.1)$$

For a non-trivial solution the matrix quantity above must, by Cramer's rule, be such that its determinant equals zero. Furthermore, if $\{e(t)\}$ is to go to zero as time evolves, all possible λ's must have negative real parts (see Section 2.2.3).

For an nth order system there will be n λ's and the objective here is then to choose all of these to have negative real parts. Since the determinant of $[A] - [B][C] - \lambda[I]$ must equal zero, this will place constraints on the possible choices for the heretofore undetermined $[B]$. Each λ selected will result in one constraint equation, so there will be n such equations in all.

$[B]$ must have n rows, while its number of columns, p, is equal to the number of available state vector components, i.e., the number of rows in $[C]$. Since it is desired to have only a single sensor (a single $\{V(t)\}$ component), $p = 1$ and $[B]$ is on $n \times 1$ matrix with n unknown components. The n equations will therefore determine $[B]$ precisely.

Numerically, the two mass (n = 6) problem can be attacked as follows:

Consider the 6 x 6 matrix

$$[B][C] = \begin{Bmatrix} B_1 \\ B_2 \\ B_3 \\ B_4 \\ B_5 \\ B_6 \end{Bmatrix} \{1 \quad 0 \quad 0 \quad 0 \quad 0 \quad 0\}$$

where [B] is to be determined and from the form of [C], it is seen that the sensor picks up the displacement (complex) of the first mass.

With streamlined notation and use of cofactor expansion, the development of [A] - [B][C] - λ[I] can be written as

$$\text{Det } ([A] - [B][C] - \lambda[I]) = \text{Det } [A'] = 0$$

$$= (A_{11} - B_1 - \lambda)\text{COF } A'_{11} + (A_{21} - B_2)\text{COF } A'_{21} + (A_{31} - B_3)\text{COF } A'_{31}$$

$$+ (A_{41} - B_4)\text{COF } A'_{41} + (A_{51} - B_5)\text{COF } A'_{51} + (A_{61} - B_6)\text{COF } A'_{61}$$

Rearranged this is

$$\sum_{i=1}^{6} A_{i1} \text{ COF } A'_{i1} - \lambda \text{ COF } A'_{11} = \sum_{i=1}^{6} (\text{COF } A'_{i1})B_i. \qquad (G.2)$$

Choosing $\lambda = \lambda_1$ with negative real part (the imaginary part is arbitrary, though a choice of zero is most convenient) results in a

definite numerical value for the LHS of (G.2). For the present purposes this will be called d_1, and

$$d_1 = \sum_{i=1}^{6} (\text{COF } A'_{i1}) B_i . \qquad (G.3)$$

Repeating this process for 6 different negative choices for $\text{Re}\{\lambda\}$ will result in a total of 6 such independent equations in 6 unknown B_i's.

$$\begin{Bmatrix} d_1 \\ d_2 \\ d_3 \\ d_4 \\ d_5 \\ d_6 \end{Bmatrix} = \sum_{i=1}^{6} (\text{COF } A'_{i1_j}) B_i$$

where "j" corresponds to the jth choice for λ.

Solving this for the B_i is straightforward. These are then used as the components in the 6 x 1 [B] matrix of the Luenberger observer (equation (4.3)).

Experience indicates that choice of largest $\text{Re}\{\lambda\}$ slightly more negative than the dominant $\text{Re}\{\lambda\}$ of the fully available controlled system (see Figure 2.3) is best (see [22] page 317).

The two page vita has been removed from the scanned document. Page 1 of 2

The two page vita has been removed from the scanned document. Page 2 of 2

OPTIMAL CONTROL OF A ROTATING CYLINDER PARTIALLY FILLED WITH IDEAL FLUID

by

Robert D. Klauber

(ABSTRACT)

Optimal control theory analysis is applied to a rotating cylinder partially filled with an inviscid, incompressible fluid. Two models of the system are investigated: (1) a two discrete mass system with fluid inside one mass and the control force applied to the other, and (2) a continuously distributed cylindrical mass system with control force applied to a discrete lower suspension mass. For (2) the method of assumed modes is used to discretize the system and obtain a set of n linear algebraic equations. In both cases the treatment is two dimensional and axial motion of the fluid is considered negligible.

In both models, the uncontrolled system, shown by earlier researchers to be inherently unstable, is found to be controllable. The appropriate optimal feedback control is derived and system responses investigated.

In addition, both models are shown to be observable. Direct measurement of only a portion of the components of the state vector are sufficient, using a Luenberger Observer, to estimate the entire state vector.